Oncology and Translational Medicine

Volume 8 • Number 2 • April 2022

Oncology and Translational Medicine Volume 8 • Number 2 • April 2022 pp 57-108

邮发代号：38-121
ISSN 2095-9621

GENERAL INFORMATION
≫otm.tjh.com.cn

ISSN 2095-9621
CN 42-1865/R

Oncology and Translational Medicine

肿瘤学与转化医学（英文）

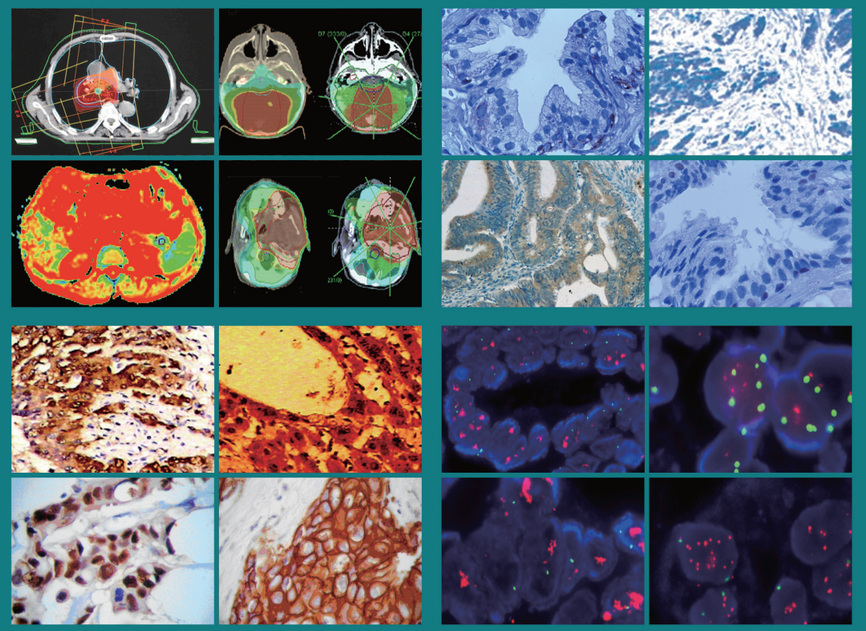

Volume 8
Number 2
April 2022

Oncology and Translational Medicine

Oncology and Translational Medicine
April 2022 Volume 8 Number 2

Contents

Oncology and Translational Medicine

Volume 8 • Number 2 • April 2022

Aims & Scope

Oncology and Translational Medicine is an international professional academic periodical. The Journal is designed to report progress in research and the latest findings in domestic and international oncology and translational medicine, to facilitate international academic exchanges, and to promote research in oncology and translational medicine as well as levels of service in clinical practice. The entire journal is published in English for a domestic and international readership.

Copyright

Supervised by

Ministry of Education of the People's Republic of China.

Administered by

Tongji Medical College, Huazhong University of Science and Technology.

Submission information

Manuscripts should be submitted to:
http://otm.tjh.com.cn
dmedizin@sina.com

Subscription information

ISSN edition: 2095-9621
CN: 42-1865/R

■ Subscription rates
Subscription may begin at any time. Remittances made by check, draft or express money order should be made payable to this journal. The price for 2022 is as follows: US $ 30 per issue; RMB ￥28.00 per issue.

Database

Oncology and Translational Medicine is abstracted and indexed in EMBASE, Index Copernicus, Chinese Science and Technology Paper Citation Database (CSTPCD), Chinese Core Journals Database, Chinese Journal Full-text Database (CJFD), Wanfang Data; Weipu Data; Chinese Academic Journal Comprehensive Evaluation Database.

Business correspondence

All matters relating to orders, subscriptions, back issues, offprints, advertisement booking and general enquiries should be addressed to the editorial office.

Mailing address
Editorial office of
Oncology and Translational Medicine
Tongji Hospital
Tongji Medical College
Huazhong University of Science and Technology
Jie Fang Da Dao 1095
430030 Wuhan, China
Tel.: +86-27-69378388
Email: dmedizin@sina.com

Printer
Changjiang Spatial Information Technology Engineering Co., Ltd. (Wuhan) Hangce Information Cartorgraphy Printing Filial, Wuhan, China
Printed in People's Republic of China

Editors-in-Chief

Managing director

Executive editors

Oncology and Translational Medicine
DOI 10.1007/s10330-022-0573-3

April 2022, Vol. 8, No. 2, P57–P73

REVIEW ARTICLE

The interaction between end-metabolites and immune escape

Tong Zhu, Guihua Wang (✉)

GI Cancer Research Institute, Tongji Hospital, Huazhong University of Science and Technology, Wuhan 430030, China

Abstract

Emerging data from metabolites-relating trails in cancers demonstrate that a common mechanism of resistance to many novel classes of immune therapeutics is the emergence of immune escape due to the reprogramming of cellular metabolism. Among them, current work about end-metabolites mostly focuses on the intersection between lactate acid, adenosine, reactive oxygen species (ROS), and tumour immune escape. In this article, we aim to review the evidence to date for the dynamic interplay between the three end-metabolites and tumour immune escape for potential approaches to overcome obstacles in the efficacy and durability of immune cancer therapies. We have organized known end-metabolites-associated immune escape mechanisms into three hallmarks: (1) decreased immunogenicity of cancer cells which constitutes defective antigen presentation and the attenuated expression of costimulatory molecules on tumour cells, (2) immunosuppressive microenvironment with aberrant angiogenesis inhibits the differentiation, maturation, and immune deviation of immune cells while drives the activation of immunosuppressive cells by immune-suppressive mediators (cytokines and other factors), (3) immune tolerance retained by inhibitory molecules and depletion of immune cells.

Received: 15 April 2022
Revised: 20 April 2022
Accepted: 25 April 2022

Key words: lactate acid; adenosine; reactive oxygen species; tumour; immune escape

Introduction

Cancer immunotherapies, such as immune adoptive T cell transfer and checkpoint blockade, have drastically improved the clinical outcomes for multiple treatment-refractory and metastatic cancers. Although these immunotherapies have demonstrated durable responses, patient response rates remain suboptimal owing to undefined suppression mechanisms. Simultaneously, the field of cancer metabolic alterations has become a topic of interest in the past decade. Aided by new molecular, biological, and biochemical tools, studies on cancer cell metabolism have advanced our understanding of the mechanisms and functional influences of tumor-associated metabolic alterations at distinct stages of tumorigenesis. Therefore, there is increasing interest in elucidating the potential impact of metabolic alterations on the immunity of tumors, because unveiling the interplay may facilitate more potent antitumor therapies.

Distinct hallmarks of tumorigenesis-associated metabolic reprogramming exist. Tumor masses often grow under hypoxic conditions, lacking glucose and other nutrients; thus, the tumor microenvironment (TME) is usually characterized by lower pH values [1]. In addition to glucose, energy can also be generated through the glutaminolysis pathway. Thus, high amounts of lactic acid are produced by both pathways and subsequently discharged into the TME. An acidic TME results from the excessive and continuous generation of lactic acid [2]. One of the most abundant extracellular metabolites is adenosine owing to the significant generation of adenosine triphosphate (ATP). Adenosine in the TME is a result of active transport through the plasma membrane or extracellular ATP dephosphorylation through the concerted function of two ectonucleotidases, CD39 and CD73 [3]. The third extensively studied end-metabolite is the reactive oxygen species (ROS). ROS can be derived as by-products from mitochondria during ATP generation in the electron transport chain (ETC), or they can represent products in enzymatic reactions mainly under the mediation of NADPH oxidase (NOX) and dual oxidase (DUOX) families (e.g., GPX) [4]. Cancer cells

✉ Correspondence to: Guihua Wang. Email: ghwang@tjh.tjmu.edu.cn

reprogram their metabolism to adapt and survive in harsh environments and, in some pathways, even utilize such adverse conditions to their benefit [5, 6]. Therefore, these metabolites may not simply be waste products of cancer metabolism, as they have widespread effects on cancer biology, such as stimulating angiogenesis, local invasion, and metastasis. In addition to reprogramming energy metabolism, evading immune destruction has also been recently described as a hallmark of tumorigenesis [6, 7]. Tumor cells evade immune surveillance and elimination using two main strategies: eluding the anticancer immunity of the immune system and promoting an immunosuppressive TME [8, 9]. The TME comprises various types of immune cells, including regulatory T cells (Tregs), myeloid-derived suppressor cells (MDSCs), and tumor-associated macrophages (TAMs), which concurrently attenuate the immune response to cancers, allowing for greater local invasion, metastasis, and occurrence of drug resistance [10, 11]. Immune cells such as macrophages and neutrophils have two subtypes: M1 and M2, and N1 and N2, respectively. M1 and N1 cells are typically activated cells that have pro-inflammatory features with antitumor activity, whereas M2 and N2 cells are immunosuppressive phenotypes that are alternatively activated to promote cancer progression.

This review focuses on the current advances in the identification of the complex and dynamic roles of lactate, adenosine, and ROS in tumor immunity. We discuss the mechanistic processes by which these three metabolites help cancer cells evade immune surveillance, break immune equilibrium, and finally escape immunity, thereby assisting tumor progression.

Lactate

The centrality of the Warburg effect in tumor metabolism has been well acknowledged [12, 13]. In accordance with the Warburg effect, the accumulation of the metabolite lactic acid and the subsequent acidic TME are the results of enhanced glycolysis. The metabolic switch of accelerated glycolysis in cancer cells is subtly mediated by increased expression levels of oncogenes, primarily hypoxia-inducible factor (HIF)-1α and c-Myc [14, 15]. In addition, to generate from aerobic glycolysis, tumor-derived lactic acid can also be produced from the catabolism of glutamine [16]. Thus, both the major pathway of aerobic glycolysis and the minor pathway of glutaminolysis are responsible for lactic acid production in cancer cells. In an acidic TME, an inverted H^+ gradient ($pH_{intracellular} > pH_{extracellular}$) is maintained by the corporate action of various transporters, such as monocarboxylic transporters (MCTs), Na^+/H^+ exchangers, H^+/K^+-ATPases, Na^+/HCO_3^- cotransporters, and carbonic anhydrases (CA IX and CA XII). This concentration inversion has been suggested to provide at least two benefits for cancer cells: (1) intracellular alkalization facilitates increased glycolysis, particularly in hypoxia, which promotes cancer cell proliferation [17]; (2) extracellular acidification hampers the initiation of an appropriate immune response [18]. Further, MCT1 and MCT4, which transport H^+-coupled molecules that contain a single carboxylate group such as lactate, pyruvate, β-hydroxybutyrate, and acetoacetate, are ubiquitously expressed in various cells, but are highly upregulated in cancer cells, where they connote a poor prognosis [19, 20]. Increased lactic acid accumulation and subsequent acidification of the TME promote multiple critical oncogenic processes, including invasion, metastasis, angiogenesis, and drug resistance. In this review, we specifically elaborate on how lactate enables cancer cells to survive immunosurveillance and elimination.

Immunogenicity

Tumor immunogenicity is the ability to induce different levels of adaptive immune responses and is dictated by two major criteria: antigen presentation and immune cell recognition. Weak immunogenicity elicits a suboptimal immune response that spares the opportunity and time for tumor cells to develop immune escape mechanisms [21]. Antigen presentation is the process by which antigen-presenting cells (APCs), such as dendritic cells (DCs), internalize tumor antigens and then present antigens to helper T (Th) cells to initiate an adaptive immune response. The recognition process is fueled by T cell receptor (TCR) and major histocompatibility complex (MHC) binding, costimulatory molecules, and some cytokines.

Presentation

Acidic and hypertonic micromilieu limit the capacity of DCs to present tumor antigens, thereby potentially contributing to cancer immune escape and partially accounting for poor clinical response to DC vaccines [22]. Moreover, the TME contains abundant immunosuppressive factors that impair the immunostimulatory capacity of DCs [23]. Exposure to high levels of lactate (e.g., 40 mM) was confirmed to hamper the differentiation and maturation of DCs [14]. As a result, the presentation of DCs is affected. In addition to the aberrant development of DCs, studies have also documented that peptide-MHC I complexes are unstable at acidic pH compared to neutral pH [15], which results in faster Ag release. The third mechanism may be that lactic acid induces a significant reduction in interleukin (IL)-12 in tumor-associated DCs, which triggers a blockage of an important stimulatory signal in the cross-priming cascade of DCs [14, 23].

Recognition

In a recent study, lactic acid suppressed the proliferation of human cytotoxic T lymphocytes (CTLs) up to 95% and led to a 50% decrease in cytotoxic cytokine production. Therefore, lactic acid promotes the development of immune evasion by establishing an anergic state of tumor-specific $CD8^+$ T lymphocytes. This is characterized by decreased cytolytic activity and cytokine secretion owing to reduced expression levels of TCRs and IL-2Ra (CD25), and diminished activation of extracellular signal-regulated kinase (ERK) and STAT5 after TCR activation both in human and mouse models [24]. Another reason for the decreased CTL function is ascribed to lactate dehydrogenase A (LDHA), which is highly expressed in cancer cells by the mediation of c-Myc and HIF-1α [23, 25]. LDHA was experimentally observed to favor tumor immune evasion [26], possibly by enabling accelerated cancer glucose consumption. LDHA has a higher affinity for pyruvate and preferentially converts pyruvate and nicotinamide adenine dinucleotide (NADH) to lactate and NAD^+ under anaerobic conditions, whereas LDHB has a higher affinity for lactate and thereby catalyzes the conversion of lactate to pyruvate. Database analyses of human melanoma patients revealed negative correlations between the expression of LDHA and T-cell activation markers. In accordance with these findings, experiments showed increased numbers of antitumor effector cells in $LDHA^{low}$ mice compared to those in the control group. By parity of reasoning, the activation and function of tumor-infiltrating immune cells (TILs), which comprise Th1 cells, NK cells, MDSCs, TAMs, CTLs, Tregs, and other immune cells, are influenced by the levels of both LDHA expression and lactic acid in the TME. Blocking LDHA or recovering the acid-base equilibrium environments in tumors may improve the efficacy of anti-programmed death-1 (PD-1) therapy [27]. However, the function of lactate anions has been relatively ignored and less studied. During an in vitro T-cell activation experiment, the addition of excess sodium lactate (NaL) enhanced the production of antitumor cytokines (such as interferon (IFN) γ, IL-2, and tumor necrosis factor (TNF)-α) more than the addition of excess sodium chloride (NaCl). This increase in cytokine production was shown to depend on TCR/CD3 activation [25].

Immunosuppressive microenvironment

High concentrations of lactate and concomitant acidification create an immunosuppressive microenvironment that limits immune cell activation and allows for immune evasion. By affecting glycolysis, oxidative phosphorylation (OXPHOS), and other metabolic signaling pathways, the distinct microenvironment changes the metabolic phenotype of immune cells, thereby impeding their normal antitumor activity. Lactic acid suppresses the proliferation and cytotoxicity of CTLs in vitro through impaired MCT1-mediated lactate and H^+ transport, resulting in the disappearance of the lactic acid gradient between the cytoplasm and extracellular space [28]. In addition, lactic acid suppresses CTL function through inhibition of p38 and JNK/c-Jun activation [29]. In natural killer T cells (NKTs), low extracellular pH inhibits NKT cell function by blocking mammalian target of rapamycin (mTOR) signaling and disturbing nuclear translocation of promyelocytic leukemia zinc finger (PLZF), thereby inhibiting IFN-γ and IL-4 production by NKT cells [30]. In contrast, Treg proliferation and function are not negatively affected by lactate, and iTreg development is favored by lactate. Tregs are less dependent on glycolysis and prefer to use OXPHOS and lipid oxidation as energy providers [31, 32]. Glucose avidity is associated with impaired functionality of Tregs because Tregs have the metabolic advantage of being invigorated by the oxidation of lactate to pyruvate mediated by LDHB; that is, Tregs can thrive on lactate as an alternative fuel. Tregs conditioned in glucose-low or glucose-deficient media upregulate the expression of LDHA and MCT1 [33], and they activate genes involved in lactate metabolism. In addition, the Treg transcription factor forkhead box P3 (Foxp3) reprograms their metabolism by suppressing Myc and glycolysis while enhancing OXPHOS and increasing NADH oxidation. Foxp3-Myc interaction can prevent endogenous lactic acid accumulation inside Tregs by favoring the oxidation of lactate to pyruvate [34]. Indoleamine 2,3-dioxygenase (IDO) is an immune regulatory enzyme expressed by Tregs that converts tryptophan to kynurenine. Upregulated Treg levels in the acidic TME also diminish tryptophan levels, which in turn stimulate stress response pathways that sustain Treg suppressive functions [35, 36]. This dominant metabolic phenotype of Tregs provides cancer cells with a chance to evade immune destruction.

Immune suppressive mediators

Tumors can survive immune surveillance by crippling CTL functionality through the production of various immunosuppressive cytokines, either from cancer cells or from non-cancerous cells present in the TME, especially those derived from immune cells and epithelial cells. Transforming growth factor-β (TGF-β) is the chief mediator among all cytokines [37]. In addition, TNF-α, colony-stimulating factor (CSF)-1, IL-1, IL-6, IL-8, IL-10, and type I IFNs can significantly contribute to tumor growth [38-42]. Protumor factors (such as CCL2, CCL5, cathepsin G, and neutrophil elastase) produced by the N2 phenotype, which is characterized by higher arginase expression level, can also induce immune suppression in the TME [43]. Lactic acid forms an inhibitory

microenvironment by regulating these mediators in the TME. For example, lactate reduces the NK cell cytotoxic response against tumor cells by decreasing the production of IFN-γ and TNF-α [26]. In mouse NK cells, IFN-γ secretion was completely inhibited at both mRNA and protein levels under 15 mM lactic acid conditions. This indicated that lactic acid alone can diminish cytokine production [26]. Moreover, tumor-derived lactate inhibits NK cell function directly as well as indirectly by promoting the development of MDSCs [44]. Under physiological conditions, bone MDSCs can differentiate into granulocytes, macrophages, and DCs. However, this process is impaired under acidic conditions, leading to the accumulation of MDSCs [45]. MDSCs have been confirmed to inhibit lymphocyte homing, stimulate other immunosuppressive cells, deplete metabolites critical for T cell function, express ectoenzymes that regulate adenosine metabolism, and produce ROS [46]. These accumulated MDSCs in both experimental and clinical tumors are considered strong contributors to the immune-suppressive TME [47]. However, NK cell effector functions can be inhibited by lactic acid and can also be reversed when acidity is buffered back to the physiological pH of 7.4, or when lactic acid generation is blocked [48].

In addition to their function, immunosuppressive mediators are also associated with the differentiation, maturation, and immune deviation of immune cells. Lactic acid is a latent inhibitor of tumor-suppressive T cells but favors the development of tumor-permissive Tregs in vitro [18, 26, 34]. Lactate can even drive T cells toward an immunosuppressive Treg phenotype [34]. A similar phenomenon also occurs in macrophages, where the antitumor pro-inflammatory M1 phenotype has high glucose consumption, whereas the protumor M2 phenotype does not, consuming either lactate or fatty acids [49]. Intrinsically, lactic acid consumed by macrophages upregulates the neovascularization factor vascular endothelial growth factor (VEGF), and the M2-marker arginase 1 (Arg1) [50, 51]. TME acidity has a direct effect on macrophage phenotypic polarization, skewing their differentiation toward the immunosuppressive M2 phenotype through ERK/STAT3 signaling activation [51], and stimulating the secretion of CCL5 through activation of Notch signaling in macrophages [52, 53]. After recognizing CCR5, which is regulated by TGF-β signaling in breast cancer cells, CCL5 increases cell migration, induces epithelial-mesenchymal transition (EMT) in cancer cells, and promotes aerobic glycolysis in cancer cells by mediating AMPK signaling [54]. In addition, the ability of lactic acid to mediate M2 redistribution is also dependent on HIF-1α stabilization to some extent [55]. Like in macrophages, lactic acid promotes an alternative N2 functional profile in neutrophils, which is characterized by poor phagocytic ability and suppressed ROS production [56]. N2-tumor associated neutrophils (TANs) express high levels of CD11b/CD18 and β2 integrin, and they contribute to tumor growth and metastasis through multiple pathways, including the production of angiogenic factors, suppression of T cells, and secretion of proteases (such as MMP-9 and elastase) [56]. DC precursors do not express CD1a and are incapable of differentiating into DCs when cultured with IL-4 and GM-CSF derived from different tumor cell lines [14]. In addition, monocyte-derived DCs (MoDCs) developed using low cell density cultures have a superior ability to produce inflammatory cytokines, migrate toward lymphoid tissue guided by chemokine CCL19, and induce Th1 polarization. Conversely, MoDCs originating from dense culture do not produce inflammatory cytokines upon activation but secrete IL-10. This cell concentration-dependent pathway acts through lactic acid, which builds up in dense culture and induces early and long-lasting reprogramming of MoDC differentiation [57]. The differentiation deviation of these immune cells can be reacquired upon pH reversal. In addition to cytokines, other immunosuppressive factors such as VEGF secretion by tumors also hamper the differentiation of progenitors into DCs [58]. Therefore, lactic acid serves as a critical immunoregulatory molecule that influences immune cell differentiation. The role of lactate as an epigenetic regulator through histone modification has also been considered. By directly combining histone lysine acetylation sites, lactate initiates the expression of many genes in various immune cells. For example, lactic acid stimulates the expression of traditional genes associated with M2 macrophages [50, 51]. The ability of macrophages to polarize into the M2 phenotype through lactic acid-induced acidosis in the TME is likely due to histone lysine acetylation and subsequent enhanced inflammation-independent biological pathways [59]. This may explain the dedifferentiation and loss of anticancer abilities of multiple cell types in an acidic extracellular environment. However, considering lactic acid as a general epigenetic regulator still requires greater understanding and a more comprehensive acceptance of its profound role in tumor biology, especially in shaping anticancer immunity.

Angiogenesis

Angiogenesis factors drive immune escape by directly inhibiting APCs as well as immune cells and indirectly by augmenting the effects of Tregs, MDSCs, and TAMs. These immunosuppressive cells can also stimulate angiogenesis, forming a vicious cycle of impaired anti-tumor immunity [19]. VEGF inhibits the activation of nuclear factor kappa B (NF-kB) [60], differentiation, and antigen presentation of APCs [61], while increasing their PD-L1 expression level [62]. VEGF also suppresses the differentiation, proliferation, and cytotoxicity of T cells

[28] and accelerates T cell exhaustion by increasing the expression levels of checkpoints such as PD-L1, CTLA-4, lymphocyte activation gene 3 (LAG3), and TIM3 [29]. Angiogenesis driven by another angiogenic factor, angiopoietin-2 (Ang-2), is distinct from that induced by VEGF. Ang-2 increases the recruitment and adhesion of both neutrophils and Tie-2–expressing monocytes (TEMs) to the endothelium [58] and then contributes to the preference for conversion to M2 macrophages [50]. However, unlike VEGF, Ang-2 does not directly affect T cells, but can indirectly contribute to the expansion of Tregs and the suppression of effector T cells by promoting TEMs to secrete IL-10 [50, 58]. Furthermore, MDSCs can initiate the formation of a pre-metastatic niche by increasing angiogenesis and enhancing tumor cell stemness [63].

An acidic pH is required for the expression of lactate-induced VEGF [52]. Exposure to lactate enables the metabolic utilization of lactate by macrophages with LDHB-catalyzed conversion of NAD^+ to NADH, which reduces the cellular NAD^+ pool and subsequently unchecks the suppressive responses mediated by NAD^+-dependent ADP-ribose polymerase. This metabolic phenomenon has been shown to promote the synthesis of VEGF by macrophages and induce angiogenesis at the wound and tumor sites [16]. The efflux and influx of lactate in the lactate shuttle of vascular endothelial cells is mediated by MCT4 and MCT1, respectively. After being imported into the cells, lactate is oxidized to pyruvate, which initiates NF-κB/IL-8 signaling and stabilizes HIF-1α by preventing HIF-1α prolyl hydroxylation. Therefore, increased lactic acid production and the subsequent acidic environment and HIF-1α overexpression co-induce vasculogenesis and angiogenesis through the VEGF pathway also under normoxic conditions [20].

Tolerance

Inhibitory molecules, death signals, and apoptotic signals are all significant contributors to cancer immune escape by promoting undue immune tolerance against tumor cells through enervating and depleting effector cells.

Inhibitory molecules

PD-1 is an inhibitory molecule expressed mainly by activated T cells on the cell surface and serves as a negative regulator of antitumor immune responses by dephosphorylating TCR. In the acidic TME, MDSCs increase their activity through the acid-induced HIF-1α pathway, resulting in augmented PD-L1 expression and myeloid cell death [64]. Lactic acid is a pivotal inhibitory signaling molecule that plays a key role in cancer cell growth, angiogenesis, immune escape, migration, and invasion [65]. This signaling molecule function depends, at least partially, on its binding to lactic acid receptors. By activating G protein-coupled receptor 81 (GPR81) on cancer cells, lactic acid enhances tumor cell proliferation, drug resistance, and PD-L1 expression through an autocrine pathway [66–68]. In a paracrine manner, cancer cell-derived lactate activates GPR81 in endothelial cells, immune cells, and adipocytes present in the TME. Activation of GPR81 on DCs triggers downstream cascades, such as decreased generation of cyclic adenosine monophosphate (cAMP), IL-6, and IL-12, suggesting that paracrine lactic acid signaling to DCs inhibits the presentation of tumor-specific antigens to T cells [69]. In addition, GPR81 knockdown mice exhibited suppressed Treg generation [70]. Therefore, the end results of GPR81 activation promotes angiogenesis, immune escape, and chemoresistance. Migratory inhibition factor (MIF) is an emerging immunosuppressive factor. Blocking MIF-CD74 signaling reduces lactate production, as well as HIF-1α and PD-L1 expression levels in resistant cancer cells, potentiating $CD8^+$ T cell infiltration and driving macrophage conversion toward the pro-inflammatory M1 phenotype [71].

Immune cell depletion

Depleting immune cells is another approach used by cancer cells to escape immunity. Lactate can reduce immune cells in several ways, such as impeding their proliferation, promoting apoptosis, and reducing their accumulation in the TME. Tregs tend to accumulate in the acidic TME; therefore, they are increasingly being evaluated as immune therapeutic targets [176]. However, in other immune cells, the serum lactate level is negatively related to the number of effector immune cells and positively associated with tumor burden in cancer patients [161]. Upon activation, T cells (excluding Tregs) in the TME change to a cancer-like Warburg metabolic phenotype and produce more lactic acid, which theoretically supports the rapid proliferation of the cancer cells. However, monocarboxylates and H^+ bidirectional symport by MCT-1 require a lactic acid concentration gradient between the cytoplasm and extracellular space. Consequently, MCT transporters cannot function optimally, thereby disturbing intracellular pH homeostasis in activated T cells, or the resultant intracellular acidification directly kills the cells. Lactate concentrations above 20 mM can invalidate the cytotoxic activity of CTLs and NK cells by causing apoptosis through blocking the FAK family interacting protein of the 200 kDa pathway both in vitro and in vivo [13]. Lactic acid can also induce NK cell apoptosis through mitochondrial dysfunction by decreasing the intracellular pH, which can be prevented by inhibiting mitochondrial ROS accumulation [5]. A decreased intracellular PH also expedites neutrophil

apoptosis. The key regulators of apoptosis, such as caspase 3, also have reduced activation under such conditions [74]. With respect to cell accumulation, upon the influx of lactic acid through the SMCT2 transporter, either decreased phosphofructokinase or downregulated hexokinase 1 of Ths and CTLs can result in the inhibition of glycolysis, and finally, the reduction of cell motility [75]. As such, these effector cells lose responsiveness to chemokines and no longer infiltrate areas of the body, resulting in less accumulation in the TME. In contrast, resisting committed cell death, that is, evading apoptosis, is also thought to be a hallmark of cancer and represents an important mechanism in tumor resistance to oncological therapies [37, 40]. LDHA plays a role in reducing the apoptosis of tumor cells. Lack of LDHA enhances oxygen consumption, resulting in elevated levels of mitochondrial ROS (mROS) [38, 39, 41]. As ROS are powerful stimulators of $Ca2^+$ internalization, knocking down LDHA leads to increased intracellular levels of $Ca2^+$, which triggers apoptosis by activating apoptotic endonucleases [26, 43].

Lactate is not an innocuous bystander or waste metabolite. In essence, lactate exported by glycolysis-dependent hypoxic cancer cells, which cannot oxidize lactate, is taken in by neighboring normoxic cancer cells to synthesize ATP through mitochondrial respiration [76]. However, the limited direct measurements of lactate in the interstitial fluid suggest relatively modest accumulation, which is substantially lower than the levels used in the culture fluid of in vitro cell studies. The gradient between incoming and outgoing blood measurements revealed that some tumors consumed lactate. The uptake of circulating lactate is oxidized to pyruvate and serves as a tricarboxylic acid (TCA) intermediate [77–79]. Because the material exchange between tumor cells and circulation is so rapid, little pyruvate generated from glucose through the upregulated glycolysis of the tumor is involved directly in the TCA cycle. Instead, tumor-derived pyruvate is mostly converted into lactate and excreted, with most of the TCA ingredient pyruvate in the tumor coming from circulating lactate produced elsewhere in the body [79]. In summary, we need to characterize the tumor metabolic milieu more precisely, which is particularly critical because of the marked metabolic composition difference between the microenvironment and the tumor mass due to active transport processes. Direct interstitial fluid sampling and subsequent metabolomic analysis may be feasible steps in this regard. The overall mechanism network of lactate acid is showed as below (Fig.1).

Adenosine

Adenosine is an immunosuppressive end-metabolite produced at high levels within the TME, where its precursor, ATP, is abundantly released into the extracellular space in response to cell death signals, cell stress, and opening of pannexin/connexin channels on immune or endothelial cells [80, 81]. Ectonucleotidases (most prominently CD39 and CD73) favor the degradation of ATP into adenosine and thus disrupt antitumor immunity [82, 83]. CD39 and CD73 are ubiquitously expressed in various cells within the TME, including tumor, stromal, immune, and endothelial cells [84]. Exosomes derived from $CD39^+CD73^+$ tumor cells, Tregs, and mesenchymal stem cells can also generate adenosine [85]. CD39 and CD73 successively catalyze ATP to AMP and AMP to adenosine. Overexpression of CD73 in the TME reverses the immune-activating role of ATP, suppressing adenosine and promoting tumor growth. CD73 expressed on the surface of tumor cells is one of the reasons for tumor immune escape, and inhibition of CD73 may reinvigorate the activity of T cells and enhance the antitumor immune monitoring ability of immune cells decreased by adenosine. Immunosuppressive subpopulations, including Tregs and MDSCs, in both the tumor mass and lymph nodes, also upregulate CD73/CD39 expression, thereby enhancing their intrinsic immunosuppressive effect [86]. Hypoxia, which is a common phenomenon in many cancers, has also been verified as one of the main stimulators for the buildup of extracellular adenosine [87]. Adenosine can locally stimulate four subtypes of specific G protein-coupled receptors (A1, A2a, A2b, and A3) [88]. Among these, only activated A2a and A2b receptors on immune cells can trigger strong immunosuppressive responses. Upon engagement of either A2a or A2b receptors, adenosine induces increased adenylyl cyclase activity with concomitant increased generation of intracellular cAMP [89] and subsequent activation of protein kinase A (PKA) [90-96]. cAMP plays a suppressive role through cAMP/PKA-mediated blocking of the TCR, NF-kB, and Janus kinase-signal transducer and activator of transcription (JAK-STAT) signaling pathways [97]. In addition, in vitro assays using mouse and human T cells have consistently confirmed that both Ths and CTLs rapidly upregulate A2a following TCR activation in an NFAT-dependent manner [98]. As for myeloid cells, particularly TAMs, A2a expression also indirectly contributes to the suppression of antitumor immunity by suppressing $CD8^+$ T and NK cells [99]. Tregs are a significant source of adenosine in the TME; however, they can also respond to autocrine/paracrine adenosine stimulation by expressing adenosine receptors. In support of a direct promoting role for A2b signaling in Tregs, a previous study demonstrated a strong increase in A2b mRNA expression level in Tregs following TCR activation [100].

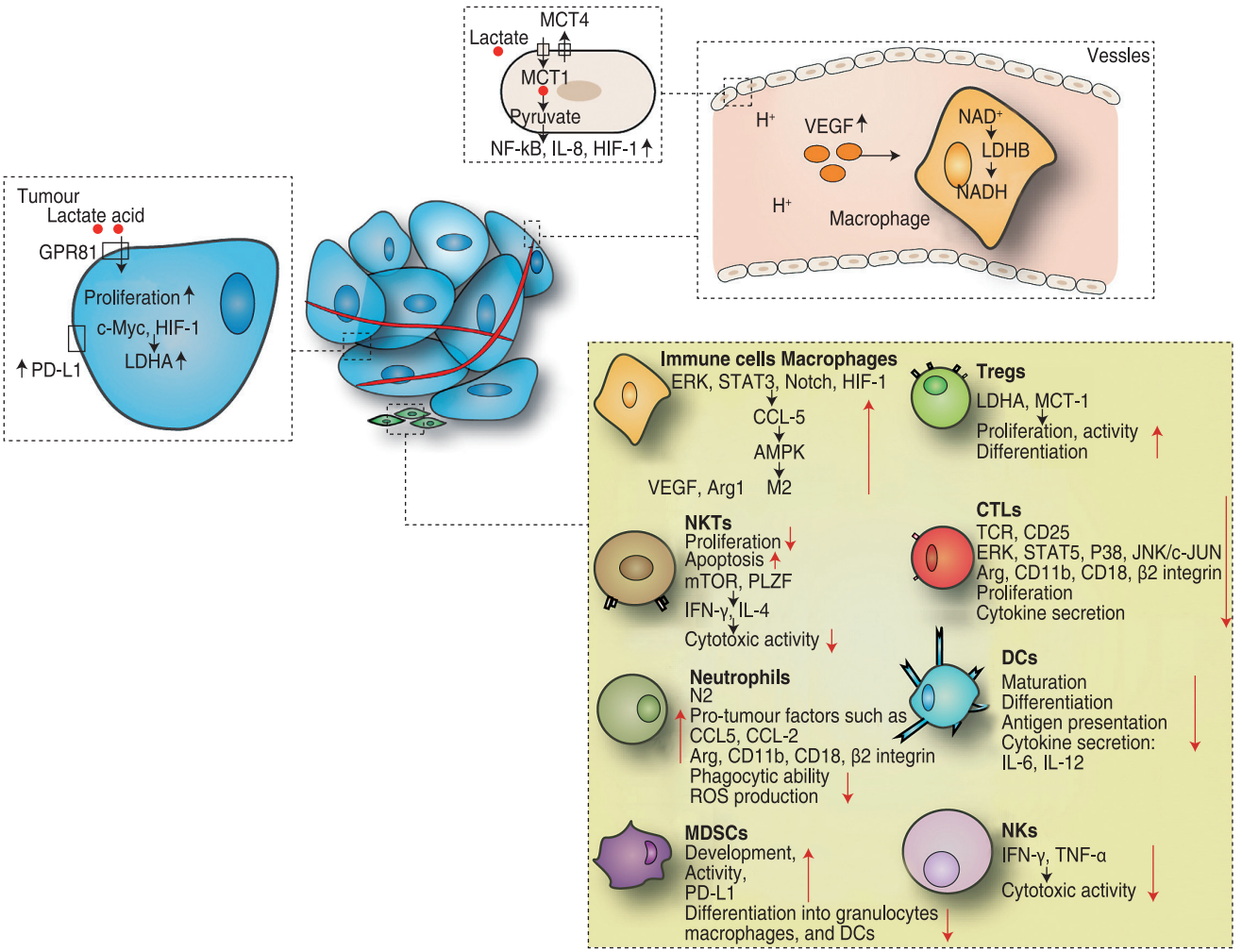

Fig. 1 The interaction between lactate acid and tumour immune escape. Lactate acid promotes tumour cells' immune escape by inducing immune cells to differentiate into immunosuppressive phenotypes and then secreting immune-suppressive mediators. The proliferating effects of lactate acid applied to tumour cells and vascular epithelial cells also contribute to the immune escape

Immunogenicity

Presentation

Depending on A2b signaling, adenosine skews aberrant differentiation of monocytes to DCs, deviating them toward a Th2-helping, pro-angiogenic, and tolerogenic phenotype characterized by the production of IL-6, IL-8, IL-10, and VEGF, as well as the expression of immunosuppressive markers such as TGF-β, IDO, Arg2, and cyclooxygenase (COX2) [101]. Blocking A2b receptors promotes DCs activation and the subsequent CXCR3-dependent antitumor responses [102]. Therefore, adenosine has been proven to diminish the capacity of DCs to prime and amplify Th1 immune responses by activating the CD39, CD73, and A2b receptors.

Recognition

Adenosine impairs antigen recognition and subsequent T cell activation. Increased PKA activity secondary to A2a receptor signaling in effector T cells has additional suppressive effects, including attenuation of proximal TCR signaling by inhibiting the LCK-dependent activation of ZAP70 [103, 104] and protein kinase C activity, which is critical for effector cell activation [105]. A2a receptor signaling in $CD4^+$ Ths decreases IL-2 secretion, which reduces the expression level of the costimulatory receptor CD28 [106].

Immunosuppressive microenvironment

Through the A2 receptor, adenosine creates an environment that facilitates the reduction of immunosurveillance cells, while favoring the expansion of immunosuppressive cells. A2b stimulation is beneficial

for the differentiation and proliferation of $CD11b^+ Gr1^{high}$ neutrophilic-like MDSCs characterized by high levels of CD73, thereby potentiating adenosine-mediated immunosuppressive functions [107]. In addition, A2a activation ultimately leads to decreased T cell expansion and activation [98, 100] and the rise of profound T cell anergy [98, 108].

Immune suppressive mediators

Inhibiting the mitogen-activated protein kinase (MAPK) pathway through ERK1 and JNK and promoting TNF-α secretion, A2a activation induces transcription of the c-Jun/AP-1 complex in activated T cells and stimulates the formation of $LAG3^+$ Tregs by inducing TGF-β secretion [98]. Adenosine production by Tregs through CD39 and CD73 expression reinforces anergic properties related to their function through autocrine A2a receptor signaling. To this end, A2a receptor agonism results in Treg expansion and can be adoptively transferred before ischemia-reperfusion injury to enhance the protective capacity [109-111]. Stimulation of the A2a receptor on naive $CD4^+$ T cells also promotes the development of Tregs by activating and increasing Foxp3 and LAG3 synthesis [112]. This is the effect of adenosine on the proliferation of immune cells.

As for immune cell functions, in murine models, studies have found that metastasis of $CD73^+$ tumor cells is associated with A2a/cAMP/PKA-mediated suppression of NK cell anti-tumor activities in a manner of decreased perforin and IFN-γ production [113, 114]. The downstream mTORC1 pathway functions as the main axis for adenosine-mediated impairment of T cell function and metabolic fitness [115]. In addition, the A2a/cAMP/PKA pathway results in the inhibition of pro-inflammatory NF-kB signaling [100]. Accordingly, A2a activation in T cells has been shown to increase the secretion levels of TGFβ, IL-10, PD-1, and LAG-3, as well as decrease the levels of pro-inflammatory cytokines, such as IFN-γ, TNF-α, and IL-6 in vivo and in vitro [93, 98, 100]. In the TME, tumor-associated endothelial cell (TEC)-derived CD73 can produce adenosine that downregulates ICAM-1, thereby repressing the adhesion and the transmigration of antitumor T cells [96]. Thus, adenosine signaling in TECs hinders T cell homing to tumors. Changes in B cell functionality have also been reported due to alterations in T cells within germinal centers [116, 117]. CD39, CD73, and A2a receptor expression on B cells also suppresses effector T cell functions and impairs the secretion of immunoglobulin (Ig)A- and IgG-type antibodies.

Adenosine also affects immune cell differentiation. TGF-β mediates the maturation of MDSCs into tumor-associated terminally differentiated myeloid mononuclear cells, which exhibit high levels of CD39/CD73 expression and adenosine-generating capacity [118]. A2a-deficient TAMs, in sharp contrast to A2a-proficient TAMs, display characteristics similar to antitumor M1, which possesses increased MHC II and IL-12 levels while decreasing IL-10 expression level. Through A2a and A2b receptor signaling, TAMs are stimulated to secrete IL-13 and IL-4, thereby increasing Arg level that inclines TAMs to initiate M2 activation and inhibit $CD4^+$ T cells.

Angiogenesis

In A2a receptor-deficient mice, tumor angiogenesis was decreased, and the subsequent starvation of tumor cells ultimately caused their death [94, 119]. Similarly, A2b receptor activation in MDSCs induces VEGF secretion and angiogenesis. Global loss of CD39/CD73 or A2a/A2b receptors resulted in decreased VEGF and CD31 (also known as PECAM1) staining of tumor vessels in mouse models [120-123]. CD73 has pro-angiogenic effects through both enzymatic and non-enzymatic pathways, which was confirmed by reduced tumor levels of VEGF and suppressed tumor angiogenesis in a breast cancer mouse model after treatment with a monoclonal antibody targeting CD73 [120].

Tolerance

Inhibitory molecules and immune cell depletion

A2a receptor signaling of both effector and regulatory T cells triggers the upregulated expression of immune checkpoint molecules, including PD-1, CTLA-4, and LAG-3 [105, 120, 124, 125]. In addition, the tumor suppression induced by A2a receptor antagonism may function through $CD8^+$ T cells and the release of cytotoxic granules as well as FAS ligand ligation with the death receptor FAS (also known as CD95) of tumor cells [113, 119]. However, there are no relevant studies on the effects of adenosine on immune cells and tumor cell apoptosis in the TME. The overall mechanism network of adenosine acid is showed as below (Fig.2).

ROS

ROS are mainly present as by-products of the OXPHOS system or in specific enzymatic reactions (such as nicotinamide adenine dinucleotide phosphate oxidase and dual oxidase), which have two faces depending on their balance in the TME. Therefore, ROS homeostasis is rigorously regulated by antioxidative machinery comprising superoxide dismutase, catalase, and glutathione peroxidase. ROS are produced not only by tumor cells but also by cellular components that make up the TME. MDSCs are often a major source of ROS in TME. In addition to their release of oxidizing species, MDSC levels often arise in oxidative stress-prone environments, such as tumors. ROS and nitric oxide are responsible for multiple

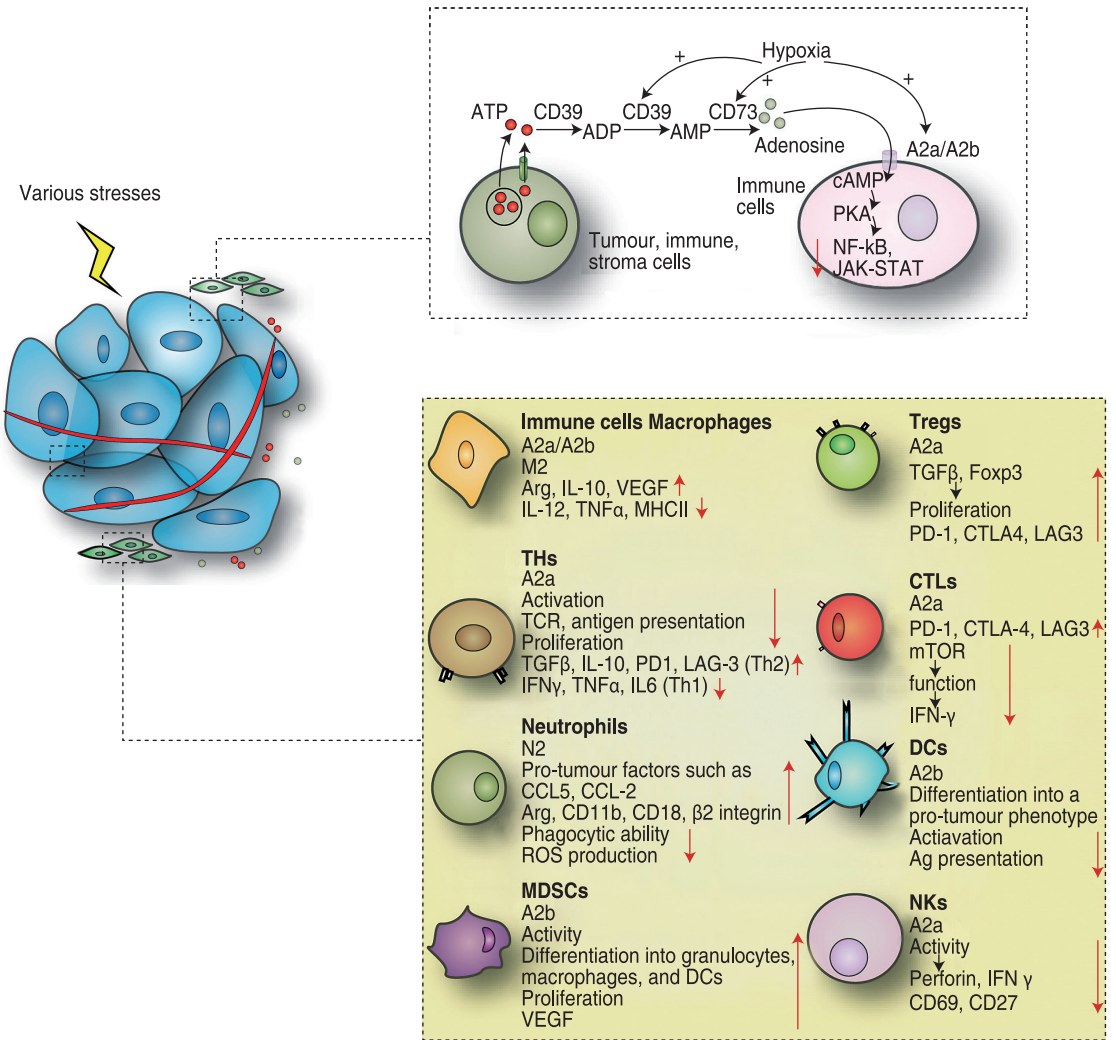

Fig. 2 The interaction between adenosine and tumour immune escape. Increased adenosine in responses to various stresses disrupts anti-tumour immunity through the A2a/A2b – cAMP – PKA pathway in many immune cells. The detailed influences can also conclude to differentiation, decreased tumour cytotoxicity, and increased immunosuppressive capacity

immune regulation responses related to tumor immune evasion; however, the differing effects on biological functions correspond to the amount of ROS. Although high levels of ROS can cause cytotoxic damage and cell death in tissues, as well as cause immune deregulation, their low cytostatic levels can have a proliferative effect that benefits tumor growth and the maintenance of biological processes. That is, ROS maximize the role of tumor promotion when ROS levels reach super-physiological or cytostatic levels, while avoiding too high levels to be conducive to cell death. Notably, ROS may be major stimulators of immunosuppression. Therefore, ROS are not only inducers of oxidative stress, but also mediators of immune regulation within the TME and are important in promoting tumorigenesis.

Immunogenicity

Presentation

In the context of cancer cells, the free oxygen radicals produced in the inflammatory TME can cause alterations in the cellular oxidative state as well as post-translational modifications of cysteine residues in proteins [126], which may alter antigenicity and contribute to T cell immunity. The redox status of antigens can modify the affinity of TCR for the antigenic peptide [127, 128]. Moreover, ROS-induced oxidative stress triggers the generation of upregulated antigenic peptides, which are counteracted by the limitation of their capacity to be loaded onto MHC molecules [129]. DCs impede antigen presentation due to chronic ER stress responses and cause oxidative damage to intracellular lipids because of excessive ROS [130, 131].

Recognition

Modest production of ROS by cancer cells can induce hypoxia [132], which can regulate T and NK cell immunity by modulating their activation through the expression of costimulatory (CD137 and OX-40) and coinhibitory (PD-L1) molecules [133]. In addition, senescent myeloma cells enhanced ligands (MICA, MICB, and PVR) to strengthen NK cell activation through NK cell activating receptors, such as natural killer group 2 member D (NKG2D) and DNAX accessory molecule-1 (DNAM1), both in an oxidant-dependent manner [39]. Moreover, upregulated gene expression of MICA and MICB was also observed in the CaCo-2 colon carcinoma cell line after oxidative stress [135], a phenomenon that could strengthen NK cell recognition and promote tumor cell elimination.

Immunosuppressive microenvironment

TILs all have decreased infiltration and cytotoxic activity [136] and embrace a differentiation skewing toward protumor type 2 as well as increased anergy [137] and apoptosis [138] in the context of ROS. ROS and oxidative stress in the TME help drive tumors to escape immunity, mainly through their effects on TILs. A high level of ROS in the TME inhibits T cell proliferation and antitumor function. Alternatively, low levels of ROS are required for T cells activation, proliferation, and function [139, 140]. ROS also affect the function of TILs, depending on the level of mROS. In renal clear cell carcinoma, $CD8^+$ TILs were present but with impaired function and metabolism. This effect was rescued by MitoQ and MitoTEMPO, both mROS scavengers, as evidenced by enhanced $CD8^+$ TILs activation [141]. Furthermore, ROS generated by other cells within the TME lead to T cell hyporesponsiveness in cancer patients [142]. The lipid raft-associated protein caveolin-1 (CAV-1) negatively regulates exosome internalization [143]. Studies have demonstrated a possible pathway by which tumor cells generate ROS, which signals to fibroblasts and causes the degradation of CAV-1, thereby increasing exosome influx. Zhao *et al*. suggested that exosomes isolated from prostate and pancreatic cancer-associated fibroblasts (CAFs) contain high amounts of lactate, glutamine, acetate, various amino acids, and many other metabolites, suggesting a potential role for exosomes in anaplerosis and lipogenesis [144]. The effect of increased exosome influx can lead to increased uptake of metabolites and metabolic reprogramming of fibroblasts to more tumorigenic CAFs, such as myofibroblasts [145, 146]. Macrophage-derived ROS affect Treg function [147]. When collaborating with large amounts of released ATP and adenosine, which are immunosuppressive, ROS and oxidative stress in the TME leads to more potent immunosuppression through Tregs [148].

Immune suppressive mediators

ROS-affected immunoregulatory factors in the TME play their role by influencing immune cell function, proliferation, and differentiation. TAMs amplify their infiltration and ROS production and promote Treg recruitment in the TME, which is ascribed to their proven high antioxidative capacity [45, 149]. And TAMs skew toward M2 is likely due to ROS-dependent TNF-α secretion [150]. TANs enhance ROS production and induce oxidative stress, which strengthens the suppression toward lymphocytes, such as inhibiting the proliferation of $IL17^+$ T cells [151] and restraining murine NK cell activity against tumor cells [152]. Tregs also exhibit increased accumulation and immunosuppression in the presence of ROS. Consistently, Kunisada *et al*. reported that metformin decreased the number of tumor-infiltrating Tregs by inhibiting the differentiation of naïve $CD4^+$ T cells into Tregs through Foxp3 protein [118]. Furthermore, metformin evokes metabolic reprogramming of Tregs toward a more glycolytic state [153]. Therefore, by reducing the levels of mROS with mitochondrial-targeted antioxidants, such as metformin, Tregs may become less immunosuppressive, allowing for an upregulated CTLs tumoricidal effect. Surrounded by ROS, MDSCs maintain their phenotype in the undifferentiated state [154, 155], have stronger immunosuppression abilities with attenuated recognition between TCR and MHC-peptide complex [156], exhaust arginine and cysteine, and generate peroxynitrite. Moreover, MDSCs also upregulate the ROS-producing enzyme COX-2 in T cells [157, 160], and through the produced ROS, tumor-induced MDSCs suppress T cell proliferation to promote colorectal cancer cell growth [123]. In support of these findings, the immunosuppressive effects of MDSCs on T cells was shown to be completely abrogated by ROS inhibitors [161, 162]. Finally, although high levels of ROS are immunosuppressive, a low level of ROS is important for T cells activation [163]. Low levels of ROS in CTLs have an anti-tumorigenic effect, but high levels of ROS in Tregs appear to be linked to reduced immunosuppression. ROS are required to induce a more locally invasive phenotype in TAMs isolated from melanoma, and this effect was regulated through ROS-dependent TNF-α secretion [164]. Taken together, this illustrates that the level of ROS within a certain cell type has different consequences for the function of that specific cell. Furthermore, similar levels of ROS can also have contradictory effects on various cell types. As shown previously, in $CD8^+$ TILs isolated from renal clear cell carcinoma, high levels of ROS resulted in impairment and even lack of antitumor response, while high levels of ROS in TILs in colon carcinoma from mice treated with anti-PD-1 blockade were related to increased tumoricidal effects.

Further research into how ROS within TILs and extracellular ROS involvement in modulating tumor

immunity will be needed to better characterize how different concentrations, types of ROS, and locations affect tumor immunity. Interestingly, healthy cells have evolved adequate adaptations to overcome the damaging protumor effects of ROS. Balanced production of ROS, sufficient antioxidant storage, and thorough cellular repair lead to low concentrations of ROS, resulting in limited tumor cell survival and proliferation. Maintenance of tumor cell metabolic activity results in high ROS levels, leading to DNA damage, genetic instability, and decreased cellular repair through functional DNA damage repair pathways. Elevated ROS levels can induce cellular damage, but tumor cells also readjust with sufficient adaptations, including hypoxia, as well as through initiation of an alternative cellular repair mechanism. Tumor cells express an elevated antioxidant capacity to remove excessive ROS while maintaining protumorigenic signaling. However, if ROS concentrations increase dramatically and approach toxic ROS levels, for example, by employing ROS-inducing agents such as chemotherapy, the resulting oxidative stress causes irreparable damage, inadequate adaptation, and eventual tumor cell death.

Angiogenesis

ROS derived from NOX and mitochondria play a pivotal role in the angiogenic transition from quiescent endothelial cells (ECs). In adults, ROS are augmented in response to growth factors (such as VEGF), ischemia, and wound injury, which promote the angiogenic switch in ECs. Excess ROS contribute to pathological angiogenesis in cancer. Exogenous ROS increase VEGF and VEGFR2 expression levels [165] and stimulates ECs proliferation and migration [166, 167]. Interestingly, VEGF-induced ROS determine VEGFR2 tyrosine phosphorylation, which is a prerequisite for ECs migration and proliferation through stimulation of small GTPase ARF6 residing in caveolae/lipid rafts in ECs [168]. Furthermore, ROS-mediated redox signaling associated with angiogenesis involves MAPKs, PI3 kinase, JAK-STAT, Akt, protein tyrosine phosphatases (PTPs) such as PTP1B, SH2-containing protein tyrosine phosphatase 2, phosphatase, and tensin homolog, as well as transcription factors, including HIF-1, AP-1, and NF-kB. Mitochondria function as an O_2 sensor that transmits a hypoxic signal by releasing ROS to the cytosol [169]. Hypoxia stimulates mROS production from mitochondrial complex III, and the mROS trigger HIF-1α stabilization [167-172], which enhances the transcription of angiogenic genes such as VEGF [172].

Tolerance

Inhibitory molecules

Although no direct and specific relationship has yet been deduced between elevation or reduction of ROS production and regulation of coinhibitory PD-L1 expression, ROS have been shown to affect the expression of PD-L1 in cancer cells in vitro [173]. Lower levels of global ROS as well as hypoxia in the TME coupled with increased intracellular mROS in specific tumor-infiltrating cells may induce the most efficacious reaction to PD-1 blockade [141, 174].

Tumor cell depletion

One of the most crucial advances in cancer research in recent years has been the recognition that tumor cell death, mostly through apoptosis, is strongly linked to the regulation of tumor formation and the critical determination of treatment efficacy. Therefore, we believe that avoiding effector immune cell-induced apoptosis can also be attributed to the manner in which tumor cells evade antitumor immunity. The killing of tumor cells, as in most anticancer strategies currently used in clinical oncology, is linked to the intrinsic (intrinsic apoptotic signal in the mitochondria) or extrinsic (extrinsic apoptotic signal by death receptors) pathway of activation of apoptosis signal transduction in cancer cells. Thus, successful apoptosis may result in reduced resistance to treatment. Binding of the TNF-α ligand to the death receptor TNFR1 induces the stimulation of initiator caspase 8, leading to the cleavage of caspase 3 [175]. Caspase 8 activation also triggers the cleavage of Bid to tBid, resulting in the release of cytochrome C in an intrinsic apoptotic pathway [176]. Toxic levels of ROS damage the mitochondrial membrane, causing the release and translocation of cytochrome C into the cytoplasm. Then, by binding with Apaf-1 and pro-caspase 9, cytochrome C forms a complex that induces the cleavage of caspase 3 and caspase 7, which finally results in apoptosis [177]. The overall mechanism network of ROS is showed as below (Fig. 3).

Conclusions

This review emphasizes that a deeper understanding of the effects of tumor metabolism and metabolite on tumors may advance the frontier of immunotherapeutic approaches. The specific focus of this work was on the three well studied end-metabolites and their roles in tumor immune escape. These end-metabolites impact the immune responses from antigen presentation and antigen recognition, to the activation, proliferation, and function of effector cells, and they are effective from the very early stages of tumor formation to local invasion and distant metastasis. Other non-immune cell activities and

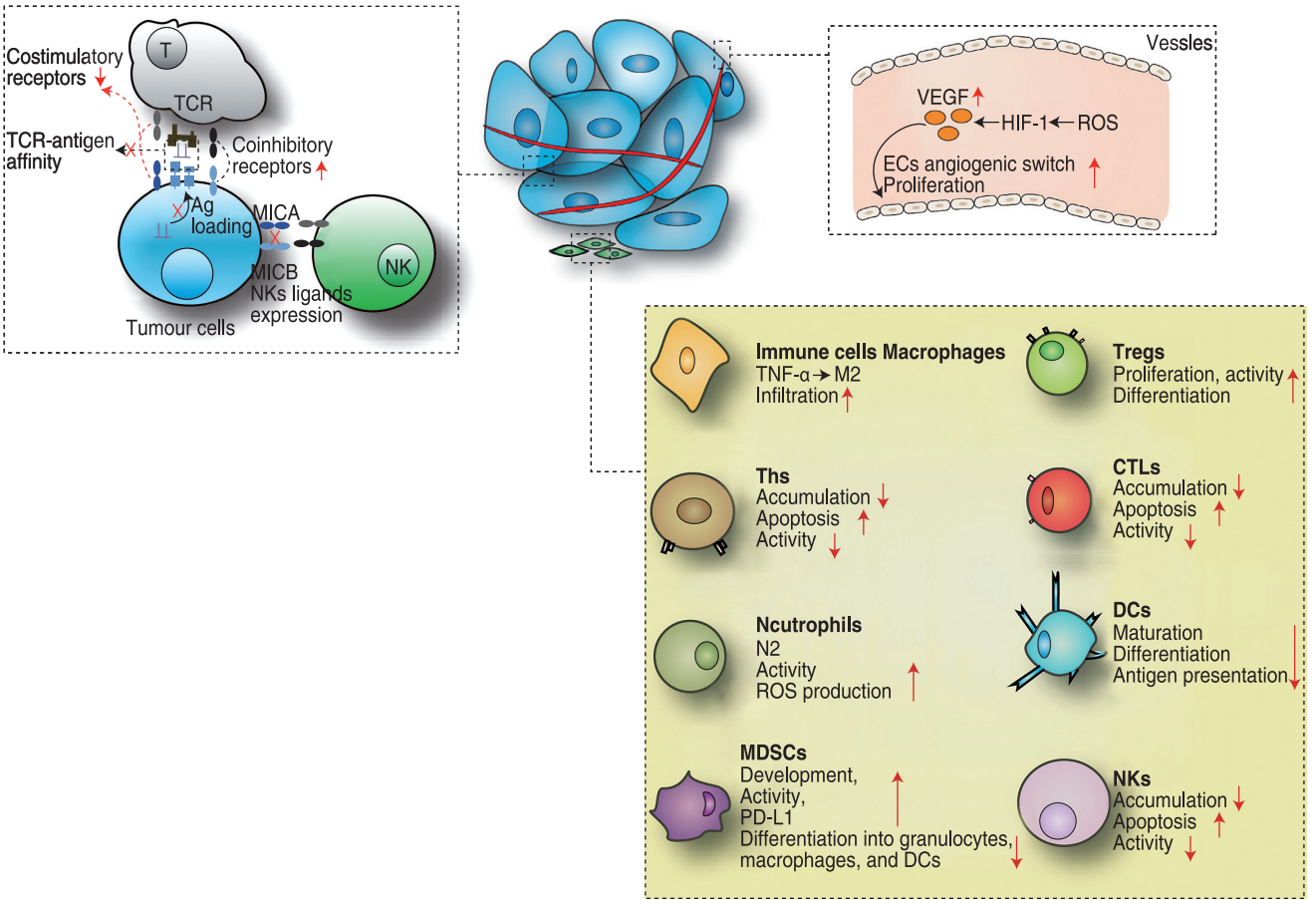

Fig. 3 The interaction between ROS and tumour immune escape. ROS impedes immunological surveillance and immune clearance by weakening the activation of tumour killer cells. Besides, ROS has the same infection on immune cells and angiogenesis as lactate acid

angiogenesis in the TME also changed in response to these metabolites. Regarding the overall interaction, there are many potential drug targets, some of which have been discovered, and corresponding drugs have been designed, which are undergoing animal or clinical trials. Some targets need to be evaluated further. However, it is not yet clear whether these three end-metabolites promote other immune escape mechanisms found in some tumors, such as (1) the silencing, loss, or mutation of related fragments in the tumor cell genome and epigenetic modifications such as RNA interference that inhibit antigen transcription and antigen presentation or promote antigen degradation; (2) the decrease of the release of tumor danger signals by tumor cells through MerTK-dependent cell burial; (3) the production of miR-214 by tumor cells, which is injected into nearby T cells through microbubbles, mediating the expansion of Tregs and causing immunosuppression; and (4) the independent production of mitotic signals and growth factors by tumor cells, which increases genetic instability to accelerate evolution and fast adaptation to the immune environment. Other end-metabolites, such as NO, bile acids, bilirubin, and uric acid, also require further exploration to assess their association with the tumor immune escape. An in-depth understanding of how tumors evade immune surveillance fueled by these end-metabolites will help researchers elucidate the essence of tumor occurrence and development as well as develop more effective therapeutic strategies.

Acknowledgments

Not applicable.

Funding

Not applicable.

Conflicts of interest

The authors indicated no potential conflicts of interest.

Author contributions

Not applicable.

Data availability statement

Not applicable.

References

1. Cairns RA, Harris IS, Mak TW. Regulation of cancer cell metabolism. Nat Rev Cancer. 2011;11(2):85-95.
2. Warburg O, Wind F, Negelein E. The metabolism of tumors in the body. J Gen Physiol. 1927;8(6):519-530.
3. Eltzschig HK. Extracellular adenosine signaling in molecular medicine. J Mol Med (Berl). 2013;91(2):141-146.
4. Hegedűs C, Kovács K, Polgár Z, et al. Redox control of cancer cell destruction. Redox Biol. 2018;16:59-74.
5. Anderson NM, Simon MC. The tumor microenvironment. Curr Biol. 2020 Aug 17;30(16):R921-R925.
6. Hanahan D, Weinberg RA. Hallmarks of cancer: the next generation. Cell. 2011;144(5):646-674.
7. Cives M, Strosberg J, Al Diffalha S, et al. Analysis of the immune landscape of small bowel neuroendocrine tumors. Endocr Relat Cancer. 2019;26(1):119-130.
8. Beatty GL, Gladney WL. Immune escape mechanisms as a guide for cancer immunotherapy. Clin Cancer Res. 2015;21(4):687-692.
9. Vinay DS, Ryan EP, Pawelec G, et al. Immune evasion in cancer: Mechanistic basis and therapeutic strategies. Semin Cancer Biol. 2015;35 Suppl:S185-S198.
10. Hornsveld M, Dansen TB. The hallmarks of cancer from a redox perspective. Antioxid Redox Signal. 2016;25(6):300-325.
11. Vasievich EA, Huang L. The suppressive tumor microenvironment: a challenge in cancer immunotherapy. Mol Pharm. 2011;8(3):635-641.
12. Goveia J, Pircher A, Conradi LC, et al. Meta-analysis of clinical metabolic profiling studies in cancer: challenges and opportunities. EMBO Mol Med. 2016;8(10):1134-1142.
13. Reznik E, Luna A, Aksoy BA, et al. A landscape of metabolic variation across tumor types. Cell Syst. 2018;6(3):301-313.e3.
14. Gottfried E, Kunz-Schughart LA, Ebner S, et al. Tumor-derived lactic acid modulates dendritic cell activation and antigen expression. Blood. 2006;107(5):2013-2021.
15. Stryhn A, Pedersen LO, Romme T, et al. pH dependence of MHC class I-restricted peptide presentation. J Immunol. 1996;156(11):4191-4197.
16. Constant JS, Feng JJ, Zabel DD, et al. Lactate elicits vascular endothelial growth factor from macrophages: a possible alternative to hypoxia. Wound Repair Regen. 2000;8(5):353-360.
17. Persi E, Duran-Frigola M, Damaghi M, et al. Systems analysis of intracellular pH vulnerabilities for cancer therapy. Nat Commun. 2018;9(1):2997.
18. Fischer K, Hoffmann P, Voelkl S, et al. Inhibitory effect of tumor cell-derived lactic acid on human T cells. Blood. 2007;109(9):3812-3819.
19. Rahma OE, Hodi FS. The intersection between tumor angiogenesis and immune suppression. Clin Cancer Res. 2019;25(18):5449-5457.
20. Vallée A, Guillevin R, Vallée JN. Vasculogenesis and angiogenesis initiation under normoxic conditions through Wnt/β-catenin pathway in gliomas. Rev Neurosci. 2018;29(1):71-91.
21. Blankenstein T, Coulie PG, Gilboa E, et al. The determinants of tumour immunogenicity. Nat Rev Cancer. 2012;12(4):307-313.
22. Burgdorf S, Porubsky S, Marx A, et al. Cancer acidity and hypertonicity contribute to dysfunction of tumor-associated dendritic cells: Potential impact on antigen cross-presentation machinery. Cancers (Basel). 2020;12(9):2403.
23. Romero-Garcia S, Moreno-Altamirano MM, Prado-Garcia H, et al. Lactate contribution to the tumor microenvironment: mechanisms, effects on immune cells and therapeutic relevance. Front Immunol. 2016;7:52.
24. Calcinotto A, Filipazzi P, Grioni M, et al. Modulation of microenvironment acidity reverses anergy in human and murine tumor-infiltrating T lymphocytes. Cancer Res. 2012;72(11):2746-2756.
25. Wen J, Cheng S, Zhang Y, et al. Lactate anions participate in T cell cytokine production and function. Sci China Life Sci. 2021;64(11):1895-1905.
26. Brand A, Singer K, Koehl GE, et al. LDHA-associated lactic acid production blunts tumor immunosurveillance by T and NK cells. Cell Metab. 2016;24(5):657-671.
27. Daneshmandi S, Wegiel B, Seth P. Blockade of lactate dehydrogenase-A (LDH-A) improves efficacy of anti-programmed cell death-1 (PD-1) therapy in melanoma. Cancers (Basel). 2019;11(4):450.
28. Ohm JE, Carbone DP. VEGF as a mediator of tumor-associated immunodeficiency. Immunol Res. 2001;23(2-3):263-72.
29. Voron T, Colussi O, Marcheteau E, et al. VEGF-A modulates expression of inhibitory checkpoints on CD8+ T cells in tumors. J Exp Med. 2015;212(2):139-148.
30. Xie D, Zhu S, Bai L. Lactic acid in tumor microenvironments causes dysfunction of NKT cells by interfering with mTOR signaling. Sci China Life Sci. 2016;59(12):1290-1296.
31. Gerriets VA, Kishton RJ, Nichols AG, et al. Metabolic programming and PDHK1 control CD4+ T cell subsets and inflammation. J Clin Invest. 2015;125(1):194-207.
32. Michalek RD, Gerriets VA, Jacobs SR, et al. Cutting edge: distinct glycolytic and lipid oxidative metabolic programs are essential for effector and regulatory CD4+ T cell subsets. J Immunol. 2011;186(6):3299-3303.
33. Watson MJ, Vignali PDA, Mullett SJ, et al. Metabolic support of tumour-infiltrating regulatory T cells by lactic acid. Nature. 2021;591(7851):645-651.
34. Angelin A, Gil-de-Gómez L, Dahiya S, et al. Foxp3 reprograms T cell metabolism to function in low-glucose, high-lactate environments. Cell Metab. 2017;25(6):1282-1293.e7.
35. Nakamura T, Shima T, Saeki A, et al. Expression of indoleamine 2, 3-dioxygenase and the recruitment of Foxp3-expressing regulatory T cells in the development and progression of uterine cervical cancer. Cancer Sci. 2007;98(6):874-881.
36. Sharma MD, Shinde R, McGaha TL, et al. The PTEN pathway in Tregs is a critical driver of the suppressive tumor microenvironment. Sci Adv. 2015;1(10):e1500845.
37. Galliher AJ, Neil JR, Schiemann WP. Role of transforming growth factor-beta in cancer progression. Future Oncol. 2006;2(6):743-763.
38. Klein SC, Jücker M, Abts H, et al. IL6 and IL6 receptor expression in Burkitt's lymphoma and lymphoblastoid cell lines: promotion of IL6 receptor expression by EBV. Hematol Oncol. 1995;13(3):121-130.
39. Lin EY, Gouon-Evans V, Nguyen AV, et al. The macrophage growth factor CSF-1 in mammary gland development and tumor progression. J Mammary Gland Biol Neoplasia. 2002;7(2):147-162.
40. Lind MH, Rozell B, Wallin RP, et al. Tumor necrosis factor receptor 1-mediated signaling is required for skin cancer development induced by NF-kappaB inhibition. Proc Natl Acad Sci U S A. 2004;101(14):4972-4977.
41. Matsuda M, Salazar F, Petersson M, et al. Interleukin 10 pretreatment protects target cells from tumor- and allo-specific cytotoxic T cells and downregulates HLA class I expression. J Exp Med. 1994;180(6):2371-2376.
42. Sotomayor EM, Fu YX, Lopez-Cepero M, et al. Role of tumor-derived cytokines on the immune system of mice bearing a mammary

adenocarcinoma. II. Down-regulation of macrophage-mediated cytotoxicity by tumor-derived granulocyte-macrophage colony-stimulating factor. J Immunol. 1991;147(8):2816-2823.
43. Wu L, Saxena S, Awaji M, et al. Tumor-associated neutrophils in cancer: going pro. Cancers (Basel). 2019;11(4):564.
44. Husain Z, Huang Y, Seth P, et al. Tumor-derived lactate modifies antitumor immune response: effect on myeloid-derived suppressor cells and NK cells. J Immunol. 2013;191(3):1486-1495.
45. Mougiakakos D, Johansson CC, Kiessling R. Naturally occurring regulatory T cells show reduced sensitivity toward oxidative stress-induced cell death. Blood. 2009;113(15):3542-3545.
46. Groth C, Hu X, Weber R, et al. Immunosuppression mediated by myeloid-derived suppressor cells (MDSCs) during tumour progression. Br J Cancer. 2019;120(1):16-25.
47. Monti M, Vescovi R, Consoli F, et al. Plasmacytoid dendritic cell impairment in metastatic melanoma by lactic acidosis. Cancers (Basel). 2020;12(8):2085.
48. Long Y, Gao Z, Hu X, et al. Downregulation of MCT4 for lactate exchange promotes the cytotoxicity of NK cells in breast carcinoma. Cancer Med. 2018;7(9):4690-4700.
49. Andrejeva G, Rathmell JC. Similarities and distinctions of cancer and immune metabolism in inflammation and tumors. Cell Metab. 2017;26(1):49-70.
50. Liao ZX, Fa YC, Kempson IM, et al. Repolarization of M2 to M1 macrophages triggered by lactate oxidase released from methylcellulose hydrogel. Bioconjug Chem. 2019;30(10):2697-2702.
51. Mu X, Shi W, Xu Y, et al. Tumor-derived lactate induces M2 macrophage polarization via the activation of the ERK/STAT3 signaling pathway in breast cancer. Cell Cycle. 2018;17(4):428-438.
52. Colegio OR, Chu NQ, Szabo AL, et al. Functional polarization of tumour-associated macrophages by tumour-derived lactic acid. Nature. 2014;513(7519):559-563.
53. El-Kenawi A, Gatenbee C, Robertson-Tessi M, et al. Acidity promotes tumour progression by altering macrophage phenotype in prostate cancer. Br J Cancer. 2019;121(7):556-566.
54. Lin S, Sun L, Lyu X, et al. Lactate-activated macrophages induced aerobic glycolysis and epithelial-mesenchymal transition in breast cancer by regulation of CCL5-CCR5 axis: a positive metabolic feedback loop. Oncotarget. 2017;8(66):110426-110443.
55. Shan T, Chen S, Chen X, et al. M2-TAM subsets altered by lactic acid promote T-cell apoptosis through the PD-L1/PD-1 pathway. Oncol Rep. 2020;44(5):1885-1894.
56. Driessens G, Kline J, Gajewski TF. Costimulatory and coinhibitory receptors in anti-tumor immunity. Immunol Rev. 2009;229(1):126-144.
57. Nasi A, Fekete T, Krishnamurthy A, et al. Dendritic cell reprogramming by endogenously produced lactic acid. J Immunol. 2013;191(6):3090-3099.
58. Gabrilovich DI, Chen HL, Girgis KR, et al. Production of vascular endothelial growth factor by human tumors inhibits the functional maturation of dendritic cells. Nat Med. 1996;2(10):1096-1103.
59. Zhang D, Tang Z, Huang H, et al. Metabolic regulation of gene expression by histone lactylation. Nature. 2019;574(7779):575-580.
60. Oyama T, Ran S, Ishida T, et al. Vascular endothelial growth factor affects dendritic cell maturation through the inhibition of nuclear factor-kappa B activation in hemopoietic progenitor cells. J Immunol. 1998;160(3):1224-1232.
61. Ohm JE, Gabrilovich DI, Sempowski GD, et al. VEGF inhibits T-cell development and may contribute to tumor-induced immune suppression. Blood. 2003;101(12):4878-4886.
62. Curiel TJ, Wei S, Dong H, et al. Blockade of B7-H1 improves myeloid dendritic cell-mediated antitumor immunity. Nat Med. 2003;9(5):562-567.
63. Condamine T, Ramachandran I, Youn JI, et al. Regulation of tumor metastasis by myeloid-derived suppressor cells. Annu Rev Med. 2015;66:97-110.
64. Damgaci S, Ibrahim-Hashim A, Enriquez-Navas PM, et al. Hypoxia and acidosis: immune suppressors and therapeutic targets. Immunology. 2018;154(3):354-362.
65. Feichtinger RG, Lang R. Targeting L-Lactate metabolism to overcome resistance to immune therapy of melanoma and other tumor entities. J Oncol. 2019;2019:2084195.
66. Feng J, Yang H, Zhang Y, et al. Tumor cell-derived lactate induces TAZ-dependent upregulation of PD-L1 through GPR81 in human lung cancer cells. Oncogene. 2017;36(42):5829-5839.
67. Lee YJ, Shin KJ, Park SA, et al. G-protein-coupled receptor 81 promotes a malignant phenotype in breast cancer through angiogenic factor secretion. Oncotarget. 2016;7(43):70898-70911.
68. Wagner W, Kania KD, Blauz A, et al. The lactate receptor (HCAR1/GPR81) contributes to doxorubicin chemoresistance via ABCB1 transporter up-regulation in human cervical cancer HeLa cells. J Physiol Pharmacol. 2017;68(4):555-564.
69. Brown TP, Bhattacharjee P, Ramachandran S, et al. The lactate receptor GPR81 promotes breast cancer growth via a paracrine mechanism involving antigen-presenting cells in the tumor microenvironment. Oncogene. 2020;39(16):3292-3304.
70. Ranganathan P, Shanmugam A, Swafford D, et al. GPR81, a cell-surface receptor for lactate, regulates intestinal homeostasis and protects mice from experimental colitis. J Immunol. 2018;200(5):1781-1789.
71. de Azevedo RA, Shoshan E, Whang S, et al. MIF inhibition as a strategy for overcoming resistance to immune checkpoint blockade therapy in melanoma. Oncoimmunology. 2020;9(1):1846915.
72. Tanaka A, Sakaguchi S. Regulatory T cells in cancer immunotherapy. Cell Res. 2017;27(1):109-118.
73. Harmon C, Robinson MW, Hand F, et al. Lactate-mediated acidification of tumor microenvironment induces apoptosis of liver-resident NK cells in colorectal liver metastasis. Cancer Immunol Res. 2019;7(2):335-346.
74. Cao S, Liu P, Zhu H, et al. Extracellular acidification acts as a key modulator of neutrophil apoptosis and functions. PLoS One. 2015;10(9):e0137221.
75. Pucino V, Certo M, Bulusu V, et al. Lactate Buildup at the Site of Chronic Inflammation Promotes Disease by Inducing CD4+ T Cell Metabolic Rewiring. Cell Metab. 2019;30(6):1055-1074.e8.
76. Sonveaux P, Végran F, Schroeder T, et al. Targeting lactate-fueled respiration selectively kills hypoxic tumor cells in mice. J Clin Invest. 2008;118(12):3930-3942.
77. Faubert B, Li KY, Cai L, et al. Lactate Metabolism in Human Lung Tumors. Cell. 2017;171(2):358-371.e9.
78. Hensley CT, Faubert B, Yuan Q, et al. Metabolic heterogeneity in human lung tumors. Cell. 2016;164(4):681-694.
79. Hui S, Ghergurovich JM, Morscher RJ, et al. Glucose feeds the TCA cycle via circulating lactate. Nature. 2017;551(7678):115-118.
80. Coffelt SB, Chen YY, Muthana M, et al. Angiopoietin 2 stimulates TIE2-expressing monocytes to suppress T cell activation and to promote regulatory T cell expansion. J Immunol. 2011;186(7):4183-4190.
81. Coffelt SB, Tal AO, Scholz A, et al. Angiopoietin-2 regulates gene expression in TIE2-expressing monocytes and augments their

inherent proangiogenic functions. Cancer Res. 2010;70(13):5270-5280.
82. Billard C. Apoptosis inducers in chronic lymphocytic leukemia. Oncotarget. 2014;5(2):309-325.
83. Urbańska K, Orzechowski A. Unappreciated role of LDHA and LDHB to control apoptosis and autophagy in tumor cells. Int J Mol Sci. 2019;20(9):2085.
84. Allard B, Longhi MS, Robson SC, et al. The ectonucleotidases CD39 and CD73: Novel checkpoint inhibitor targets. Immunol Rev. 2017;276(1):121-144.
85. Allard B, Beavis PA, Darcy PK, Stagg J. Immunosuppressive activities of adenosine in cancer. Curr Opin Pharmacol. 2016;29:7-16.
86. Umansky V, Abschuetz O, Osen W, et al. Melanoma-specific memory T cells are functionally active in Ret transgenic mice without macroscopic tumors. Cancer Res. 2008;68(22):9451-9458.
87. Sitkovsky MV, Hatfield S, Abbott R, et al. Hostile, hypoxia-A2-adenosinergic tumor biology as the next barrier to overcome for tumor immunologists. Cancer Immunol Res. 2014;2(7):598-605.
88. Chen JF, Eltzschig HK, Fredholm BB. Adenosine receptors as drug targets–what are the challenges? Nat Rev Drug Discov. 2013;12(4):265-286.
89. Ohta A, Sitkovsky M. Role of G-protein-coupled adenosine receptors in downregulation of inflammation and protection from tissue damage. Nature. 2001;414(6866):916-920.
90. Häusler SF, Del Barrio IM, Diessner J, et al. Anti-CD39 and anti-CD73 antibodies A1 and 7G2 improve targeted therapy in ovarian cancer by blocking adenosine-dependent immune evasion. Am J Transl Res. 2014;6(2):129-139.
91. Häusler SF, Montalbán del Barrio I, Strohschein J, et al. Ectonucleotidases CD39 and CD73 on OvCA cells are potent adenosine-generating enzymes responsible for adenosine receptor 2A-dependent suppression of T cell function and NK cell cytotoxicity. Cancer Immunol Immunother. 2011;60(10):1405-1418.
92. Loi S, Pommey S, Haibe-Kains B, et al. CD73 promotes anthracycline resistance and poor prognosis in triple negative breast cancer. Proc Natl Acad Sci U S A. 2013;110(27):11091-11096.
93. Lokshin A, Raskovalova T, Huang X, et al. Adenosine-mediated inhibition of the cytotoxic activity and cytokine production by activated natural killer cells. Cancer Res. 2006;66(15):7758-7765.
94. Ohta A, Gorelik E, Prasad SJ, et al. A2A adenosine receptor protects tumors from antitumor T cells. Proc Natl Acad Sci U S A. 2006;103(35):13132-13137.
95. Stagg J, Beavis PA, Divisekera U, et al. CD73-deficient mice are resistant to carcinogenesis. Cancer Res. 2012;72(9):2190-2196.
96. Wang L, Fan J, Thompson LF, et al. CD73 has distinct roles in nonhematopoietic and hematopoietic cells to promote tumor growth in mice. J Clin Invest. 2011;121(6):2371-2382.
97. Palmer TM, Trevethick MA. Suppression of inflammatory and immune responses by the A(2A) adenosine receptor: an introduction. Br J Pharmacol. 2008;153 Suppl 1(Suppl 1):S27-34.
98. Zarek PE, Huang CT, Lutz ER, et al. A2A receptor signaling promotes peripheral tolerance by inducing T-cell anergy and the generation of adaptive regulatory T cells. Blood. 2008;111(1):251-259.
99. Cekic C, Day YJ, Sag D, et al. Myeloid expression of adenosine A2A receptor suppresses T and NK cell responses in the solid tumor microenvironment. Cancer Res. 2014;74(24):7250-7259.
100. Romio M, Reinbeck B, Bongardt S, et al. Extracellular purine metabolism and signaling of CD73-derived adenosine in murine Treg and Teff cells. Am J Physiol Cell Physiol. 2011;301(2):C530-C539.
101. Novitskiy SV, Ryzhov S, Zaynagetdinov R, et al. Adenosine receptors in regulation of dendritic cell differentiation and function. Blood. 2008;112(5):1822-1831.
102. Cekic C, Sag D, Li Y, et al. Adenosine A2B receptor blockade slows growth of bladder and breast tumors. J Immunol. 2012;188(1):198-205.
103. Linnemann C, Schildberg FA, Schurich A, et al. Adenosine regulates CD8 T-cell priming by inhibition of membrane-proximal T-cell receptor signalling. Immunology. 2009;128(1 Suppl):e728-e737.
104. Vang T, Torgersen KM, Sundvold V, et al. Activation of the COOH-terminal Src kinase (Csk) by cAMP-dependent protein kinase inhibits signaling through the T cell receptor. J Exp Med. 2001;193(4):497-507.
105. Cekic C, Linden J. Purinergic regulation of the immune system. Nat Rev Immunol. 2016;16(3):177-192.
106. Butler JJ, Mader JS, Watson CL, et al. Adenosine inhibits activation-induced T cell expression of CD2 and CD28 co-stimulatory molecules: role of interleukin-2 and cyclic AMP signaling pathways. J Cell Biochem. 2003;89(5):975-991.
107. Ryzhov S, Novitskiy SV, Goldstein AE, et al. Adenosinergic regulation of the expansion and immunosuppressive activity of CD11b+Gr1+ cells. J Immunol. 2011;187(11):6120-6129.
108. Ohta A, Madasu M, Subramanian M, et al. Hypoxia-induced and A2A adenosine receptor-independent T-cell suppression is short lived and easily reversible. Int Immunol. 2014;26(2):83-91.
109. Deaglio S, Dwyer KM, Gao W, et al. Adenosine generation catalyzed by CD39 and CD73 expressed on regulatory T cells mediates immune suppression. J Exp Med. 2007;204(6):1257-1265.
110. Kinsey GR, Huang L, Jaworska K, et al. Autocrine adenosine signaling promotes regulatory T cell-mediated renal protection. J Am Soc Nephrol. 2012;23(9):1528-1537.
111. Ohta A, Kini R, Ohta A, et al. The development and immunosuppressive functions of CD4(+) CD25(+) FoxP3(+) regulatory T cells are under influence of the adenosine-A2A adenosine receptor pathway. Front Immunol. 2012;3:190.
112. Bao R, Hou J, Li Y, et al. Adenosine promotes Foxp3 expression in Treg cells in sepsis model by activating JNK/AP-1 pathway. Am J Transl Res. 2016;8(5):2284-2292.
113. Beavis PA, Divisekera U, Paget C, et al. Blockade of A2A receptors potently suppresses the metastasis of CD73+ tumors. Proc Natl Acad Sci U S A. 2013;110(36):14711-14716.
114. Mittal D, Young A, Stannard K, et al. Antimetastatic effects of blocking PD-1 and the adenosine A2A receptor. Cancer Res. 2014;74(14):3652-3658.
115. Mastelic-Gavillet B, Navarro Rodrigo B, Décombaz L, et al. Adenosine mediates functional and metabolic suppression of peripheral and tumor-infiltrating CD8+ T cells. J Immunother Cancer. 2019;7(1):257.
116. Abbott RK, Silva M, Labuda J, et al. The GS Protein-coupled A2a Adenosine Receptor Controls T Cell Help in the Germinal Center. J Biol Chem. 2017;292(4):1211-1217.
117. Chrobak P, Charlebois R, Rejtar P, et al. CD73 plays a protective role in collagen-induced arthritis. J Immunol. 2015;194(6):2487-2492.
118. Ryzhov SV, Pickup MW, Chytil A, et al. Role of TGF-β signaling in generation of CD39+CD73+ myeloid cells in tumors. J Immunol. 2014;193(6):3155-3164.
119. Sitkovsky MV, Kjaergaard J, Lukashev D, et al. Hypoxia-adenosinergic immunosuppression: tumor protection by T regulatory cells and cancerous tissue hypoxia. Clin Cancer Res. 2008;14(19):5947-5952.
120. Allard B, Turcotte M, Spring K, et al. Anti-CD73 therapy impairs tumor angiogenesis. Int J Cancer. 2014;134(6):1466-1473.
121. Feng L, Sun X, Csizmadia E, et al. Vascular CD39/ENTPD1 directly

promotes tumor cell growth by scavenging extracellular adenosine triphosphate. Neoplasia. 2011;13(3):206-216.
122. Jackson SW, Hoshi T, Wu Y, et al. Disordered purinergic signaling inhibits pathological angiogenesis in cd39/Entpd1-null mice. Am J Pathol. 2007;171(4):1395-1404.
123. Ryzhov S, Novitskiy SV, Zaynagetdinov R, et al. Host A(2B) adenosine receptors promote carcinoma growth. Neoplasia. 2008;10(9):987-995.
124. Allard D, Turcotte M, Stagg J. Targeting A2 adenosine receptors in cancer. Immunol Cell Biol. 2017;95(4):333-339.
125. Ohta A. A Metabolic immune checkpoint: adenosine in tumor microenvironment. Front Immunol. 2016;7:109.
126. Martínez-Cayuela M. Oxygen free radicals and human disease. Biochimie. 1995;77(3):147-161.
127. Trujillo JA, Croft NP, Dudek NL, et al. The cellular redox environment alters antigen presentation. J Biol Chem. 2014;289(40):27979-27991.
128. Weiskopf D, Schwanninger A, Weinberger B, et al. Oxidative stress can alter the antigenicity of immunodominant peptides. J Leukoc Biol. 2010;87(1):165-172.
129. Preynat-Seauve O, Coudurier S, Favier A, et al. Oxidative stress impairs intracellular events involved in antigen processing and presentation to T cells. Cell Stress Chaperones. 2003;8(2):162-171.
130. Cubillos-Ruiz JR, Silberman PC, Rutkowski MR, Chopra S, Perales-Puchalt A, Song M, Zhang S, Bettigole SE, Gupta D, Holcomb K, Ellenson LH, Caputo T, Lee AH, Conejo-Garcia JR, Glimcher LH. ER Stress Sensor XBP1 Controls Anti-tumor Immunity by Disrupting Dendritic Cell Homeostasis. Cell. 2015;161(7):1527-1538.
131. Veglia F, Tyurin VA, Mohammadyani D, et al. Lipid bodies containing oxidatively truncated lipids block antigen cross-presentation by dendritic cells in cancer. Nat Commun. 2017;8(1):2122.
132. Farhood B, Najafi M, Salehi E, et al. Disruption of the redox balance with either oxidative or anti-oxidative overloading as a promising target for cancer therapy. J Cell Biochem. 2019;120(1):71-76.
133. Labiano S, Palazon A, Melero I. Immune response regulation in the tumor microenvironment by hypoxia. Semin Oncol. 2015;42(3):378-386.
134. Soriani A, Iannitto ML, Ricci B, et al. Reactive oxygen species- and DNA damage response-dependent NK cell activating ligand upregulation occurs at transcriptional levels and requires the transcriptional factor E2F1. J Immunol. 2014;193(2):950-960.
135. Yamamoto K, Fujiyama Y, Andoh A, et al. Oxidative stress increases MICA and MICB gene expression in the human colon carcinoma cell line (CaCo-2). Biochim Biophys Acta. 2001;1526(1):10-12.
136. Scharping NE, Menk AV, Moreci RS, et al. The tumor microenvironment represses T cell mitochondrial biogenesis to drive intratumoral T cell metabolic insufficiency and dysfunction. Immunity. 2016;45(3):701-703.
137. Ligtenberg MA, Mougiakakos D, Mukhopadhyay M, et al. Coexpressed catalase protects chimeric antigen receptor-redirected T cells as well as bystander cells from oxidative stress-induced loss of antitumor activity. J Immunol. 2016;196(2):759-766.
138. Izawa S, Kono K, Mimura K, et al. H_2O_2 production within tumor microenvironment inversely correlated with infiltration of CD56(dim) NK cells in gastric and esophageal cancer: possible mechanisms of NK cell dysfunction. Cancer Immunol Immunother. 2011;60(12):1801-1810.
139. Devadas S, Zaritskaya L, Rhee SG, et al. Discrete generation of superoxide and hydrogen peroxide by T cell receptor stimulation: selective regulation of mitogen-activated protein kinase activation and fas ligand expression. J Exp Med. 2002;195(1):59-70.
140. Jackson SH, Devadas S, Kwon J, et al. T cells express a phagocyte-type NADPH oxidase that is activated after T cell receptor stimulation. Nat Immunol. 2004;5(8):818-827.
141. Siska PJ, Beckermann KE, Mason FM, et al. Mitochondrial dysregulation and glycolytic insufficiency functionally impair CD8 T cells infiltrating human renal cell carcinoma. JCI Insight. 2017;2(12):e93411.
142. Cemerski S, Cantagrel A, Van Meerwijk JP, et al. Reactive oxygen species differentially affect T cell receptor-signaling pathways. J Biol Chem. 2002;277(22):19585-19593.
143. Svensson KJ, Christianson HC, Wittrup A, et al. Exosome uptake depends on ERK1/2-heat shock protein 27 signaling and lipid Raft-mediated endocytosis negatively regulated by caveolin-1. J Biol Chem. 2013;288(24):17713-17724.
144. Zhao H, Yang L, Baddour J, et al. Tumor microenvironment derived exosomes pleiotropically modulate cancer cell metabolism. Elife. 2016;5:e10250.
145. Martinez-Outschoorn UE, Balliet RM, Rivadeneira DB, et al. Oxidative stress in cancer associated fibroblasts drives tumor-stroma co-evolution: A new paradigm for understanding tumor metabolism, the field effect and genomic instability in cancer cells. Cell Cycle. 2010;9(16):3256-3276.
146. Martinez-Outschoorn UE, Trimmer C, Lin Z, et al. Autophagy in cancer associated fibroblasts promotes tumor cell survival: Role of hypoxia, HIF1 induction and NFκB activation in the tumor stromal microenvironment. Cell Cycle. 2010;9(17):3515-3533.
147. Kraaij MD, Savage ND, van der Kooij SW, et al. Induction of regulatory T cells by macrophages is dependent on production of reactive oxygen species. Proc Natl Acad Sci U S A. 2010;107(41):17686-17691.
148. Maj T, Wang W, Crespo J, et al. Oxidative stress controls regulatory T cell apoptosis and suppressor activity and PD-L1-blockade resistance in tumor. Nat Immunol. 2017;18(12):1332-1341.
149. Whiteside TL. Human regulatory T cells (Treg) and their response to cancer. Expert Rev Precis Med Drug Dev. 2019;4(4):215-228.
150. Zhang Y, Choksi S, Chen K, et al. ROS play a critical role in the differentiation of alternatively activated macrophages and the occurrence of tumor-associated macrophages. Cell Res. 2013;23(7):898-914.
151. Mensurado S, Rei M, Lança T, et al. Tumor-associated neutrophils suppress pro-tumoral IL-17+ γδ T cells through induction of oxidative stress. PLoS Biol. 2018;16(5):e2004990.
152. El-Hag A, Clark RA. Down-regulation of human natural killer activity against tumors by the neutrophil myeloperoxidase system and hydrogen peroxide. J Immunol. 1984;133(6):3291-3297.
153. Kunisada Y, Eikawa S, Tomonobu N, et al. Attenuation of CD4+CD25+ regulatory T cells in the tumor microenvironment by metformin, a type 2 diabetes drug. EBioMedicine. 2017;25:154-164.
154. Corzo CA, Cotter MJ, Cheng P, et al. Mechanism regulating reactive oxygen species in tumor-induced myeloid-derived suppressor cells. J Immunol. 2009;182(9):5693-5701.
155. Kusmartsev S, Gabrilovich DI. Inhibition of myeloid cell differentiation in cancer: the role of reactive oxygen species. J Leukoc Biol. 2003;74(2):186-196.
156. Nagaraj S, Gupta K, Pisarev V, et al. Altered recognition of antigen is a mechanism of CD8+ T cell tolerance in cancer. Nat Med. 2007;13(7):828-835.
157. Bronte V, Serafini P, Mazzoni A, et al. L-arginine metabolism in myeloid cells controls T-lymphocyte functions. Trends Immunol.

2003;24(6):302-306.
158. Gabrilovich DI, Nagaraj S. Myeloid-derived suppressor cells as regulators of the immune system. Nat Rev Immunol. 2009;9(3):162-174.
159. Khaled YS, Ammori BJ, Elkord E. Myeloid-derived suppressor cells in cancer: recent progress and prospects. Immunol Cell Biol. 2013;91(8):493-502.
160. Srivastava MK, Sinha P, Clements VK, et al. Myeloid-derived suppressor cells inhibit T-cell activation by depleting cystine and cysteine. Cancer Res. 2010;70(1):68-77.
161. OuYang LY, Wu XJ, Ye SB, et al. Tumor-induced myeloid-derived suppressor cells promote tumor progression through oxidative metabolism in human colorectal cancer. J Transl Med. 2015;13:47.
162. Wei J, Zhang M, Zhou J. Myeloid-derived suppressor cells in major depression patients suppress T-cell responses through the production of reactive oxygen species. Psychiatry Res. 2015;228(3):695-701.
163. Weinberg SE, Sena LA, Chandel NS. Mitochondria in the regulation of innate and adaptive immunity. Immunity. 2015;42(3):406-417.
164. Lin X, Zheng W, Liu J, et al. Oxidative stress in malignant melanoma enhances tumor necrosis factor-α secretion of tumor-associated macrophages that promote cancer cell invasion. Antioxid Redox Signal. 2013;19(12):1337-1355.
165. González-Pacheco FR, Deudero JJ, Castellanos MC, et al. Mechanisms of endothelial response to oxidative aggression: protective role of autologous VEGF and induction of VEGFR2 by H2O2. Am J Physiol Heart Circ Physiol. 2006;291(3):H1395-H1401.
166. Chua CC, Hamdy RC, Chua BH. Upregulation of vascular endothelial growth factor by H2O2 in rat heart endothelial cells. Free Radic Biol Med. 1998;25(8):891-897.
167. Yasuda M, Shimizu S, Tokuyama S, et al. A novel effect of polymorphonuclear leukocytes in the facilitation of angiogenesis. Life Sci. 2000;66(21):2113-2121.
168. Ikeda S, Ushio-Fukai M, Zuo L, et al. Novel role of ARF6 in vascular endothelial growth factor-induced signaling and angiogenesis. Circ Res. 2005;96(4):467-475.
169. Chandel NS, McClintock DS, Feliciano CE, et al. Reactive oxygen species generated at mitochondrial complex III stabilize hypoxia-inducible factor-1alpha during hypoxia: a mechanism of O2 sensing. J Biol Chem. 2000;275(33):25130-25138.
170. Guzy RD, Hoyos B, Robin E, et al. Mitochondrial complex III is required for hypoxia-induced ROS production and cellular oxygen sensing. Cell Metab. 2005;1(6):401-408.
171. Klimova T, Chandel NS. Mitochondrial complex III regulates hypoxic activation of HIF. Cell Death Differ. 2008;15(4):660-666.
172. Reichard A, Asosingh K. The role of mitochondria in angiogenesis. Mol Biol Rep. 2019;46(1):1393-1400.
173. Bailly C. Regulation of PD-L1 expression on cancer cells with ROS-modulating drugs. Life Sci. 2020;246:117403.
174. Scharping NE, Menk AV, Whetstone RD, et al. Efficacy of PD-1 blockade is potentiated by metformin-induced reduction of tumor hypoxia. Cancer Immunol Res. 2017;5(1):9-16.
175. Berg D, Lehne M, Müller N, et al. Enforced covalent trimerization increases the activity of the TNF ligand family members TRAIL and CD95L. Cell Death Differ. 2007;14(12):2021-2034.
176. Fulda S, Debatin KM. Extrinsic versus intrinsic apoptosis pathways in anticancer chemotherapy. Oncogene. 2006;25(34):4798-4811.
177. Susin SA, Lorenzo HK, Zamzami N, et al. Molecular characterization of mitochondrial apoptosis-inducing factor. Nature. 1999;397(6718):441-446.

DOI 10.1007/s10330-022-0573-3
Cite this article as: Zhu T, Wang GH. The interaction between end-metabolites and immune escape. Oncol Transl Med. 2022;8(2):57–73.

Oncology and Translational Medicine
DOI 10.1007/s10330-022-0551-1

April 2022, Vol. 8, No. 2, P74–P82

REVIEW ARTICLE

Research progress on immune checkpoint inhibitors in neoadjuvant therapy for gastric cancer

Wenting Li, Shiying Yu (✉)

Department of Oncology, Tongji Hospital, Tongji Medical College, Huazhong University of Science and Technology, Wuhan 430030, China

Abstract

In recent years, immune checkpoint inhibitors (ICIs) have become an important treatment strategy for advanced gastric cancer. Immunotherapy has gradually transitioned from a later-line to a first-line treatment for advanced gastric cancer. Simultaneously, more and more researchers have begun to pay attention to whether immunotherapy can be used for resectable gastric cancer. The current use of ICIs in the neoadjuvant treatment of gastric cancer is still in its exploratory stage, with a number of clinical trials currently underway. However, the available data show good application prospects. This article reviews the research progress on ICIs in the neoadjuvant therapy for gastric cancer and evokes some unresolved problems.

Received: 13 January 2022
Revised: 24 March 2022
Accepted: 2 April 2022

Key words: gastric cancer; immune checkpoint inhibitors (ICIs); neoadjuvant therapy

Gastric cancer is a common malignant tumor of the digestive system that ranks fifth in cancer incidence and fourth in mortality worldwide [1]. Approximately 44% of gastric cancer cases worldwide occur in China [2]. The China Gastrointestinal Cancer Surgery Union counted the gastric cancer surgery cases in 85 centers across the country from 2014 to 2016 and found that the proportion of locally advanced gastric cancers was as high as 70.8% [3]. The current treatment of resectable gastric cancer is based on clinical stage evaluation, and the importance of comprehensive perioperative treatment has been recognized; however, the perioperative treatment strategy for gastric cancer has not yet reached a global consensus [4–5]. In recent years, immune checkpoint inhibitors (ICIs) have gradually become a research hotspot in tumor immunotherapy. Based on the results of the CheckMate-649 study [6], in April 2021, the US Food and Drug Administration (FDA) approved nivolumab in combination with fluoropyrimidine- and platinum-containing chemotherapeutic drugs as a first-line treatment for patients with advanced or metastatic gastric cancer, gastroesophageal junction cancer, and esophageal adenocarcinoma. This is the first FDA-approved first-line immunotherapy for gastric cancer. Immunotherapy has transitioned from the later-line treatment of gastric cancer to the first-line treatment and has evolvedas a neoadjuvant therapy. A number of clinical trials on neoadjuvant immunotherapy for gastric cancer are currently underway. This article reviews the research progress of ICIs in neoadjuvant therapy for gastric cancer.

Immune checkpoint inhibitors (ICIs)

Immune checkpoints, including programmed cell death receptor-1 (PD-1), programmed cell death ligand-1 (PD-L1), cytotoxic T lymphocyte-associated molecule-4 (CTLA-4), lymphocyte activation gene 3 (LAG3), and T cell immunoglobulin 3 (TIM3), are a class of molecules expressed on immune cells, antigen-presenting cells, and tumor cells that can regulate immune responses [7]. PD-1/PD-L1 and CTLA-4 inhibitors are the most widely used ICIs in clinical practice. PD-1/PD-L1 and CTLA-4 are negative regulators of T cell immune responses, and their inhibition enhances antitumor immune responses by blocking these factor-mediated immunosuppressive pathways [8].

PD-1 is an inhibitory receptor that is expressed on a variety of immune cells, such as activated T cells, B cells, and natural killer cells [9–10]. When it binds to PD-L1 expressed on tumor cells, it activates an

✉ Correspondence to: Shiying Yu. Email: syyu@tjh.tjmu.edu.cn

immunosuppressive signaling pathway, resulting in tumor immune escape [11]. PD-1/PD-L1 inhibitors relieve the immunosuppression and restore the anti-tumor immune function of T cells by blocking the interaction between PD-1 and PD-L1 [12]. Common PD-1 inhibitors include pembrolizumab, nivolumab, camrelizumab, sintilimab, tislelizumab, and toripalimab. PD-L1 inhibitors include atezolizumab, avelumab, and durvalumab.

CTLA-4 is homologous to the immunostimulatory receptor CD28, but it binds to the CD80 (B7-1) and CD86 (B7-2) ligands expressed on antigen-presenting cells with a higher affinity than CD28. CTLA-4 and CD28 competitively bind to B7 ligands, thereby inhibiting T cell activation [13–15]. CTLA-4 inhibitors specifically bind to CTLA-4 and release T cellinhibition, thereby promoting their proliferation and activation [12, 16]. Tang *et al* proposed that anti-CTLA-4 antibodies exert therapeutic effects by selectively depleting T-regulatory cells in tumors [17]. However, their relevant mechanism of action is still under investigation. CTLA-4 inhibitors include ipilimumab and tremelimumab.

Neoadjuvant immune monotherapy

Nivolumab

A phase I clinical study of neoadjuvant nivolumab monotherapy for resectable gastric cancer was reported at the 2021 American Society of Clinical Oncology (ASCO) annual meeting [18]. A total of 31 patients received two cycles of neoadjuvant therapy, of which one discontinued the trial preoperatively due to disease progression. The remaining 30 patients underwent surgery, of which five (16.7%) achieved major pathological response (MPR), including one (3.3%) pathological complete response (pCR). Among seven patients with microsatellite instability-high (MSI-H), four (57.1%) achieved MPR (including one pCR). Treatment-related adverse events (TRAEs) occurred in seven patients (22.6%); one patient had grade 3 asymptomatic lipase elevation, and the rest developed grade 1–2 TRAEs. The results of the study showed that nivolumab is feasible and safe for neoadjuvant treatment of gastric cancer. However, because one patient had disease progression before surgery, the efficacy of immune monotherapy needs further validation.

Pembrolizumab

The 2021 ASCO annual meeting announced the results of an interim study on pre- and postoperative pembrolizumab and adjuvant chemoradiotherapy in patients with MSI-H, Epstein-Barr virus-positive, or PD-L1-positive locally advanced gastric cancer (NCT03257163) [19]. Of the 15 patients enrolled in the study, six had MSI-H status and two did not undergo surgical resection because they were considered too frail and were found to have peritoneal disease on exploration. Of the 13 patients that completed the operation, two (15.4%) MSI-H patients achieved pCR, five patients had downstaged clinical T stage, and two patients had downstaged clinical N stage. No recurrence was observed in the short-term follow-up (1–22 months). The incidence of specific adverse events was not disclosed.

It is worth noting that the patients who achieved pCR in the above two studies had an MSI-H status, and immunotherapy generally has a positive effect on MSI-H patients. Zhang *et al* reported a retrospective study of six patients with MSI-H gastrointestinal tumors [20], including four with gastric cancer and two with colorectal cancer. Two patients switched to immunotherapy after chemotherapy failure and were treated with nivolumab monotherapy and sintilimab combined with bevacizumab, respectively; three patients received ICIs combined with chemotherapy; and one patient received nivolumab combined with ipilimumab. Of these patients, five achieved pCR and one achieved clinical TNM downstaging after surgery. No grade 3–4 TRAES or surgery-related complications occurred. The median follow-up time was 10.5 (7–18) months after surgery, and no recurrence or long-term complications were reported. These data suggest the potential of MSI-H as a predictive marker for the efficacy of neoadjuvant therapy for gastric cancer.

Neoadjuvant immunotherapy combined with chemotherapy

Sintilimab in combination with chemotherapy

In 2021, the ASCO Gastrointestinal Cancers Symposium (ASCO-GI) reported a phase II clinical study on sintilimab combined with FLOT regimen (docetaxel + oxaliplatin + fluorouracil + leucovorin) as the neoadjuvant treatment of gastric or gastroesophageal junction adenocarcinoma (NCT04341857) [21]. The enrolled patients received four cycles of FLOT chemotherapy combined with three cycles of sintilimab before surgery and four cycles of FLOT chemotherapy after surgery. Seventeen patients underwent surgery with a pCR rate of 17.6% and an MPR rate of 58.8%. Grade 3–4 TRAEs included anemia (20%), leukopenia (10%), and abnormal liver function (5%). In the FLOT4-AIO study [22], the pCR and MPR rates following perioperative FLOT regimen chemotherapy were 16% and 37%, respectively. Therefore, compared with the FLOT4-AIO study, the combination of sintilimab and FLOT chemotherapy used in the NCT04341857 study improved the pCR rate and MPR rate, especially the MPR rate increased by 21.8%. The current survival rate of this study is still in the follow-up stage, and the efficacy and safety of the regimen need to be further confirmed.

A phase II clinical study of sintilimab combined

with oxaliplatin/capecitabine (CapeOx) as the neoadjuvant treatment of locally advanced resectable gastric/gastroesophageal junction adenocarcinoma was reported at the 2021 ASCO-GI [23]. The patients received three cycles of sintilimab combined with CapeOx regimen neoadjuvant therapy before surgery and three cycles of CapeOx regimen adjuvant chemotherapy postoperatively. Twenty-five patients completed three cycles of neoadjuvant therapy, one patient completed only 2 cycles due to grade 3 aspartate aminotransferase elevation, and 26 patients underwent surgery. The pCR and MPR rates were 23.1% and 53.8%, respectively. To assess the validity of positron emission tomography and computed tomography (PET-CT) evaluation, 18 patients underwent PET-CT scanning; of which, 11 patients (61.1%) showed partial metabolic remission. Six patients (23.1%) had grade 3 neoadjuvant TRAEs, including neutropenia, leukopenia, and thrombocytopenia. One patient developed hypothyroidism as agrade 1 immune-related adverse event (irAE). The pCR and MPR rates of this regimen exceeded the results of the study on sintilimab/FLOT combination and the safety was acceptable. However, whether PET-CT can better predict the response to focal immunotherapy remains to be explored [24–25].

Camrelizumab in combination with chemotherapy

The ChiCTR2000030610 study was a single-center, randomized, controlled clinical study evaluating FLOT chemotherapy combined with camrelizumab as a neoadjuvant therapy [26]. Twenty-four patients with locally advanced gastric and gastroesophageal junction adenocarcinoma were randomly divided into a FLOT (arm A) and a FLOT/camrelizumab (arm B) groups. Nineteen patients completed four cycles of neoadjuvant therapy and 17 underwent surgery. The R0 resection rate in arm B (100%) was higher than that in arm A (71.4%). In terms of tumor regression and lymph node downstaging, 10% and 60% of patients in arm B achieved TRG1 and ypN0, respectively, whereas no such observations were reported in arm A. No pCR was observed in either group; this may be related to the small number of enrolled patients, and the efficacy and safety of this regiment need to be further explored.

The 2021 ASCO meeting updated the results of a study on camrelizumab combined with FOLFOX regimen (oxaliplatin + fluorouracil + leucovorin) for the neoadjuvant treatment of resectable locally advanced gastric and gastroesophageal junction adenocarcinoma [27]. Of the 60 enrolled patients that received four cycles of neoadjuvant therapy, one was assessed for disease progression, three refused surgery, and four were found to have intra-abdominal metastases during surgery. The 52 surgically resected patients had pCR and MPR rates of 10% and 31%, respectively. Grade 3–4 TRAEs included leukopenia (17%). One patient had grade 3 irAEs (increased alanine and aspartate aminotransferases). The neoadjuvant combination of camrelizumab and FOLFOX is a safe and effective treatment option for patients with gastric or gastroesophageal junction adenocarcinomas.

Avelumab in combination with chemotherapy

The ICONIC study was a phase II clinical study of perioperative FLOT chemotherapy combined with avelumab for the treatment of resectable esophagogastric adenocarcinoma, and its interim safety results were announced at the 2021 ASCO-GI [28]. Of the 15 enrolled patients, two switched to alternative chemotherapy due to 5-fluorouracil cardiac toxicity. All patients underwent R0 resections. Grade 3–4 adverse events occurred in 9 patients (60%) and included neutropenia and diarrhea. Three patients developed Clavien-Dindo grade IIIa postoperative complications.

A phase II clinical trial of perioperative chemotherapy combined with avelumab in the treatment of locally advanced gastric and esophageal adenocarcinoma was reported at the 2021 ASCO Annual Meeting [29]. The patients were administered 4 cycles of avelumab and mDCF regimen (docetaxel + cisplatin + fluorouracil) before and after surgery. Surgery was completed in 27 patients, with MPR and pCR rates of 22% and 11%, respectively. Toxicity events included grade 4 neutropenia (two cases), pneumonia (one case), grade 3 stomatitis (two cases), and diarrhea (one case). The 12- and 24-month disease-free survival rates were 92% (95% CI: 0.83–1.00) and 77% (95% CI: 0.58–1.00), respectively. The combination of mDCF chemotherapy with avelumab showed promising safety and efficacy.

Atezolizumab in combination with chemotherapy

The DANTE study was a multicenter, phase IIb clinical study [30]. The 295 enrolled patients with resectable gastric or gastroesophageal junction adenocarcinoma were randomly divided into two groups: arm A received four cycles of FLOT/atezolizumab combination before surgery, followed by four cycles of FLOT/atezolizumab combination and eight cycles of atezolizumab; arm B received 4 cycles of FLOT chemotherapy before and after surgery. Twenty-three patients exhibited deficient mismatch repair (dMMR), and their pCR rate (47.8%) was higher than that of proficient mismatch repair (pMMR) patients (21.2%). Among dMMR patients, pCR and MPR rates were also higher in arm A (60% and 80%, respectively) than in arm B (38.5% and 53.9%, respectively). The data from the DANTE study once again demonstrated the favorable therapeutic effects of

immunotherapy in patients with MSI-H gastric cancer. Additionally, comparison of this study with the two aforementioned clinical trials on immune monotherapy revealed that atezolizumab combined with chemotherapy results in the highest pCR and MPR rates in patients with MSI-H gastric cancer.

Toripalimab in combination with chemotherapy

The Gastrim 001 study was a single-arm phase II clinical trial that assessed the effects of toripalimab/chemotherapy combination in patients with locally advanced resectable gastric/gastroesophageal junction adenocarcinoma [31]. The treatment plan consisted of four cycles of toripalimab combined with FLOT chemotherapy before and after surgery. Thirty-six patients were included, of which 28 had completed the surgery. The pCR and the MPR rates were 25% and 42.9%, respectively, higher than those of the FLOT4-AIO study. In terms of safety, eight patients developed Clavien-Dindo grade II postoperative complications and two had grade IIIa complications. Grade 3–4 adverse events included neutropenia (30.6%), leukopenia (25.0%), and anemia (5.6%). Among the three clinical studies using immunization combined with FLOT chemotherapy as the treatment plan, the most effective treatment was toripalizumab, followed by sintilimab and camrelizumab. The DANTE study was not included in this comparison because it analyzed patients according to dMMR and pMMR groups. Toripalimab combined with FLOT chemotherapy has high pCR and MPR rates, with good tolerability and safety.

Neoadjuvant immunotherapy combined with chemotherapy and targeted therapy

The 2021 ASCO Annual Meeting reported a phase II clinical study on camrelizumab, apatinib, and S-1 ± oxaliplatin in neoadjuvant/conversion therapy for gastric cancer treatment (cT4a/bN+M0) [32]. Twenty-five patients received at least two cycles of neoadjuvant therapy before surgery. Twenty-four patients completed the reassessment, and the tumor downstaging rate was 79.2%. Conversion failed in three cases and surgery was refused in two cases and postponed in one case because of immune-related pneumonia. Among the 18 patients who underwent R0 resection, the pCR and MPR rates were 16.7% and 27.8%, respectively. No TRAEs of grade 3 or higher were found.

Lin *et al* [33] and Zheng *et al* [34] conducted a study of S-1/oxaliplatin combined with apatinib (SOXA) as the neoadjuvant therapy for locally advanced gastric cancer, with pCR rates of 6.3% and 13.7%, respectively. However, camrelizumab, apatinib, and S-1 ± oxaliplatin neoadjuvant/conversion therapy for gastric cancer treatment (cT4a/bN+M0) achieved a higher pCR rate (16.7%) than those reported in the previous studies, suggesting that neoadjuvant immunetherapy combined with chemotherapy and antiangiogenic drugs may have a synergistic effect [35]. Preliminary results indicated that the treatment regimen is effective and safe. The multicenter phase II–III clinical trial DRAGON-IV/Ahead-G208 study on SOXA and camrelizumab for the perioperative treatment of resectable locally advanced gastric or esophagogastric junction adenocarcinoma is also underway, and we look forward to the results.

Neoadjuvant immunotherapy combined with chemoradiotherapy

Sintilimab in combination with chemoradiotherapy

The SHARED study was designed to evaluate the efficacy and safety of perioperative sintilimab combined with concurrent chemoradiotherapy (S-1 + Nab-PTX) for the treatment of locally advanced gastric or gastroesophageal junction adenocarcinoma [36]. Gastrectomy was completed in 19 patients, with pCR and MPR rates of 42.1% and 73.7%, respectively. Eleven (39.3%) patients had grade 3–4 TRAEs, including myelosuppression (39.3%) and increased transaminase levels (10.7%). The incidence of irAEs was 21.4%; these included one case of grade 4 hepatitis; the remaining irAEs were grade 1–2. Perioperative complications occurred in three patients. Despite the small sample size, the results of the SHARED study are encouraging. The final results of this study will be available once the follow-up of patients is completeand the survival data are reported.

Camrelizumab in combination with chemoradiotherapy

The Neo-PLANET study was a phase II clinical study on neoadjuvant camrelizumab combined with chemoradiotherapy (oxaliplatin + capecitabine) for the treatment of locally advanced proximal gastric cancer [37]. Of the 36 enrolled patients, 33 were subjected to radical surgery; three patients were excluded from surgery because of liver metastasis, peritoneal metastasis, and surgery refusal. The pCR and MPR rates were 33.3% and 44.4%, respectively. Twenty-nine patients (80.56%) had grade 3–4 adverse events, including decreased lymphocyte count (75%) and leukopenia (5.6%). From the above-mentioned clinical studies, the efficacy of this regimen is second only to that obtained by sintilimab combined with concurrent chemoradiotherapy. However, the Neo-PLANET study had a high rate of grade 3–4 adverse events that required close monitoring.

Efficacy and safety

At present, the administration of ICIs in the perioperative period of gastric cancer is still being explored. Theoretically, due to the presence of the preoperative primary tumor, high levels of endogenous tumor antigens are present in the patient's body and can be presented to tumor-specific T cells by dendritic cells; these activated tumor-specific T cells can enter the blood circulation to act on metastatic lesions and enhance systemic anti-tumor immunity [38]. These effects may persist even after surgical resection of the primary tumor and regional lymph nodes. The long-term immune memory generated preoperatively may be superior to that induced by postoperative adjuvant therapy, thereby reducing the risk of recurrence [39]. Neoadjuvant therapy can increase the strength, breadth, and durability of tumor-specific T-cell responses compared with adjuvant therapy, which primarily targets micrometastases or residual lesions after resection [40]. A preclinical study also confirmed that neoadjuvant therapy, compared with adjuvant immunotherapy, can improve efficacy [41].

Owing to the different clinical characteristics and treatment plans of the patients enrolled in each clinical trial, the reported therapeutic effects also differ. Based on the existing studies, the efficacy of immune combination therapy is better than that of immune monotherapy and the combination of immune therapy and chemoradiotherapy has the best efficacy. Several previous studies have explored the application of neoadjuvant chemoradiotherapy in gastric cancer [42–46]. For example, the POET study included patients with locally advanced gastroesophageal junction adenocarcinoma and showed that neoadjuvant chemoradiation could significantly improve the pCR rate compared with neoadjuvant chemotherapy (15.6% *vs.* 2.0%) [42]. However, because most studies on neoadjuvant chemoradiation focus on gastroesophageal junction cancer, their validity for gastric corpus and distal gastric cancer is limited. The impressive pCR rate of 42.1% in the SHARED study is a significant improvement over the pCR rates in the RTOG 9904 (neoadjuvant chemoradiotherapy) and FLOT4-AIO studies (26% and 16%, respectively) [22, 44]. Whether the high pCR rate of neoadjuvant immunotherapy combined with chemoradiotherapy can be translated into long-term survival benefit is worth looking forward to. It is also worth noting that the results of some of the above clinical trials are not better than those on neoadjuvant chemo- and radiochemotherapy, possibly due to the small number of patients included. Additionally, whether the combination therapy can exert a synergistic effect needs to be determined in afollow-up with a large sample size. Owing to the lack of data on CTLA-4 inhibitors and dual immune combination therapy in clinical practice, it remains to be determinedwhether better treatments will be developed in the future.

A number of clinical trials have also analyzed MSI-H patients, and the results have shown that these patients can achieve high pCR rates regardless of whether they receive immune monotherapy or combination therapy. Increasing evidence suggests that patients with MSI-H gastric cancer do not benefit from neoadjuvant chemotherapy [47–48]. Neoadjuvant immunotherapy may provide a new treatment option for these patients. However, the proportion of the MSI-H/dMMR population among gastric cancer patients is only 8%–10% [20], and MSI-H alone as the selection criterion for the appropriate population is limited. Therefore, the active search for markers or targets is critical for the precise treatment of gastric cancer. In recent years, the perioperative treatment of human epidermal growth factor receptor 2 (HER2)-positive gastric cancer has also attracted attention. Trastuzumab is a targeted therapy drug that specifically acts on HER2. The HER-FLOT study evaluated the administration of trastuzumab in combination with FLOT chemotherapy for the perioperative treatment of patients with HER2-positive gastric or esophagogastric junction adenocarcinomaand reported a pCR rate of 21.4% [49]. This phase II clinical trial confirmed the feasibility and effectiveness of trastuzumab combined with chemotherapy. However, there are currently no data on the application of immune combined anti-HER2 therapy in the perioperative period of HER2-positive gastric cancer. The KEYNOTE-811 study explored trastuzumab and chemotherapy combined with pembrolizumab as the first-line treatment for HER2-positive gastric or gastroesophageal junction cancer. The objective response rate was 74.4% (95% CI: 66.2–81.6) in the combined pembrolizumab group and 51.9% (95% CI: 43.0–60.7) in the control group; the incidence of adverse events was similar in both groups [50]. The high objective response rate of the KEYNOTE-811 study suggests that this treatment strategy has great potential for further development for the perioperative treatment of HER2-positive gastric cancer. Currently, most clinical trials use the clinical stage of patients as the main inclusion criteria. With the increasing understanding of the molecular typing of gastric cancer, the combination of MSI-H and other markers as inclusion criteria may more accurately screen the dominant population and improve the efficacy. It may also provide ideas for the design of clinical studies. Finally, in the NCT03257163 study, one patient was too frail to undergo surgery. Poor nutritional status increases the incidence of postoperative complications and affects the prognosis of patients with gastric cancer [51–52]. Therefore, clinically, the nutritional status of patients should be actively evaluated and nutritional support treatment should be provided accordingly.

In terms of safety, the most commonly observed grade 3–4 adverse reactions were chemotherapy-related bone marrow suppression and gastrointestinal reactions. Based on the available studies, the incidence of postoperative complications and irAEs is low, and the overall safety is acceptable. It is worth noting that although neoadjuvant immunotherapy combined with chemoradiotherapy achieved an outstanding efficacy, the incidence of adverse reactions also significantly increased. The incidences of irAEs in the SHARED study and grade 3–4 adverse events in the Neo-PLANET study were 21.4% and 80.56%, respectively. In addition, patients may need to delay surgery or suspend the follow-up treatment because of the disease progression or irAEs after neoadjuvant therapy. Researchers should carefully consider these potential risks in clinical practice and choose a treatment plan with a high disease control rate and safety to improve efficacy while minimizing adverse reactions. As most of the currently available data comes from phase II clinical trials with small samples and research is still in progress, the evidence is not yet strong and further data accumulation and evaluation are needed. The available data show the development prospects of ICIs as the neoadjuvant therapy of gastric cancer. We look forward to updating these data on efficacy, safety, postoperative recurrence and metastasis, and survival in the future multicenter, large-sample, and long-term follow-up phase III clinical trials. The ongoing phase III clinical trials of ICIs for the neoadjuvant treatment of gastric cancer are shown in Table 1.

Problems to be addressed

The exploration of biomarkers

Immunotherapy is not beneficial for all patients. To prevent disease progression due to unfavorable treatment plans or serious adverse reactions, it is crucial to find biomarkers that accurately screen beneficiaries. Currently, there are no clear biomarkers for neoadjuvant immunotherapy for gastric cancer. Potential predictive markers found in immunotherapy studies for advanced gastric cancer include PD-L1, tumor mutational burden, MSI-H, Epstein-Barr virus-positive, and gut microbiota [53]. Whether these can be used in the perioperative treatment of gastric cancer remains to be verified. We look forward to the identification of reliable biomarkers and multiple indicators that may help identify dominant populations, guide treatment, predict efficacy, and monitor prognosis.

Best treatment strategy

Several factors must be considered and optimized when establishing a treatment plan: the treatment mode; the dose, sequence, cycle, and interval of neoadjuvant therapy; the potential negative effects of neoadjuvant immunotherapy on surgery prospects; the need of adjuvant therapy after surgery; the adjuvant therapy regimen and timing of administration; the survival benefit of neoadjuvant or adjuvant immunotherapy; and the compromise between efficacy and safety. These factors still remain unresolved.

Choice of the surgery timing

The optimal timing for surgery after neoadjuvant chemotherapy in patients with gastric cancer is still controversial [54–56]. A preclinical study, where a mouse model of breast cancer received immunotherapy before surgery, showed that different surgical intervals after neoadjuvant therapy affect survival [57]. Exploring the optimal duration of immunotherapy action may help determine the timing of surgery.

Endpoints of clinical trials

Overall survival is the generally accepted gold standard to measure the benefit of a treatment. However, determining the overall survival requires an extended

Table 1 Ongoing phase III clinical trials on immune checkpoint inhibitors as a neoadjuvant treatment of gastric cancer

ClinicalTrials.gov Identifier	Phase	Cases	Treatment method	Primary outcome	Estimated primary completion date
NCT04882241	III	120	pembrolizumab + chemotherapy	EFS, pCR rate, OS, The percentage of participants who experience at least one AE, The percentage of participants who discontinue study treatment due to an AE	2025.10.31
NCT03221426	III	1007	pembrolizumab + chemotherapy	EFS, pCRrate, OS, The percentage of participants who experience at least one AE, The percentage of participants who discontinue study treatment due to an AE	2024.06.28
NCT04208347	II/III	258	camrelizumab + apatinib + chemotherapy	MPR	2021.07
NCT04592913	III	900	durvalumab + chemotherapy	EFS	2025.02.14
NCT04139135	III	642	HLX10 + chemotherapy	3-year EFS rate	2023.10.15

Note: AE, adverse events; EFS, event-free survival; MPR, major pathological response; OS, overall survival; pCR, pathological complete response

follow-up, which increases the trial costs [58]. Scholars have suggested MPR as a surrogate endpoint in studies related to neoadjuvant chemotherapy in resectable lung cancer [59]. Most studies on neoadjuvant immunotherapy now use MPR or pCR as the primary endpoint; however, their prognostic value is inconclusive. At present, survival data are still being followed up. The relationship between pathological remission and remission degree and long-term survival, as well as whether there are other surrogate endpoints, such as the lymph node status, remains to be determined [60–61].

Efficacy assessment

Previous studies have reported that patients who received neoadjuvant immunotherapy showed tumor enlargement on preoperative imaging, but postoperative pathological evaluation was based on the pCR or MPR [62]. This discrepancy between imaging and pathological evaluations is a pseudoprogression, a phenomenon that may result from transient immune cell infiltration in the tumor bed [63]. Hyperprogression, another specific immune response pattern characterized by accelerated disease progression and shortened survival, is also of concern [64]. Failure to correctly identify pseudo- and hyperprogression in a timely manner may result in delayed surgery or even loss of the opportunity for surgical resection. With the continuous improvement of the efficacy evaluation criteria, researchers have developed a number of response evaluation criteria in solid tumors (RECISTs) for immunotherapy, such as the immune-related RECIST (irRECIST), immune-modified RECIST (imRECIST), and immune RECIST (iRECIST). However, these new criteria cannot assess hyperprogression, and it is unclear whether they should be used in clinical practice [65]. Additional efficacy assessment tools are also being explored, such as circulating tumor DNA [66] and PET-CT [67–69].

Some scholars have also explored the pathological evaluation standard and proposed immune-related pathologic response criteria for the immunotherapy of non-small cell lung cancer; these have been extended to multiple tumor types and need to be further verified and standardized [70–71].

Epilogue

ICIs have shown promising potential in the neoadjuvant therapy for gastric cancer, especially neoadjuvant immunotherapy combined with chemoradiotherapy. However, questions such as the optimal treatment strategy and the timing of surgery remain to be answered, and the current survival data are immature. Thus, more large-scale clinical trials are still needed. In addition, because gastric cancer is a highly heterogeneous tumor, a future development trend will be the search for reliable biomarkers to screen beneficial populations, formulate personalized targeted treatment plans, and achieve precise treatment.

Acknowledgments

Not applicable.

Funding

Not applicable.

Conflicts of interest

The authors declare that they have no conflicts of interest.

Author contributions

All authors contributed to data acquisitionand interpretation, and reviewed and approved the final version of this manuscript.

Data availability statement

Not applicable.

Ethical approval

Not applicable.

References

1. Sung H, Ferlay J, Siegel RL, et al. Global cancer statistics 2020: GLOBOCAN estimates of incidence and mortality worldwide for 36 cancers in 185 countries. CA Cancer J Clin. 2021;71(3):209-249.
2. Yang L, Ying XJ, Liu S, et al. Gastric cancer: Epidemiology, risk factors and prevention strategies. Chin J Cancer Res. 2020;32(6):695-704.
3. Wang YK, Li ZY, Shan F, et al. Current status of diagnosis and treatment of early gastric cancer in China – Data from China Gastrointestinal Cancer Surgery Union. Chin J Gastrointest Surg (Chinese). 2018;21(2):168-174.
4. Beeharry MK, Zhang TQ, Liu WT, et al. Optimization of perioperative approaches for advanced and late stages of gastric cancer: clinical proposal based on literature evidence, personal experience, and ongoing trials and research. World J Surg Oncol. 2020;18(1):51.
5. Wang FH, Zhang XT, Li YF, et al. The Chinese Society of Clinical Oncology (CSCO): Clinical guidelines for the diagnosis and treatment of gastric cancer, 2021. Cancer Commun (Lond). 2021;41(8):747-795.
6. Janjigian YY, Shitara K, Moehler M, et al. First-line nivolumab plus chemotherapy versus chemotherapy alone for advanced gastric, gastro-oesophageal junction, and oesophageal adenocarcinoma (CheckMate 649): a randomised, open-label, phase 3 trial. Lancet. 2021;398(10294):27-40.
7. Zhang Y, Zheng J. Functions of immune checkpoint molecules beyond immune evasion. Adv Exp Med Biol. 2020;1248:201-226.
8. Grosso JF, Kelleher CC, Harris TJ, et al. LAG-3 regulates CD8+ T cell accumulation and effector function in murine self- and tumor-tolerance systems. J Clin Invest. 2007;117(11):3383-3392.
9. Sharpe AH, Pauken KE. The diverse functions of the PD1 inhibitory pathway. Nat Rev Immunol. 2018;18(3):153-167.
10. Saha D, Martuza RL, Rabkin SD. Macrophage polarization contributes to glioblastoma eradication by combination immunovirotherapy and

immune checkpoint blockade. Cancer Cell. 2017;32(2):253-267.
11. Xu Y, Poggio M, Jin HY, et al. Translation control of the immune checkpoint in cancer and its therapeutic targeting. Nat Med. 2019;25(2):301-311.
12. Buchbinder EI, Desai A. CTLA-4 and PD-1 pathways: Similarities, differences, and implications of their inhibition. Am J Clin Oncol. 2016;39(1):98-106.
13. Wing K, Yamaguchi T, Sakaguchi S. Cell-autonomous and -non-autonomous roles of CTLA-4 in immune regulation. Trends Immunol. 2011;32(9):428-433.
14. Zelle-Rieser C, Thangavadivel S, Biedermann R, et al. T cells in multiple myeloma display features of exhaustion and senescence at the tumor site. J Hematol Oncol. 2016;9(1):116.
15. Yi JS, Ready N, Healy P, et al. Immune activation in early-stage non-small cell lung cancer patients receiving neoadjuvant chemotherapy plus ipilimumab. Clin Cancer Res. 2017;23(24):7474-7482.
16. Li K, Zhang A, Li X, et al. Advances in clinical immunotherapy for gastric cancer. Biochim Biophys Acta Rev Cancer. 2021;1876(2):188615.
17. Tang F, Du X, Liu M, et al. Anti-CTLA-4 antibodies in cancer immunotherapy: selective depletion of intratumoral regulatory T cells or checkpoint blockade? Cell Biosci. 2018;8:30.
18. Takiguchi S, Shitara K, Takiguchi N, et al. Neoadjuvant nivolumab monotherapy in patients with resectable gastric cancer: Preliminary results from a multicenter study. J Clin Oncol. 2021;39(15 suppl):4026.
19. Kennedy T, Shah MM, In H, et al. Preoperative pembrolizumab for MSI high, EBV positive or PD-L1 positive locally advanced gastric cancer followed by surgery and adjuvant chemoradiation with pembrolizumab: Interim results of a phase 2 multi-center trial (NCT03257163). J Clin Oncol. 2021;39(15 suppl):e16111.
20. Zhang Z, Cheng S, Gong J, et al. Efficacy and safety of neoadjuvant immunotherapy in patients with microsatellite instability-high gastrointestinal malignancies: A case series. Eur J Surg Oncol. 2020;46(10 Pt B):e33-e39.
21. Li N, Li Z, Fu Q, et al. Phase II study of sintilimab combined with FLOT regimen for neoadjuvant treatment of gastric or gastroesophageal junction (GEJ) adenocarcinoma. J Clin Oncol. 2021;39(3 suppl):216.
22. Al-Batran SE, Hofheinz RD, Pauligk C, et al. Histopathological regression after neoadjuvant docetaxel, oxaliplatin, fluorouracil, and leucovorin versus epirubicin, cisplatin, and fluorouracil or capecitabine in patients with resectable gastric or gastro-oesophageal junction adenocarcinoma (FLOT4-AIO): results from the phase 2 part of a multicentre, open-label, randomised phase 2/3 trial. Lancet Oncol. 2016;17(12):1697-1708.
23. Jiang HP, Yu XF, Kong M, et al. Sintilimab plus oxaliplatin/capecitabine (CapeOx) as neoadjuvant therapy in patients with locally advanced, resectable gastric (G)/esophagogastric junction (GEJ) adenocarcinoma. J Clin Oncol. 2021;39(3 suppl):211.
24. Cho SY, Lipson EJ, Im HJ, et al. Prediction of response to immune checkpoint inhibitor therapy using early-time-point ^{18}F-FDG PET/CT imaging in patients with advanced melanoma. J Nucl Med. 2017;58(9):1421-1428.
25. Anwar H, Sachpekidis C, Winkler J, et al. Absolute number of new lesions on ^{18}F-FDG PET/CT is more predictive of clinical response than SUV changes in metastatic melanoma patients receiving ipilimumab. Eur J Nucl Med Mol Imaging. 2018;45(3):376-383.
26. Liu N, Liu ZM, Zhou YB, et al. Efficacy and safety of camrelizumab combined with FLOT versus FLOT alone as neoadjuvant therapy in patients with resectable locally advanced gastric and gastroesophageal junction adenocarcinoma who received D2 radical gastrectomy. J Clin Oncol. 2021;39(15 suppl):e16020.
27. Liu Y, Han GS, Li HL, et al. Camrelizumab combined with FLOFOX as neoadjuvant therapy for resectable locally advanced gastric and gastroesophageal junction adenocarcinoma: Updated results of efficacy and safety. J Clin Oncol. 2021;39(15 suppl):4036.
28. Athauda A, Starling N, Chau I, et al. Perioperative FLOT plus anti-PD-L1 avelumab (FLOT-A) in resectable oesophagogastric adenocarcinoma (OGA): Interim safety analysis results from the ICONIC trial. J Clin Oncol. 2021;39(3 suppl):201.
29. Alcindor T, Opu T, Elkrief A, et al. Phase II trial of perioperative chemotherapy + avelumab in locally advanced gastroesophageal adenocarcinoma: Preliminary results. J Clin Oncol. 2021;39(15 suppl):4046.
30. Al-Batran S-E, Lorenzen S, Homann N, et al. Pathological regression in patients with microsatellite instability (MSI) receiving perioperative atezolizumab in combination with FLOT vs. FLOT alone for resectable esophagogastric adenocarcinoma: Results from the DANTE trial of the German Gastric Group at the AIO and SAKK. Ann Oncol. 2021;32(S5):S1069.
31. Li HL, Deng JY, Ge SH, et al. Phase II study of perioperative toripalimab in combination with FLOT in patients with locally advanced resectable gastric/gastroesophageal junction (GEJ) adenocarcinoma. J Clin Oncol. 2021;39(15 suppl):4050.
32. Li S, Yu WB, Xie F, et al. A prospective, phase II, single-arm study of neoadjuvant/conversion therapy with camrelizumab, apatinib, S-1 ± oxaliplatin for locally advanced cT4a/bN+ gastric cancer. J Clin Oncol. 2021;39(15 suppl):4061.
33. Lin JX, Xu YC, Lin W, et al. Effectiveness and safety of apatinib plus chemotherapy as neoadjuvant treatment for locally advanced gastric cancer: A nonrandomized controlled trial. JAMA Netw Open. 2021;4(7):e2116240.
34. Zheng Y, Yang X, Yan C, et al. Effect of apatinib plus neoadjuvant chemotherapy followed by resection on pathologic response in patients with locally advanced gastric adenocarcinoma: A single-arm, open-label, phase II trial. Eur J Cancer. 2020;130:12-19.
35. Yi M, Jiao D, Qin S, et al. Synergistic effect of immune checkpoint blockade and anti-angiogenesis in cancer treatment. Mol Cancer. 2019;18(1):60.
36. Wei J, Lu XF, Liu Q, et al. SHARED: Efficacy and safety of sintilimab in combination with concurrent chemoradiotherapy (cCRT) in patients with locally advanced gastric (G) or gastroesophageal junction (GEJ) adenocarcinoma. J Clin Oncol. 2021;39(15 suppl):4040.
37. Tang ZQ, Wang Y, Liu D, et al. Phase II study of neoadjuvant camrelizumab combined with chemoradiation for locally advanced proximal gastric cancer (Neo-PLANET, NCT03631615). Ann Oncol. 2021;32(S5):S1049.
38. Topalian SL, Taube JM, Pardoll DM. Neoadjuvant checkpoint blockade for cancer immunotherapy. Science. 2020;367(6477):eaax0182.
39. Keung EZ, Ukponmwan EU, Cogdill AP, et al. The rationale and emerging use of neoadjuvant immune checkpoint blockade for solid malignancies. Ann Surg Oncol. 2018;25(7):1814-1827.
40. O'Donnell JS, Hoefsmit EP, Smyth MJ, et al. The promise of neoadjuvant immunotherapy and surgery for cancer treatment. Clin Cancer Res. 2019;25(19):5743-5751.
41. Liu J, Blake SJ, Yong MC, et al. Improved efficacy of neoadjuvant compared to adjuvant immunotherapy to eradicate metastatic disease. Cancer Discov. 2016;6(12):1382-1399.
42. Stahl M, Walz MK, Stuschke M, et al. Phase III comparison of preoperative chemotherapy compared with chemoradiotherapy in patients with locally advanced adenocarcinoma of the esophagogastric junction. J Clin Oncol. 2009;27(6):851-856.

43. Stahl M, Walz MK, Riera-Knorrenschild J, et al. Preoperative chemotherapy versus chemoradiotherapy in locally advanced adenocarcinomas of the oesophagogastric junction (POET): Long-term results of a controlled randomised trial. Eur J Cancer. 2017;81:183-190.
44. Ajani JA, Winter K, Okawara GS, et al. Phase II trial of preoperative chemoradiation in patients with localized gastric adenocarcinoma (RTOG 9904): quality of combined modality therapy and pathologic response. J Clin Oncol. 2006;24(24):3953-3958.
45. van Hagen P, Hulshof MC, van Lanschot JJ, et al. Preoperative chemoradiotherapy for esophageal or junctional cancer. N Engl J Med. 2012;366(22):2074-2084.
46. Klevebro F, Alexandersson von Döbeln G, Wang N, et al. A randomized clinical trial of neoadjuvant chemotherapy versus neoadjuvant chemoradiotherapy for cancer of the oesophagus or gastro-oesophageal junction. Ann Oncol. 2016;27(4):660-667.
47. Pietrantonio F, Miceli R, Raimondi A, et al. Individual patient data meta-analysis of the value of microsatellite instability as a biomarker in gastric cancer. J Clin Oncol. 2019;37(35):3392-3400.
48. Smyth EC, Wotherspoon A, Peckitt C, et al. Mismatch repair deficiency, microsatellite instability, and survival: An exploratory analysis of the medical research council adjuvant gastric infusional chemotherapy (MAGIC) trial. JAMA Oncol. 2017;3(9):1197-1203.
49. Hofheinz RD, Hegewisch-Becker S, Kunzmann V, et al. Trastuzumab in combination with 5-fluorouracil, leucovorin, oxaliplatin and docetaxel as perioperative treatment for patients with human epidermal growth factor receptor 2-positive locally advanced esophagogastric adenocarcinoma: A phase II trial of the Arbeitsgemeinschaft Internistische Onkologie Gastric Cancer Study Group. Int J Cancer. 2021;149(6):1322-1331.
50. Janjigian YY, Kawazoe A, Yañez P, et al. The KEYNOTE-811 trial of dual PD-1 and HER2 blockade in HER2-positive gastric cancer. Nature. 2021;600(7890):727-730.
51. Nishigori T, Tsunoda S, Obama K, et al. Optimal cutoff values of skeletal muscle index to define sarcopenia for prediction of survival in patients with advanced gastric cancer. Ann Surg Oncol. 2018;25(12):3596-3603.
52. Guo W, Ou G, Li X, et al. Screening of the nutritional risk of patients with gastric carcinoma before operation by NRS 2002 and its relationship with postoperative results. J Gastroenterol Hepatol. 2010;25(4):800-803.
53. Kang BW, Chau I. Current status and future potential of predictive biomarkers for immune checkpoint inhibitors in gastric cancer. ESMO Open. 2020;5(4):e000791.
54. Wang Y, Liu Z, Shan F, et al. Optimal timing to surgery after neoadjuvant chemotherapy for locally advanced gastric cancer. Front Oncol. 2020;10:613988.
55. Liu Y, Zhang KC, Huang XH, et al. Timing of surgery after neoadjuvant chemotherapy for gastric cancer: Impact on outcomes. World J Gastroenterol. 2018;24(2):257-265.
56. Ocaña Jiménez J, Priego P, Cuadrado M, et al. Impact of interval timing to surgery on tumor response after neoadjuvant treatment for gastric cancer. Rev Esp Enferm Dig. 2020;112(8):598-604.
57. Liu J, O'Donnell JS, Yan J, et al. Timing of neoadjuvant immunotherapy in relation to surgery is crucial for outcome. Oncoimmunology. 2019;8(5):e1581530.
58. Fiteni F, Westeel V, Pivot X, et al. Endpoints in cancer clinical trials. J Visc Surg. 2014;151(1):17-22.
59. Hellmann MD, Chaft JE, William WN Jr, et al. Pathological response after neoadjuvant chemotherapy in resectable non-small-cell lung cancers: proposal for the use of major pathological response as a surrogate endpoint. Lancet Oncol. 2014;15(1):e42-50.
60. Pataer A, Weissferdt A, Vaporciyan AA, et al. Evaluation of pathologic response in lymph nodes of patients with lung cancer receiving neoadjuvant chemotherapy. J Thorac Oncol. 2021;16(8):1289-1297.
61. Smyth EC, Fassan M, Cunningham D, et al. Effect of pathologic tumor response and nodal status on survival in the medical research council adjuvant gastric infusional chemotherapy trial. J Clin Oncol. 2016;34(23):2721-2727.
62. Forde PM, Chaft JE, Smith KN, et al. Neoadjuvant PD-1 blockade in resectable lung cancer. N Engl J Med. 2018;378(21):1976-1986.
63. Borcoman E, Kanjanapan Y, Champiat S, et al. Novel patterns of response under immunotherapy. Ann Oncol. 2019;30(3):385-396.
64. Han XJ, Alu A, Xiao YN, et al. Hyperprogression: A novel response pattern under immunotherapy. Clin Transl Med. 2020;10(5):e167.
65. Frelaut M, du Rusquec P, de Moura A, et al. Pseudoprogression and hyperprogression as new forms of response to immunotherapy. BioDrugs. 2020;34(4):463-476.
66. Lee JH, Long GV, Menzies AM, et al. Association between circulating tumor DNA and pseudoprogression in patients with metastatic melanoma treated with anti-programmed cell death 1 antibodies. JAMA Oncol. 2018;4(5):717-721.
67. Aide N, Hicks RJ, Le Tourneau C, et al. FDG PET/CT for assessing tumour response to immunotherapy: Report on the EANM symposium on immune modulation and recent review of the literature. Eur J Nucl Med Mol Imaging. 2019;46(1):238-250.
68. Goldfarb L, Duchemann B, Chouahnia K, et al. Monitoring anti-PD-1-based immunotherapy in non-small cell lung cancer with FDG PET: introduction of iPERCIST. EJNMMI Res. 2019;9(1):8.
69. Tao X, Li N, Wu N, et al. The efficiency of ^{18}F-FDG PET-CT for predicting the major pathologic response to the neoadjuvant PD-1 blockade in resectable non-small cell lung cancer. Eur J Nucl Med Mol Imaging. 2020;47(5):1209-1219.
70. Cottrell TR, Thompson ED, Forde PM, et al. Pathologic features of response to neoadjuvant anti-PD-1 in resected non-small-cell lung carcinoma: a proposal for quantitative immune-related pathologic response criteria (irPRC). Ann Oncol. 2018;29(8):1853-1860.
71. Stein JE, Lipson EJ, Cottrell TR, et al. Pan-tumor pathologic scoring of response to PD-(L)1 blockade. Clin Cancer Res. 2020;26(3):545-551.

DOI 10.1007/s10330-022-0551-1
Cite this article as: Li WT, Yu SY. Research progress on immune checkpoint inhibitors in neoadjuvant therapy for gastric cancer. Oncol Transl Med. 2022;8(2):74–82.

Oncology and Translational Medicine
DOI 10.1007/s10330-022-0553-3
April 2022, Vol. 8, No. 2, P83–P88

ORIGINAL ARTICLE

Automatic delineation of organs at risk in non-small cell lung cancer radiotherapy based on deep learning networks*

Anning Yang[1], Na Lu[2], Huayong Jiang[2], Diandian Chen[2], Yanjun Yu[2], Yadi Wang[2], Qiusheng Wang[1], Fuli Zhang[2] (✉)

[1] School of Automation Science and Electrical Engineering, Beihang University, Beijing 100191, China
[2] Department of Radiation Oncology, the Seventh Medical Center of Chinese PLA General Hospital, Beijing 100700, China

Abstract

Objective To introduce an end-to-end automatic segmentation method for organs at risk (OARs) in chest computed tomography (CT) images based on dense connection deep learning and to provide an accurate auto-segmentation model to reduce the workload on radiation oncologists.

Methods CT images of 36 lung cancer cases were included in this study. Of these, 27 cases were randomly selected as the training set, six cases as the validation set, and nine cases as the testing set. The left and right lungs, cord, and heart were auto-segmented, and the training time was set to approximately 5 h. The testing set was evaluated using geometric metrics including the Dice similarity coefficient (DSC), 95% Hausdorff distance (HD95), and average surface distance (ASD). Thereafter, two sets of treatment plans were optimized based on manually contoured OARs and automatically contoured OARs, respectively. Dosimetric parameters including Dmax and Vx of the OARs were obtained and compared.

Results The proposed model was superior to U-Net in terms of the DSC, HD95, and ASD, although there was no significant difference in the segmentation results yielded by both networks ($P > 0.05$). Compared to manual segmentation, auto-segmentation significantly reduced the segmentation time by nearly 40.7% ($P < 0.05$). Moreover, the differences in dose-volume parameters between the two sets of plans were not statistically significant ($P > 0.05$).

Conclusion The bilateral lung, cord, and heart could be accurately delineated using the DenseNet-based deep learning method. Thus, feature map reuse can be a novel approach to medical image auto-segmentation .

Received: 15 January 2022
Revised: 11 March 2022
Accepted: 10 April 2022

Key words: non-small cell lung cancer; organs at risk; medical image segmentation; deep learning; DenseNet

In a typical clinical workflow of radiotherapy (RT), a radiation oncologist manually segments a tumor target and the organs at risk (OARs) based on the information provided by the computed tomography (CT), magnetic resonance, and/or positron emission tomography/CT images [1, 2]. However, this process is usually time-consuming and laborious, and the quality of segmentation significantly depends on the prior knowledge and/or experience of the radiation oncologist. Although it is easy to distinguish organs with high contrast in CT images, distinguishing the boundary between a tumor tissue and surrounding normal tissue with similar contrast is difficult. Furthermore, inconsistencies in the target and OARs segmentations have been reported for both inter- and intra-observer segmentation variability [3-7]. These factors affect the accuracy and efficacy of RT. Therefore, it is imperative to improve the consistency and efficiency of image segmentation.

✉ Correspondence to: Fuli Zhang. Email: radiozfli@163.com
* Supported by a grant from the Beijing Municipal Science and Technology Commission Foundation Programme (No. Z181100001718011).

In recent years, deep learning-based automatic medical image segmentation learning has emerged as a popular topic in the field of RT [8-10]. Huang *et al.* [11] proposed the DenseNet network, which deploys the concept of feature map reuse for small training datasets in supervised learning. DenseNet connects multiple dense blocks with a transition layer and concatenates the channels of each dense block feature map in series to increase the number of feature maps and improve their utilization rate.

In this study, FC_DenseNet, a deep learning model based on DenseNet and fully convolutional networks, was employed. The model learns the planar distribution characteristics of the OARs in CT images through the dense block module to achieve end-to-end accurate OARs delineation for non-small cell lung cancer (NSCLC) patients.

Materials and methods

Data acquisition and preprocessing

CT images of 36 NSCLC patients from the Seventh Medical Center of the PLA General Hospital were acquired. The obtained four-dimensional-CT images were scanned using a Philips Brilliance Big Bore simulator (Philips Medical Systems, Madison, WI, USA) from the level of the larynx to the bottom of the lungs with a 3-mm slice thickness in the helical scan mode. This study was approved by the Ethics Committee of the Seventh Medical Center at the Chinese PLA General Hospital. All the patients provided written consent towards recording their medical information in the hospital database. By analyzing the DICOM file, the grey value of the original CT image was mapped to a range of 0–255, and the window width and level were set to 400 and 40, respectively. Different OARs were filled with different grayscale values to generate masked images as training labels, as shown in Fig. 1.

The training and validation datasets comprised 3803 CT images recorded from 27 patients and 650 images recorded from six patients, respectively. The testing set included 567 images recorded from nine patients. After data cleaning and enhancement, the images were sent to FC_DenseNet. All the training, validation, and testing tasks were performed on an 11-GB NVIDIA GeForce GTX 1080 Ti GPU. The start and end times of the manual and auto-segmentation operations for each patient in the testing set were recorded.

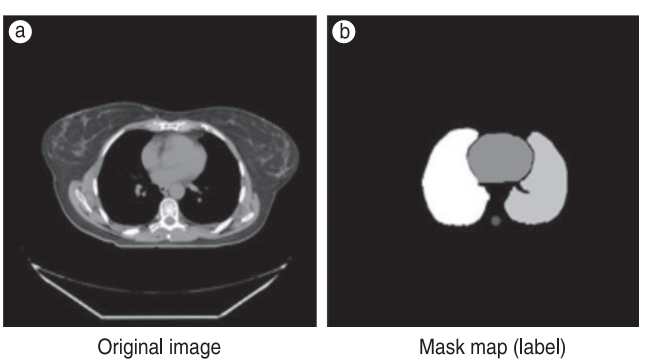

Fig. 1 Original image and mask map (label)

FC_DenseNet model for segmentation

In this study, FC_DenseNet was trained to auto-segment four types of OARs for diagnosing or monitoring NSCLC. The specific architecture of the model is illustrated in Fig. 2. The segmentation process was primarily divided into two parts: (a) The left half, called the analysis path, was composed of a density block module and transition down module connected by a short cut layer to extract image features. (b) The right half, called the synthesis path, was upsampled by the transition-up transposition convolution module to recover the size of the feature image layer. To improve the accuracy of the reconstructed image and accelerate the convergence of the network parameters, feature maps of the same size in the analysis path were connected in series as the input to the next layer of the

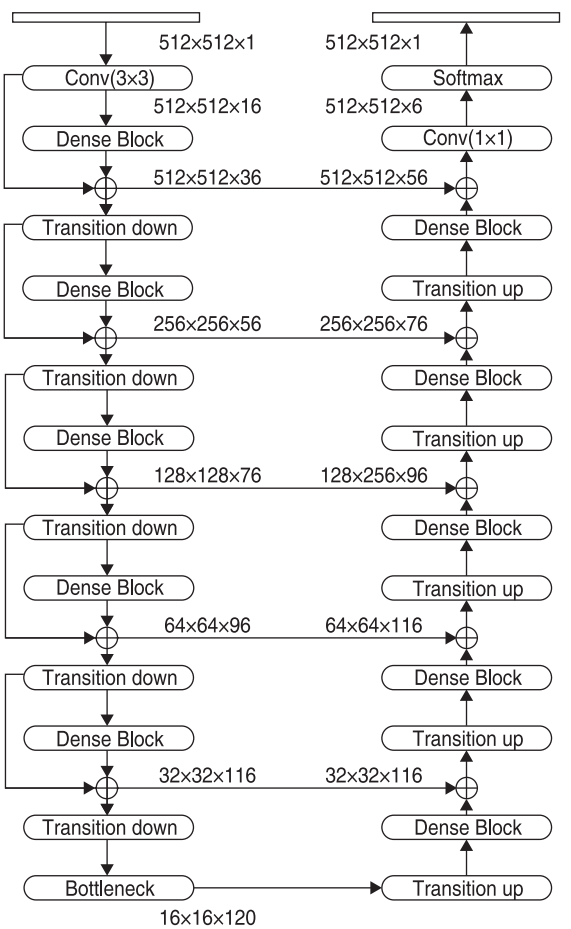

Fig. 2 Scheme of FC_DenseNet

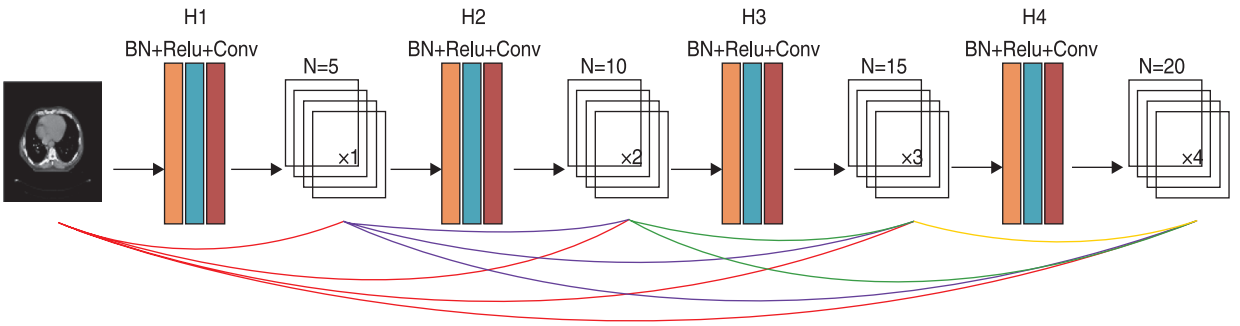

Fig. 3 Scheme of Dense Block

density block.

The input to each layer of the dense block was composed of all the outputs of the front layer after a dense connection (as shown in Fig. 3). The output of each layer possessed the following corresponding functional relationship with the output of the other front layers:

$$X_{i+1} = H(X_1, X_2, \ldots, X_i) \quad (1)$$

where H (*) is a nonlinear function, denoting a series of operations, including batch normalization, ReLU activation, pooling, and convolution, that were used to extract features, adjust the size of the feature map, and reduce the channel dimension. A bottleneck architecture was set in each network, as the operation of dense connections could induce a surge in the number of channels and increase the training difficulty. The bottleneck architecture uses a 1 × 1 convolution kernel to realize cross-channel feature fusion and enhance the feature extraction ability of the network.

FC_DenseNet training

Following cleaning and augmentation, the data were sent to the FC_DenseNet for training. The weight and bias of the network were updated using the cross-entropy loss function, as follows:

$$L_S = -\sum_{i=1}^{k}\left(y\log\hat{y} + (1-y)\log(1-\hat{y})\right) \quad (2)$$

$$\hat{y} = (1+e^{-w^T x+b})^{-1} \quad (3)$$

where χ is the input of the network, $\hat{y}$ is the posterior probability output after network regression, and κ is the number of categories.

In this study, an early stop module was incorporated to detect the network accuracy and loss function value with an increase in the iterative epoch, and the network architecture of DensNet56 in the 30th epoch was selected. During the network training process, the initial learning rate was set to 1e-3, which decreased with an increase in the epoch. This ensured that the network could converge quickly in the initial stage of training while preventing poor feature generalization arising from network overfitting. The average segmentation time of the training set and that of a single 512 × 512 CT image were set to approximately 12.58 min/epoch and 0.17s, respectively. Approximately 13.4 s were required to delineate all the CT images of a patient.

Accuracy evaluation

The auto-segmentation performance was evaluated based on geometric evaluation indices, including the Dice coefficient (DSC), 95% Hausdorff distance (HD95), and average surface distance (ASD). The OAR segmentation performance of the FC_DenseNet network was compared with that of U-Net. Thereafter, two sets of RT plans were optimized with manually contoured OARs and automatically contoured OARs, respectively. Dosimetric parameters including Dmax (i.e., the dose received by 2% of the volume) and V_x (i.e., the volume receiving more than x Gy dose as a percentage of the total volume) were obtained and compared.

Statistical analysis

SPSS 20.0, a statistical software (version 20.0, SPSS Inc., Chicago, USA), was used for the Wilcoxon signed rank test, and the difference, at a significance level of $\alpha = 0.05$, $P < 0.05$, was found to be statistically significant.

Table 1 Comparison of Dice parameters for both networks ($\bar{\chi} \pm s$)

	Cord	Heart	Right lung	Left lung
Densenet	0.90 ± 0.02	0.84 ± 0.10	0.93 ± 0.06	0.97 ± 0.01
U-Net	0.87±0.05	0.82 ± 0.12	0.92 ± 0.07	0.96 ± 0.02
P value	0.106	0.752	0.904	0.141

Table 2 Comparison of HD95 parameters for both networks ($\bar{\chi} \pm s$)

	Cord	Heart	Right lung	Left lung
Densenet	1.85 ± 0.36	15.95 ± 16.0	9.48 ± 5.50	6.97 ± 3.41
U-Net	2.42 ± 0.66	18.65 ± 15.2	13.2 ± 8.99	9.56 ± 4.62
P value	0.109	0.930	0.642	0.255

Table 3 Comparison of ASD parameters for both networks ($\bar{\chi} \pm s$)

	Cord	Heart	Right lung	Left lung
Densenet	0.69±0.13	6.98±5.55	1.81±1.61	1.11±0.51
U-Net	0.86±0.26	7.52±4.65	2.55±2.82	1.72±0.60
P value	0.304	0.900	0.789	0.053

Results

The geometric evaluation indices including DSC, HD95, ASD for the FC_DenseNet and U-Net networks are listed in Tables 1–3, respectively. As can be inferred, DenseNet outperforms U-Net, although there is no significant difference between the two ($P > 0.05$). A comparison of the results obtained for automatic and manual segmentation based on DenseNet for a typical patient is presented in Figure 4. The dose-volume parameters of the OARs based on manual and automatic segmentation are listed in Table 4. There are no statistically significant differences between the dosimetric parameters of the manually and automatically delineated OARs ($P > 0.05$). The average time of manual segmentation by a radiation oncologist for nine patients in the testing set is 15.2 min. Whereas, auto-segmentation, which can be achieved with an average segmentation time of 9.0 min, significantly improves the delineation efficiency ($P < 0.05$).

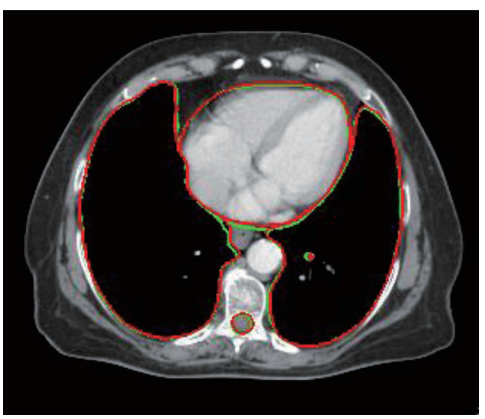

Fig. 4 Schematic of automatic OAR segmentation using the DenseNet network (green and red lines represent manual and automatic segmentation contours, respectively)

Table 4 Dosimetric comparison of the OARs between manual and DenseNet auto-segmentation.

Dosimetric parameters		Manual	AI	*P* value
Spinal Cord	Dmax	16.15±8.62	18.75±7.41	0.314
Heart	V30	0.40±1.09	0.06±0.12	0.180
	V40	0.19±0.56	0.03±0.07	0.180
	Mean (Gy)	1.71±1.58	1.33±1.17	0.110
Lung All	V5	27.55±6.81	28.19±6.78	0.515
	V10	15.49±4.41	14.83±4.54	0.953
	V20	9.40±3.69	9.44±3.89	0.859
	V30	6.57±3.25	6.64±3.36	0.263
	Mean (Gy)	6.49±1.94	6.56±2.01	0.173
MU		979.56±97.49	977.11±102.19	0.515

Discussion

As can be observed from the results produced by both networks, it is easier to segment the lungs than it is to segment the spinal cord and heart. In the original CT image, there are obvious boundaries between the left and right lungs; further, the deep learning network makes it easier to extract the edge features. Compared to the lungs, although the spinal cord possesses a bone structure as a support and obvious texture and edge differentiation, it accounts for less area in the image. The negative samples in the background image significantly outnumber the positive samples in the spinal cord, thereby producing an imbalance that degrades the segmentation accuracy. The heart is at the center of the slice and is surrounded by other organs such as the larynx and esophagus. The image features at the center are not strong, which makes the segmentation result slightly worse than that of the lungs.

Compared to U-Net, the average DSC of FC_DenseNet is slightly higher, and the variance is small, which indicates that the auto-segmentation performance of FC_DenseNet is more stable, and the generalization of the model is better. The HD95 score is an index used to measure the maximum distortion of the segmentation results, and it is influenced by the number of outliers. FC_DenseNet had better continuity and produced fewer outliers. The number of CT layers for each patient was not the same; therefore, the segmentation time for each patient was different. According to the evaluation benchmark [12] provided by the report on the thoracic organs auto-segmentation challenge organized by the American Association of Medical Physicists annual meeting in 2017, the organ with the highest DSC is the lung, with an average value between 0.95 and 0.98. The results of our study are relatively consistent with this value. Zhang *et al.* [13] developed a two-dimensional-AS-CNN based on the ResNet101 network using a dataset of 250 lung cancer patients. The average DSC scores for the left lung, heart, right lung, spinal cord, and esophagus were 0.94, 0.89, 0.94, 0.82, and 0.73, respectively. The DSC score of the spinal cord obtained by the proposed model was 0.89, which was significantly better than that of the AS-CNN. FC_DenseNet, used in this study, is a lightweight model with a more concise architecture.

Owing to the difference in the training datasets, it was difficult to compare the advantages and disadvantages of the proposed method and those of the extant method. However, although significantly fewer training cases were used in this study, FC_DenseNet exhibited a strong feature extraction ability in the training of small samples, and the segmentation results were similar to those of the training model with large datasets.

Zhu *et al.* [14] proposed an auto-segmentation model based on depth convolution to segment the CT images

of patients with lung cancer. In this model, a U-shaped network with a three-dimensional convolution kernel was used. The HD95 score was between 7.96 mm and 8.74 mm, and the ASD was between 1.81 mm and 2.92 mm. The resulting segmentation performance was significantly better than that of DenseNet. This may be because DenseNet, used in this study, is a two-dimensional model, and the extracted features are different owing to the poor continuity of the feature sequence in space.

Currently, there exist three primary development directions for deep learning networks in medical image segmentation. The first direction is to deepen the network level and depth, extract deeper semantic features to obtain a stronger expression ability, or widen the network to increase the number of channels to obtain additional information in the same layer such as the texture features of different frequencies and boundary features in different directions. The second direction is to achieve a more effective spatial feature extraction ability by learning the sequence association properties of multiple CT levels of a given case, represented by three-dimensional U-Net and several other derivative networks. The third direction, represented by DenseNet, is to improve the utilization rate of feature maps by sharing them layer by layer to enhance the feature expression ability of the image and improve the generalization performance of the network [15].

Herein, the results demonstrated that FC_DenseNet outperforms U-Net with regard to the segmentation of OARs; even when the training set contained fewer images, FC_DenseNet still effectively prevented overfitting. Simultaneously, it prevented gradient disappearance during the training process by repeatedly using different levels of feature maps. Thus, this study provides a new approach for medical-image segmentation.

Acknowledgments
Not applicable.

Funding
Supported by a grant from the Beijing Municipal Science and Technology Commission Programme (No. Z181100001718011).

Conflicts of interest
The authors indicated no potential conflicts of interest.

Author contributions
Fuli Zhang and Qiusheng Wang contributed conception and design of the study. Fuli Zhang and Anning Yang trained the deep learning models, Anning Yang drafted the manuscript. Na Lu, Huayong Jiang, Diandian Chen, Yanjun Yu and Yadi Wang helped to collect the data and evaluate radiotherapy planning. All authors read, discussed and approved the final manuscript.

Data availability statement
The data that support the findings of this study are available from the corresponding author upon reasonable request.

Ethical approval
Not applicable.

References

1. Eaton BR, Pugh SL, Bradley JD, et al. Institutional Enrollment and Survival Among NSCLC Patients Receiving Chemoradiation: NRG Oncology Radiation Therapy Oncology Group (RTOG) 0617. J Natl Cancer Inst. 2016;108(9):djw034.
2. Wang EH, Rutter CE, Corso CD, et al. Patients selected for definitive concurrent chemoradiation at high-volume facilities achieve improved survival in stage III non-small-cell lung cancer. J Thorac Oncol. 2015;10(6):937-943.
3. Martin S, Johnson C, Brophy M, et al. Impact of target volume segmentation accuracy and variability on treatment planning for 4D-CT-based non-small cell lung cancer radiotherapy. Acta Oncol. 2015;54(3):322-332.
4. Speight R, Sykes J, Lindsay R, et al. The evaluation of a deformable image registration segmentation technique for semi-automating internal target volume (ITV) production from 4DCT images of lung stereotactic body radiotherapy (SBRT) patients. Radiother Oncol. 2011;98(2):277-283.
5. van Dam IE, van Sornsen de Koste JR, Hanna GG, et al. Improving target delineation on 4-dimensional CT scans in stage I NSCLC using a deformable registration tool. Radiother Oncol. 2010;96(1):67-72.
6. Jameson MG, Holloway LC, Vial PJ, et al. A review of methods of analysis in contouring studies for radiation oncology. J Med Imaging Radiat Oncol. 2010;54(5):401-410.
7. Brouwer CL, Steenbakkers RJ, van den Heuvel E, et al. 3D Variation in delineation of head and neck organs at risk. Radiat Oncol. 2012;7:32.
8. Wong J, Fong A, McVicar N, et al. Comparing deep learning-based auto-segmentation of organs at risk and clinical target volumes to expert inter-observer variability in radiotherapy planning. Radiother Oncol. 2020;144:152-158.
9. Wang Z, Chang Y, Peng Z, et al. Evaluation of deep learning-based auto-segmentation algorithms for delineating clinical target volume and organs at risk involving data for 125 cervical cancer patients. J Appl Clin Med Phys. 2020;21(12):272-279.
10. Men K, Dai J, Li Y. Automatic segmentation of the clinical target volume and organs at risk in the planning CT for rectal cancer using deep dilated convolutional neural networks. Med Phys. 2017;44(12):6377-6389.
11. Huang G, Liu Z, Van Der Maaten L, et al. Densely Connected Convolutional Networks. IEEE Conference on Computer Vision and Pattern Recognition; 2017. Available at: https://doi.org/10.48550/arXiv.1608.06993
12. Yang J, Veeraraghavan H, Armato SG 3rd, et al. Autosegmentation for thoracic radiation treatment planning: A grand challenge at AAPM 2017. Med Phys. 2018;45(10):4568-4581.
13. Zhang T, Yang Y, Wang J, et al. Comparison between atlas and convolutional neural network based automatic segmentation of multiple organs at risk in non-small cell lung cancer. Medicine (Baltimore). 2020;99(34):e21800.
14. Zhu J, Zhang J, Qiu B, et al. Comparison of the automatic

segmentation of multiple organs at risk in CT images of lung cancer between deep convolutional neural network-based and atlas-based techniques. Acta Oncol. 2019;58(2):257-264.
15. Ke L, Deng Y, Xia W, et al. Development of a self-constrained 3D DenseNet model in automatic detection and segmentation of nasopharyngeal carcinoma using magnetic resonance images. Oral Oncol. 2020;110:104862.

DOI 10.1007/s10330-022-0553-3
Cite this article as: Yang AN, Lu N, Jiang HY, et al. Automatic delineation of organs at risk (OARs) in NSCLC radiotherapy based on deep learning network. Oncol Transl Med. 2022;8(2):83–88.

Oncology and Translational Medicine
DOI 10.1007/s10330-021-0538-8

April 2022, Vol. 8, No. 2, P89–P93

ORIGINAL ARTICLE

Risk factors for lymph node metastasis of cN0 papillary thyroid carcinoma

Guangcai Niu, Hao Guo (✉)

Department of Oncological Surgery, Xuzhou Central Hospital, Xuzhou 221000, China

Abstract

Objective To investigate the risk factors for cervical lymph node metastasis of clinically lymph node-negative (cN0) papillary thyroid carcinoma (PTC).

Methods Patients and Methods: The clinicopathologic data of patients with cN0 PTC who underwent at least one lobectomy plus central lymph node dissection at Xuzhou Central Hospital from January 2018 to December 2020 were retrospectively collected and the risk factors of lymph node metastasis analyzed. Univariate and multivariate analyses were performed to detect the risk factors for cervical lymph node metastasis.

Results A total of 312 patients with cN0 PTC were enrolled in this study. The postoperative pathology results showed that 134 patients (42.9%) had central lymph node metastasis, of whom 24 (17.9%) had lateral lymph node metastasis (LLNM). The univariate analysis results showed that male gender, age <45 years, tumor diameter ≥10 mm, bilateral cancer, capsule invasion, and multiple foci were associated with cervical lymph node metastasis of cN0 PTC ($P < 0.05$). Further logistic regression analysis results showed that these factors, except age, were independent risk factors for cervical lymph node metastasis of cN0 PTC ($P < 0.05$). The results also showed that the risk of LLNM increased with an increase in the number of positive central lymph nodes in patients with cN0 PTC ($P < 0.05$).

Conclusion Cervical lymph node metastasis of cN0 PTC is related to many factors, and a high number of positive central lymph nodes indicates a high risk of LLNM. Patients with risk factors should undergo preventive central lymph node dissection at the first surgery, and in patients with a high number of positive central lymph nodes, lateral lymph node dissection should be discreetly performed.

Received: 22 November 2021
Revised: 21 December 2021
Accepted: 21 January 2022

Key words: papillary thyroid carcinoma; risk factor; complication

Papillary thyroid carcinoma (PTC) is the most well-known type of thyroid cancer, accounting for over 80% of all thyroid carcinoma cases [1]. The prognosis of patients with PTC is favorable; their 10-year survival rate is over 95% [2]. Though PTC exhibits a favorable prognosis, relatively low malignancy, and positive response to surgery, central lymph node metastasis (CLNM) is very common in PTC; it has been observed in 20%–90% of patients [3–4]. CLNM not only increases the recurrence rate and reduces disease-free survival time but also elevates the rates of lateral lymph node metastasis (LLNM) [5].

For the preoperative evaluation of patients suspected to have CLNM, central lymph node dissection (CLND) is strongly recommended in some guidelines. At present, contrast-enhanced computed tomography (CT) and neck ultrasound (US) are widely used for preoperative imaging to assess CLNM; unfortunately, the sensitivities of US (23%–53.2%) and contrast-enhanced CT (41%–66.7%) are particularly not high enough for accurate evaluation [6, 7]. For patients with cN0 stage PTC, prophylactic cervical lymph node dissection (PCLND) is still controversial.

Materials and methods

Patients

A total of 312 patients at the Xuzhou Central Hospital from January 2018 to December 2020 were eligible for the study. All the patients had to meet the following criteria: (1) all suspected cases of PTC without evidence of CLNM following US or CT examination; (2) all patients with no history of neck radiation or previous neck surgery; (3) PTC should have been diagnosed by intraoperative frozen or postoperative pathological examination; (4) all patients at the least underwent unilateral thyroidectomy with

✉ Correspondence to: Hao Guo. Email: m10046@126.com

CLND; 5) complete follow-up data.

Treatment

For patients with PTC, CLND is routinely performed in our hospital. The ipsilateral lobe and isthmus were resected for unilateral primary lesions while total thyroidectomy was performed for multiple lesions and bilateral primary lesions. According to previous studies, the rate of LLNM was associated with an increase in CLNM and tumor size. In our research, LLNM occurs only if there is CLNM and tumor diameter ≥10 mm on intraoperative frozen pathology [8]. Central lymph nodes lie in the center of the neck; they include the prelaryngeal, pretracheal, and paratracheal lymph nodes. Cervical lymph nodes are divided into levels I, II, III, IV, V, and VI. After surgery, all patients with PTC received levothyroxine (L-T4) for thyroid-stimulating hormone (TSH) suppression. Some patients with advanced disease received iodine-131 treatment.

Surgical complications

Total serum calcium and parathyroid hormone (PTH) levels were measured after surgery. The patients were considered to have permanent hypoparathyroidism when symptoms still existed or total serum calcium and PTH levels remained below the normal range for over half a year postoperatively. Direct fiber-optic laryngoscopy was performed to evaluate cord motility in all patients with PTC before and after surgery. The patients were considered to have permanent recurrent laryngeal nerve injury when the cord palsy remained unfixed for over half a year postoperatively.

Statistical analysis

Univariate and multivariate analyses were performed to determine the significant clinical characteristics. Univariate analyses were performed using the chi-squared test. Variables with $P < 0.05$ on univariate analysis were included for multivariate analysis. Multivariate analyses were performed using logistic regression analysis. The results were presented as odds ratios (OR) with 95% confidence intervals (CI) and P values. Differences associated with $P < 0.05$ were considered statistically significant. Statistical analysis was performed using SPSS 13.0 software (SPSS Inc, Chicago, USA).

Results

There were 312 patients enrolled in this study, including 217 females (69.6%) and 95 males (30.4%). Their median age at the time of PTC diagnosis was 46 years (ranged, 14–78 years). The tumor diameter ranged from 0.3–5.8 cm. A total of 139 patients had a tumor size ≤10 mm (44.6%), while 173 patients had a tumor size >10 mm (55.4%). There were 85 patients (27.2%) who exhibited multifocal disease and 227 (72.8%) had single lesions. There were 71 (22.8%) and 241 (77.2%) unilateral and bilateral tumors, respectively. Fifty-six patients had invasion of adjacent structures, such as the strap muscles, trachea, and recurrent laryngeal nerve. Thirty-eight patients had Hashimoto thyroiditis.

After the postoperative pathological examination, 134 (42.9%) patients were found to have CLNM, among whom 24 (17.9%) had LLNM. For 88 of the patients, the number of positive central lymph nodes was less than 3, and of these, only 11 had LLNM. For 46 of the patients, the number of positive central lymph nodes was greater than 3, and of these, 13 had LLNM. All patients with PTC underwent CLND. A total of 72 patients underwent both lobectomy and unilateral CLND. Total thyroidectomy combined with bilateral CLND was performed in 92 patients. Total thyroidectomy and unilateral CLND and LLND was performed in 87 patients. Total thyroidectomy combined with unilateral LLND and bilateral CLND was performed in 56 patients, and total thyroidectomy plus bilateral CLND and LLND was performed in 5 patients. The patients' surgery patterns are summarized in Table 1.

Univariate analysis revealed that male gender, age < 45 years, tumor diameter ≥10 mm, bilateral cancer, capsule invasion, and multiple foci were associated with CLNM of cN0 PTC ($P < 0.05$). Further logistic regression analysis results showed that these factors, except age, were independent risk factors for CLNM of cN0 PTC ($P < 0.05$). While it was found that the risk of LLNM increased with an increasing number of positive central lymph nodes in patients with cN0 PTC ($P < 0.05$) (Table 2 and 3), the X^2 test revealed that CLNM was an important risk factor for LLNM ($\chi^2 = 5.104$, $P = 0.024$; Table 4).

Table 5 shows the postoperative complications. Fifty-six patients (17.95%) had transient hypoparathyroidism that resolved within 6 months and 9 (2.88%) had persistent hypoparathyroidism over 6 months. Ten patients had vocal cord palsy, which implied recurrent laryngeal nerve injury: 8 (2.56%) recovered within 1 to 6 months while the other 2 (0.64%) had persistent injury. One patient (0.32%) underwent reoperation because of postoperative bleeding. Four patients (1.28%) had chyle leakage, which was cured within 30 days. Complications such as, hematoma, wound infection, and tracheal leakage were observed in 12 patients.

Table 1 Surgery pattern

Treatment	*n*
Lobectomy plus ipsilateral CLND	72
Lotal thyroidectomy plus bilateral CLND	92
Total thyroidectomy plus unilateral CLND and unilateral LLND	87
Total thyroidectomy plus bilateral CLND and unilateral LLND	56
Total thyroidectomy plus bilateral CLND and bilateral LLND	5

Table 2 Univariate analysis of cervical lymph node metastasis in cN0 PTM patients

Variables	*n*	Cervical lymph node metastasis	χ^2	*P*
Age (years)			4.1	0.043
≤ 45	131	65		
> 45	181	69		
Gender			9.191	0.002
Female	217	81		
Male	95	53		
Tumor diameter (cm)			8.539	0.003
≤1	139	47		
>1	173	87		
Bilateral neoplasms			9.852	0.002
No	241	92		
Yes	71	42		
Extrathyroid invasion			8.791	0.003
Yes	56	34		
No	256	100		
Multifocality			10.301	0.001
Yes	85	49		
No	227	85		
Thyroiditis			1.656	0.198
Yes	38	20		
No	274	114		

Table 3 Multivariable analysis of cervical lymph node metastasis in cN0 PTM patients

Variables	standard error	Wald	95%CI	*P*
Age	0.249	1.946	0.434–1.151	0.163
Gender	0.271	6.870	0.288–0.836	0.009
Tumor diameter	0.255	11.304	1.431–3.895	0.001
Location	0.300	6.815	1.216–3.942	0.009
Multifocality	0.278	5.795	0.297–0.883	0.016
Extrathyroid invasion	0.322	7.349	0.223–0.785	0.007

Table 4 Association between central lymph node metastasis and lateral lymph node metastasis

Central lymph node metastasis	*n*	Lateral lymph node metastasis		χ^2	*P*
		Positive	Negative		
1–3	88	11	77	5.104	0.024
> 3	46	13	33		

Table 5 The complications after operation

Complications	*n*	%
Transiet hypoparathyroidism	56	17.95
Persistent hypoparathyroidism	9	2.88
Transiet recurrent laryngeal nerve injury	8	2.56
Persistent recurrent laryngeal nerve injury	2	0.64
Chyle leakage	4	1.28
Bleeding	1	0.32
Others	12	3.85

Discussion

Most patients with PTC have an excellent prognosis and a low mortality rate; however, PTC also shows a high potency to spread to cervical lymph nodes [9]. CLNM existed in 20%–90% of patients with PTC. The low sensitivities of CT and US lead to inaccurate preoperative assessment. Unidentified metastatic lymph nodes remain in the neck and become the main source of recurrence, making patients suffer from reoperation, recurrence, and disease-specific mortality. In our study, the CLNM occurrence rate was 42.9%, which is comparable to that in previous studies [10, 4]. We found male gender, tumor diameter ≥10 mm, bilateral cancer, capsule invasion, and multiple foci to be closely associated with the probability of CLNM, which is consistent with previous reports [11–13]. Currently, there are no new or more accurate indicators of CLNM.

Many studies have reported that age is a risk factor for CLNM. The cut-off age of 45 years is associated with a poor prognosis and increased recurrence, and it is widely used as a clinical marker for prognosis [14]. In multivariate analyses, we observed that age was not a significant risk factor for CLNM in patients with stage cN0 PTC. Some scholars have also observed a positive correlation between age younger than 45 years and a higher rate of CLNM, while others used 55 years as the cut-off age [15–16].

There were 217 females (69.6%) and 95 males (30.4%) enrolled in this study. The central lymph nodes of 81 of the 217 female patients were positive while those of 53 of the 95 male patients were positive. The difference was statistically significant (P = 0.002). Although the incidence of PTC was higher among women, the rates of CLNM were higher in men, who happened to be more prone to unhealthy lifestyles [17].

As always, tumor size and capsule invasion are important factors in TNM staging and can, therefore be used to predict aggressiveness [18]. In our data, we found that tumor size >1 cm and capsule invasion exhibited a high association with the risk of CLNM in patients with cN0 PTC.

Multifocal PTC was always considered to involve intraglandular spread and be more aggressive than unifocal PTC. It was also reported that multiple tumors were associated with more aggressive clinicopathological features and a poor prognosis in patients with PTC [19]. Forty-nine of the 85 patients with multifocal disease had multifocal CLNM, while 85 of the 227 patients with single lesions had unifocal CLNM. The difference was statistically significant (P = 0.001). We also observed that cN0 CLNM was associated with bilateral tumors. However, Sun *et al.* [20] reported that bilateral tumors were not a significant risk factor for CLNM in patients with cN0. Our data also showed that there was no correlation

between Hashimoto's thyroiditis and CLNM in patients with cN0.

There is still no uniform conclusion on CLND, and whether PCLND is needed remains controversial. The Japanese Association of Endocrine Surgeons (JAES) routinely recommends [21]. Performing PCLND provides the most real and adequate TNM staging, allows for speculation about the prognosis, and contributes to the decision whether to administer TSH suppressive therapy or radioactive iodine (RAI) therapy. It also decreases recurrence, increases disease-free survival, and reduces the thyroglobulin levels during postoperative follow-up. In addition, PCLND can help reduce the chances of reoperation and any other associated complications. Some scholars have suggested performing PCLND only in a selected group of patients with the recognized factors of higher locoregional recurrence [22]. The American Thyroid Association (ATA) guidelines suggest that PCLND should be routinely performed only in patients with advanced disease: stages T3 and T4 [23]. One reason why the ATA discourages PCLND is that CLNM seems to affect recurrence rather than disease-free survival and the other is that most thyroid surgeons in the United States are not considered to be competent enough in the procedure [24].

Some scholars insist that PCLND may increase the chances of complications and has no benefits of survival for patients with PTC. Kim SK *et al.* [25] suggested that PCLND may not be suggested in PTC due to the absence of increased survival time and clear evidence of complications. Nonetheless, reoperation due to recurrence in cervical lymph nodes is inevitably associated with postoperative complications, such as hypoparathyroidism and recurrent laryngeal nerve injury. Lymph node resection means wide dissection; it may result in temporary or permanent dysphonia in up to 1%–3% of cases [26]. In our study, there were 10 patients with vocal cord palsy, which implied recurrent laryngeal nerve injury: 8 (2.56%) recovered within 1 to 6 months while the other 2 (0.64%) had persistent damage. Clearance of all the fatty and lymphatic tissues around the parathyroid glands, which may be unintentional, could cause permanent or transient hypoparathyroidism in up to 2%–5% and 10%–50% of cases, respectively [27]. We reported that 56 patients (17.95%) had transient hypoparathyroidism and 9 (2.88%) had persistent hypoparathyroidism. Our results are consistent with the results from previous studies. It was reported in some previous papers that the incidence of chyle leakage ranges from 0.5%–8.3% [28], and in our study, 4 patients (1.28%) had chyle leakage and they were cured within a month. According to our study, routine PCLND did not increase the chances of complications, but it helped in avoiding the potential risk of a second operation and in defining a more accurate stage.

We also found that there is a strong correlation between CLNM and LLNM. The incidence of LLNM increased with an increasing number of positive central lymph nodes. This can be explained by the dissemination of PTC. CLNM seldom occurs rapidly, and it tends to occur in a consecutive order from the central compartment to the lateral compartment lymph nodes. Chen *et al.* [16] reported in their study that 21 patients had skip metastasis, that is to say, there was LLNM with no CLNM. Hu *et al.* [29] reported that age >55 years, primary tumor located in the upper portion of the thyroid lobe, and unilaterality were associated with the risk of skip metastasis. The underlying mechanism of this form of metastasis is still unclear. In our study, there were 88 patients for whom the number of positive central lymph nodes was under 3, and of these, only 11 had LLNM. On the other hand, there were 46 patients for whom the number of positive central lymph nodes was greater than 3, and of these, 13 had LLNM. The difference was statistically significant ($P = 0.024$).

Conclusion

CLNM occurs frequently and it is not easy to detect preoperatively. Our results showed that there was an association between CLNM and male gender, tumor diameter ≥10 mm, bilateral cancer, capsule invasion, and presence of multiple foci. Patients whose number of positive central lymph nodes was greater than 3 were extremely prone to LLNM. The incidence of postoperative complications potentially caused by CLND was acceptable according to our study. Effectively assessing the risk factors for lymph node metastasis preoperatively is crucial for the development of individualized surgical plans. Routine PCLND does not increase the risk of postoperative complications and should be discreetly considered as a reasonable surgical treatment for patients with PTC.

Acknowledgments

Not applicable.

Funding

Not applicable.

Conflicts of interest

The authors indicated no potential conflicts of interest.

Author contributions

Not applicable.

Data availability statement

Not applicable.

Ethical approval

Not applicable.

References

1. Lundgren CI, Hall P, Dickman PW, et al. Clinically significant prognostic factors for differentiated thyroid carcinoma: a population-based, nested case-control study. Cancer. 2006;106(3):524-531.
2. Hay ID, Hutchinson ME, Gonzalez-Losada T, et al. Papillary thyroid microcarcinoma: a study of 900 cases observed in a 60-year period. Surgery. 2008;144(6):980-987; discussion 987-988.
3. Viola D, Materazzi G, Valerio L, et al. Prophylactic central compartment lymph node dissection in papillary thyroid carcinoma: clinical implications derived from the first prospective randomized controlled single institution study. J Clin Endocrinol Metab. 2015;100(4):1316-1324.
4. Kutler DI, Crummey AD, Kuhel WI. Routine central compartment lymph node dissection for patients with papillary thyroid carcinoma. Head Neck. 2012;34(2):260-263.
5. Liu FH, Kuo SF, Hsueh C, et al. Postoperative recurrence of papillary thyroid carcinoma with lymph node metastasis. J Surg Oncol. 2015;112(2):149-154.
6. Choi JS, Kim J, Kwak JY, et al. Preoperative staging of papillary thyroid carcinoma: comparison of ultrasound imaging and CT. AJR Am J Roentgenol. 2009;193(3):871-878.
7. Hwang HS, Orloff LA. Efficacy of preoperative neck ultrasound in the detection of cervical lymph node metastasis from thyroid cancer. Laryngoscope. 2011;121(3):487-491.
8. Zeng RC, Zhang W, Gao EL, et al. Number of central lymph node metastasis for predicting lateral lymph node metastasis in papillary thyroid microcarcinoma. Head Neck. 2014;36(1):101-106.
9. Malterling RR, Andersson RE, Falkmer S, et al. Differentiated thyroid cancer in a Swedish county–long-term results and quality of life. Acta Oncol. 2010;49(4):454-459.
10. Lim YS, Lee JC, Lee YS, et al. Lateral cervical lymph node metastases from papillary thyroid carcinoma: predictive factors of nodal metastasis. Surgery. 2011;150(1):116-121.
11. Tao Y, Wang C, Li L, et al. Clinicopathological features for predicting central and lateral lymph node metastasis in papillary thyroid microcarcinoma: Analysis of 66 cases that underwent central and lateral lymph node dissection. Mol Clin Oncol. 2017;6(1):49-55.
12. Zhao C, Jiang W, Gao Y, et al. Risk factors for lymph node metastasis (LNM) in patients with papillary thyroid microcarcinoma (PTMC): role of preoperative ultrasound. J Int Med Res. 2017;45(3):1221-1230.
13. Sapuppo G, Palermo F, Russo M, et al Latero-cervical lymph node metastases (N1b) represent an additional risk factor for papillary thyroid cancer outcome. J Endocrinol Invest. 2017;40(12):1355-1363.
14. Londero SC, Krogdahl A, Bastholt L, et al; Danish Thyroid Cancer Group-DATHYRCA (part of the DAHANCA organization). Papillary thyroid carcinoma in Denmark, 1996-2008: outcome and evaluation of established prognostic scoring systems in a prospective national cohort. Thyroid. 2015;25(1):78-84.
15. Obregón-Guerrero G, Martínez-Ordaz JL, Peña-García JF, et al. Factors associated with malignancy in patients with thyroid nodules. Cir Cir. 2010;78(6):479-484.
16. Chen Y, Chen S, Lin X, et al. Clinical analysis of cervical lymph node metastasis risk factors and the feasibility of prophylactic central lymph node dissection in papillary thyroid carcinoma. Int J Endocrinol. 2021;2021:6635686.
17. Rahbari R, Zhang L, Kebebew E. Thyroid cancer gender disparity. Future Oncol. 2010;6(11):1771-1779.
18. Tuttle RM, Haddad RI, Ball DW, et al. Thyroid carcinoma, version 2.2014. J Natl Compr Canc Netw. 2014;12(12):1671-1680; quiz 1680.
19. Lee SH, Lee SS, Jin SM, et al. Predictive factors for central compartment lymph node metastasis in thyroid papillary microcarcinoma. Laryngoscope. 2008;118(4):659-662.
20. Sun W, Lan X, Zhang H, et al. Risk factors for central lymph node metastasis in CN0 papillary thyroid carcinoma: A systematic review and meta-analysis. PLoS One. 2015;10(10):e0139021.
21. Takami H, Ito Y, Okamoto T, et al. Therapeutic strategy for differentiated thyroid carcinoma in Japan based on a newly established guideline managed by Japanese Society of Thyroid Surgeons and Japanese Association of Endocrine Surgeons. World J Surg. 2011;35(1):111-121.
22. Haddad RI, Nasr C, Bischoff L, et al. NCCN Guidelines Insights: Thyroid Carcinoma, Version 2.2018. J Natl Compr Canc Netw. 2018;16(12):1429-1440.
23. American Thyroid Association (ATA) Guidelines Taskforce on Thyroid Nodules and Differentiated Thyroid Cancer, Cooper DS, Doherty GM, Haugen BR, et al. Revised American Thyroid Association management guidelines for patients with thyroid nodules and differentiated thyroid cancer. Thyroid. 2009;19(11):1167-1214.
24. Saunders BD, Wainess RM, Dimick JB, et al. Who performs endocrine operations in the United States? Surgery. 2003;134(6):924-931; discussion 931.
25. Kim SK, Woo JW, Lee JH, et al. Prophylactic central neck dissection might not be necessary in papillary thyroid carcinoma: analysis of 11,569 cases from a single Institution. J Am Coll Surg. 2016;222(5):853-864.
26. Chisholm EJ, Kulinskaya E, Tolley NS. Systematic review and meta-analysis of the adverse effects of thyroidectomy combined with central neck dissection as compared with thyroidectomy alone. Laryngoscope. 2009;119(6):1135-1139.
27. Sadowski BM, Snyder SK, Lairmore TC. Routine bilateral central lymph node clearance for papillary thyroid cancer. Surgery. 2009;146(4):696-703; discussion 703-705.
28. Wu G, Chang X, Xia Y, et al. Prospective randomized trial of high versus low negative pressure suction in management of chyle fistula after neck dissection for metastatic thyroid carcinoma. Head Neck. 2012;34(12):1711-1715.
29. Hu D, Lin H, Zeng X, et al. Risk factors for and prediction model of skip metastasis to lateral lymph nodes in papillary thyroid carcinoma. World J Surg. 2020;44(5):1498-1505.

DOI 10.1007/s10330-021-0538-8
Cite this article as: Niu GC, Guo H. Risk factors for lymph node metastasis of cN0 papillary thyroid carcinoma. Oncol Transl Med. 2022;8(2):89–93.

Oncology and Translational Medicine
DOI 10.1007/s10330-021-0523-3

April 2022, Vol. 8, No. 2, P94–P99

ORIGINAL ARTICLE

Differential gene screening and functional analysis in docetaxel-resistant prostate cancer cell lines*

Ming Wang[1], Lei Wang[1] (Co-first author), Yan Zhang[1] (Co-first author), Chaoqi Wang[1] (✉), Shuang Li[2], Tao Fan[3]

[1] Department of Urinary Surgery, Affiliated Hospital of Inner Mongolia University for the Nationalities, Tongliao 028007, China
[2] Department of Pathology, The People's Hospital of China Three Gorges University, The First People's Hospital of Yichang, Yichang 443000, China
[3] Department of Oncology & Hematology, Hubei Provincial Hospital of Integrated Chinese and Western Medicine, Wuhan 430015, China

Abstract

Objective Docetaxel-based combination chemotherapy has traditionally been the standard treatment for metastatic castration-resistant prostate cancer (PCa). However, most patients eventually develop resistance to this treatment, which further reduces their survival. This study aimed to determine key molecular genes in docetaxel-resistant PCa cell lines using bioinformatic approaches.

Methods The analysis of microarray data GSE33455 (including DU-145/DU-145R and PC-3/PC-3R cell lines) obtained from the Gene Expression Omnibus (GEO) database was performed using GEO2R. Differentially expressed genes (DEGs) of DU-145/DU-145R and PC-3/PC-3R cell lines were selected, and the intersection of DEGs between the two groups was obtained. DEGs were annotated with the Gene Ontology (GO) function and enriched with the Kyoto Encyclopedia of Genes and Genomes (KEGG) pathway using an online platform (https://cloud.oebiotech.cn/task/detail/array_enrichment/). The online tool Search Tool for the Retrieval of Interacting Genes (https://string-db.org/) was used to obtain the DEG network graph and matrix list, which was imported into Cytoscape 3.6.1 and analyzed using the Molecular Complex Detection plug-in to detect potential functional modules in the network.

Results A total of 131 intersection DEGs were identified between non-treated and docetaxel-resistant PCa cell lines. GO functional annotation showed that the main genes involved were present in the plasma membrane and were involved in positive regulation of ubiquitin-protein transferase activity, positive regulation of pseudopodium assembly, centriolar subdistal appendage, and heterophilic cell–cell adhesion via plasma membrane cell adhesion molecules. KEGG pathway enrichment analysis revealed that DEGs were mainly involved in IL-17 signaling pathway, cytokine-cytokine receptor interaction, rheumatoid arthritis, legionellosis, and folate biosynthesis. We identified two distinct hubs of DEGs: (1) CD274, C-X-C motif chemokine ligand (CXCL)1, DExD/H-box helicase 58, CXCL2, CXCL8, colony-stimulating factor 2, C-X-C motif chemokine receptor 4 (CXCR4), CXCL5, and CXCL6 and (2) argininosuccinate lyase, argininosuccinate synthase 1, and asparagine synthetase. Except for the CXCR4 gene that was downregulated, the other 11 genes showed upregulated expression.

Conclusion Certain differential genes may be potential targets for predicting and treating metastatic docetaxel-resistant PCa.

Received: 24 September 2021
Revised: 12 November 2021
Accepted: 21 March 2022

Key words: docetaxel-resistant; prostate cancer; differentially expressed genes; bioinformatics; hub genes

The GLOBOCAN 2020 reports that prostate cancer (PCa) accounts for 7.3% of the 19.3 million new cancer cases worldwide [1], which is the second leading cause of cancer-related deaths in men in the USA [2], and its

✉ Correspondence to: Chaoqi Wang. Email: wangchaoqi001@163.com
* Supported by grants from the Natural Science Foundation of Inner Mongolia Autonomous Region, China (No. 2021MS08071), and the Medical and Health Science Research Program Project of Inner Mongolia Autonomous Region Health and Family Planning Commission, China (No. 202202264).

incidence in China is rapidly increasing [3]. Between 10% and 15% of patients present with advanced disease and receive hormone therapy as their initial treatment. However, most cases acquire therapy resistance within 2 years and progress to castration-resistant prostate cancer (CRPC) [4]. Docetaxel-based chemotherapy is the standard treatment for metastatic CRPC (mCRPC) [5]. Unfortunately, there is no effective treatment strategy for docetaxel-resistant patients with mCRPC. Moreover, the molecular mechanisms underlying docetaxel resistance remain unclear. In this study, the differentially expressed genes (DEGs) from the microarray data in the Gene Expression Omnibus (GEO) database were identified between non-treated and docetaxel-resistant PCa cell lines. We aimed to explore certain differential hub genes in docetaxel-resistant PCa using bioinformatic approaches.

Materials and methods

Microarray data filtering eligible dataset

We searched and downloaded microarray data GSE33455 (including DU-145, DU-145R, PC-3, and PC-3R cell lines) from the GEO database (www.ncbi.nlm.nih.gov/geo/). The four cell lines in GSE33455 were generated in androgen-independent cell lines. Microarray data were used to analyze the eligible dataset and identify the intersection of DEGs in docetaxel-resistant cell lines (DU-145/DU-145R and PC-3/PC-3R).

DEG screening

DEGs were independently screened using the GEO2R online tool in the GEO database. In our study, DEGs between non-treated and docetaxel-resistant PCa cells (DU-145 and DU-145R and PC-3 and PC-3R) were screened and selected using the cutoff point of adj. P value < 0.05 and |log FC| > 1.0. More accurate intersection DEGs were obtained through the online Venny map (https://bioinfogp.cnb.csic.es/tools/venny/index.html) after deleting duplicate and invalid genes.

Functional enrichment and protein–protein interaction analysis

The online platform (https://cloud.oebiotech.cn/task/detail/array_enrichment/) was used to analyze Gene Ontology (GO) functional annotation and Kyoto Encyclopedia of Genes and Genomes (KEGG) pathway enrichment. Furthermore, we obtained the protein–protein interaction (PPI) of differential genes using the Search Tool for the Retrieval of Interacting Genes database (STRING, https://string-db.org/), and one big pairing picture was generated. In this study, DEGs with a confidence score of >0.4 were selected to construct the PPI network.

Established DEG network

The DEG network was generated using Cytoscape 3.6.1 software [6]. The Molecular Complex Detection (MCODE) plug-in was used for module clustering analysis to detect potential functional modules in the network. In the MCODE process, the cutoff value of the degree was set to 2, and the cutoff value of the node score was set to 0.2.

Results

DEG screening

A total of 1,311 and 2,027 DEGs were identified in the DU-145/DU-145R and PC-3/PC-3R cell lines, respectively. Using the online Venny map (https://bioinfogp.cnb.csic.es/tools/venny/index.html), we obtained 131 more accurate DEGs.

GO and functional enrichment analysis

Pathway and process enrichment analyses were performed using GO biological processes (BPs), GO cellular components (CCs), GO molecular functions (MFs), KEGG functional sets, and KEGG pathway ontology sources. There were 73 BP annotated genes, 83 CC annotated genes, and 65 MF annotated genes. A bar chart was drawn for items in BP, CC, and MF of the GO enrichment analysis results, and the most significant top 10 GO items in the three categories of GO in the same chart were shown (Fig. 1a).

Through the BP, CC, and MF functional annotations of GO, we found that 131 DEGs were mainly involved in the plasma membrane, positive regulation of ubiquitin-protein transferase activity, positive regulation of pseudopodium assembly, centriolar subdistal appendage, heterophilic cell–cell adhesion via plasma membrane cell adhesion molecules (CAMs), helicase activity, Rho protein signal transduction, phospholipid translocation, integral component of membrane, and bicellular tight junction (Fig. 1a).

The KEGG pathway enrichment analysis showed that DEGs were mainly involved in the IL-17 signaling pathway, cytokine-cytokine receptor interaction, rheumatoid arthritis, legionellosis, folate biosynthesis, CAMs, mitophagy (animal), TNF signaling pathway, alanine, aspartate and glutamate metabolism, and Salmonella infection (Fig. 1b). A bubble chart was drawn for the KEGG pathway enrichment analysis results, and the most significant top 30 GO items in the KEGG database were shown (Fig. 1b).

Construction of DEG network analysis

Considering the selected 131 DEGs, we identified 103 PPI pairs using the STRING database. One big pairing picture mentioned earlier was obtaining a complete DEG network in Cytoscape. The MCODE plug-in in

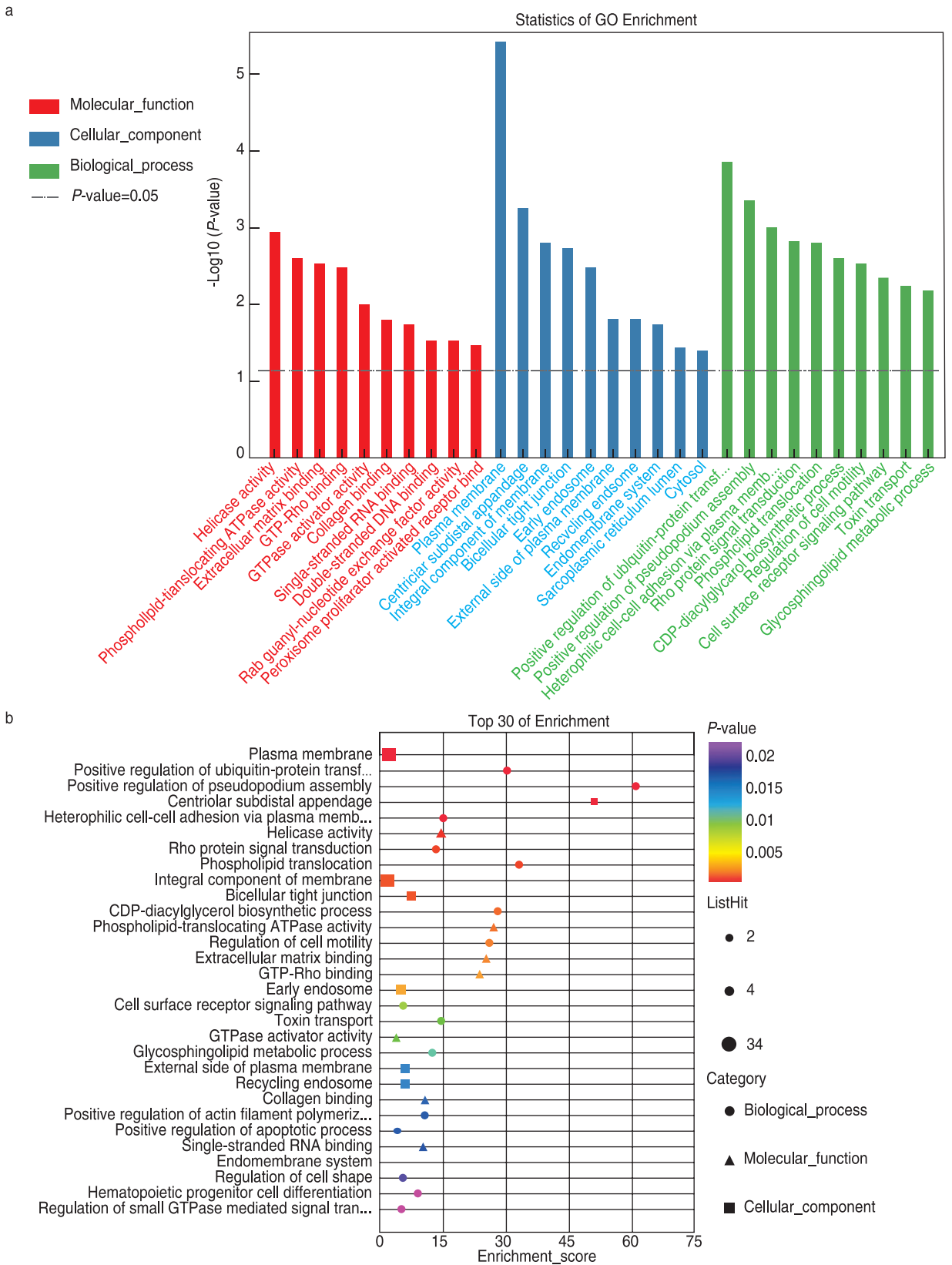

Fig. 1 (a) Gene Ontology bar graph. The y-axis is −log10 (*P* value). The higher the bar graph height, the greater the significance; (b) Kyoto Encyclopedia of Genes and Genomes bubble chart. The y-axis corresponds to the KEGG entries, the x-axis corresponds to the enrichment score, the size of the point corresponds to the number of intersection genes in the KEGG entries, and the smaller the *P* value of KEGG enrichment, the greater the significance

Cytoscape was used to perform module clustering of the DEG network mentioned earlier, after which two key functional modules of the network were evaluated (Fig. 2a). One was CD274 (CD274 molecule), C-X-C motif chemokine ligand (CXCL)1, DDX58 (DExD/H-box helicase 58), CXCL2, CXCL8, colony-stimulating factor 2 (CSF2), C-X-C motif chemokine receptor 4 (CXCR4), CXCL5, and CXCL6. The other was argininosuccinate lyase (ASL), argininosuccinate synthase 1 (ASS1), and asparagine synthetase (ASNS). These modules also occurred in the GO and KEGG enriched earlier, which were associated with the plasma membrane and signaling pathways.

Further analysis of the online volcano map (sangerbox.com/AllTools? tool_id=9699135) revealed 11 upregulated DEGs, namely CD274, CXCL1, DDX58, CXCL2, CXCL8, CSF2, CXCL5, CXCL6, ASL, ASS1, and ASNS, and one downregulated CXCR4 (Fig. 2b).

Discussion

Docetaxel is the standard first-line chemotherapy for metastatic castration-resistant PCa. However, the occurrence of docetaxel resistance is one of the main reasons for poor chemotherapy response in patients with PCa who fail androgen deprivation therapy. In our study, 1,311 DEGs were identified between the DU-145 and DU-145R cell lines and 2,027 DEGs were identified between the PC-3 and PC-3R cell lines. A total of 131 more accurate common intersection DEGs were identified between 1,311 DEGs and 2,027 DEGs by analyzing the GSE33455 dataset.

The 131 common intersection DEGs included 85 upregulated and 46 downregulated genes. The interactions among these DEGs were investigated in the KEGG and GO enrichment analyses. In the BP category, the DEGs were predominantly enriched in "positive regulation of ubiquitin-protein transferase activity," "positive regulation of pseudopodium assembly," "heterophilic cell–cell adhesion via plasma membrane CAMs," and "Rho protein signal transduction," all of which are closely associated with drug resistance and tumor metastasis. In the MF category, the DEGs were associated with "helicase activity," "phospholipid-translocating ATPase activity," "extracellular matrix binding," "GTP-Rho binding," and "GTPase activator activity"; these data suggested that the DEGs affect the binding of cadherin, proteins, and actin, as well as GTPase activity. In addition, in the CC category, the DEGs were mainly enriched in "plasma membrane," "centriolar subdistal appendage," "integral component of membrane," and "bicellular tight junction"; these data suggest that the DEGs were mainly involved in the transport and transfer of intracellular substances.

The KEGG analysis showed that the DEGs were mainly enriched in "folate biosynthesis," "viral protein interaction with cytokine and cytokine receptor," "legionellosis," "rheumatoid arthritis," "IL-17 signaling pathway," "TNF signaling pathway," and "CAMs." Wu *et al.*[7] demonstrated a novel IL-17–mediated cascade via the IL-17R-Act1-TRAF4-MEKK3-ERK5-positive circuit that directly stimulates keratinocyte proliferation and tumor formation. A previous study indicated that high

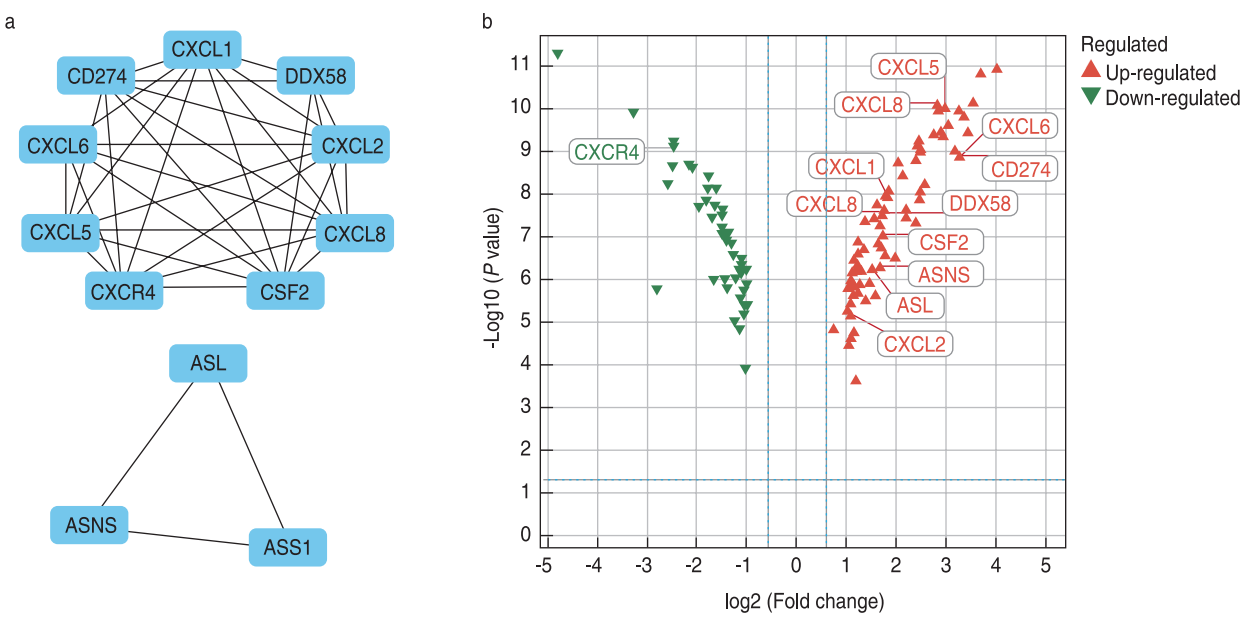

Fig. 2 (a) Two outstanding hubs of differentially expressed genes (DEGs) in metastatic docetaxel-resistant prostate cancer cell lines; (b) Volcanic map of two outstanding hubs of DEGs

serum folate levels increased cancer cell proliferation in PCa and were involved in cellular development, cell cycle, cell death, and molecular transport [8]. There is a growing body of evidence suggesting that changes in the expression or function of CAMs have been implicated in all steps of tumor progression, including detachment of tumor cells from the primary site, intravasation into the bloodstream, extravasation into distant target organs, and formation of secondary lesions [9].

In this study, a PPI network with 130 nodes and 103 edges was constructed using DEGs, and two significant modules, termed modules one and two, were obtained through the MCODE function in the Cytoscape software. Module one comprised nine genes, including the CD274 molecule, CXCL1, DDX58, CXCL2, CXCL8, CSF2, CXCR4, CXCL5, and CXCL6, which were enriched in "chemokine-mediated signaling pathway," "neutrophil chemotaxis," "antimicrobial humoral immune response mediated by antimicrobial peptide," and "cellular response to lipopolysaccharide." This enrichment results in the interaction of multiple signal transduction pathways in effector cells and the expression of related stimulating genes, which have many biological functions, including inflammation-mediated signaling pathways and humoral immune regulation [10]. Module two consisted of three genes, including ASL, ASS1, and ASNS, which were mainly associated with "arginine biosynthetic process," "urea cycle," "aspartate and glutamine family amino acid metabolic process," and "alpha-amino acid biosynthetic process." Several studies have shown that these enrichment results are mainly involved in the processes of tumor adhesion, invasion, metastasis, and drug resistance [11-12].

These 12 DEGs were considered to be hub genes, including 11 upregulated genes, namely CD274, CXCL1, DDX58, CXCL2, CXCL8, CSF2, CXCL5, CXCL6, ASL, ASS1, and ASNS, and one downregulated CXCR4, which may play a key role in docetaxel-resistant PCa [13-15]. It has been reported that CXCL8 is related to the migration and proliferation of various types of cancer cells, including PCa cells [16-17]. CXCL8 promotes the proliferation, growth, and development of cancer cells by regulating the expression of the tumor growth factor, which increases the drug resistance of androgen-independent PCa to cytotoxic chemotherapeutic drugs [18]. The data from this study suggest that these DEGs are closely related to the carcinogenesis, progression, prognosis, and drug resistance of PCa.

Conclusion

In summary, the bioinformatic analysis of the intersection gene data between DEGs in different docetaxel-resistant PCa cell lines revealed several hub genes, which may assist in the understanding of the potential molecular mechanism of docetaxel resistance. Subsequent RT-qPCR validation and in vivo experiments are required for further confirmation in the future.

Acknowledgments

Not applicable.

Funding

Supported by grants from the Natural Science Foundation of Inner Mongolia Autonomous Region, China (No. 2021MS08071), and the Medical and Health Science Research Program Project of Inner Mongolia Autonomous Region Health and Family Planning Commission, China (No. 202202264).

Conflicts of interest

The authors indicated no potential conflicts of interest.

Author contributions

Not applicable.

Data availability statement

The raw data analysis in this study were downloaded from GEO database (GSE33455).

Ethical approval

Not applicable.

References

1. Sung H, Ferlay J, Siegel RL, et al. Global Cancer Statistics 2020: GLOBOCAN Estimates of Incidence and Mortality Worldwide for 36 Cancers in 185 Countries. CA Cancer J Clin, 2021;71(3):209-249.
2. Terada N, Kamoto T, Tsukino H, et al. The efficacy and toxicity of cabazitaxel for treatment of docetaxel-resistant prostate cancer correlating with the initial doses in Japanese patients. BMC Cancer. 2019;19(1):156.
3. Yuan S, Xie SH. Urban-rural disparity in cancer incidence in China, 2008-2012: a cross-sectional analysis of data from 36 cancer registers. BMJ Open. 2021;11(4):e042762.
4. Harris WP, Mostaghel EA, Nelson PS, et al. Androgen deprivation therapy: progress in understanding mechanisms of resistance and optimizing androgen depletion. Nat Clin Pract Urol. 2009;6(2):76-85.
5. Tassinari D, Cherubini C, Roudnas B, et al. Treatment of Metastatic, Castration-resistant, Docetaxel-resistant Prostate Cancer: A Systematic Review of Literature With a Network Meta-analysis of Randomized Clinical Trials. Rev Recent Clin Trials. 2018;13(3):226-237.
6. Fan T, Wang CQ, Zhang K, *et al*. Differentially expressed genes analysis and target genes prediction of miR-22 in breast cancer. Oncol Transl Med, 2021,7: 59–64.
7. Wu L, Chen X, Zhao J, et al. A novel IL-17 signaling pathway controlling keratinocyte proliferation and tumorigenesis via the TRAF4-ERK5 axis. J Exp Med. 2015;212(10):1571-1587.
8. Tomaszewski JJ, Cummings JL, Parwani AV, et al. Increased cancer cell proliferation in prostate cancer patients with high levels of serum folate. Prostate. 2011;71(12):1287-1293.

9. Makrilia N, Kollias A, Manolopoulos L, et al. Cell adhesion molecules: role and clinical significance in cancer. Cancer Invest. 2009;27(10):1023-1037.
10. Haralambieva IH, Ovsyannikova IG, Umlauf BJ, et al. Genetic polymorphisms in host antiviral genes: associations with humoral and cellular immunity to measles vaccine. Vaccine. 2011;29(48):8988-8997.
11. Kido J, Matsumoto S, Sugawara K, et al. Variants associated with urea cycle disorders in Japanese patients: Nationwide study and literature review. Am J Med Genet A. 2021;185(7):2026-2036.
12. Wheatley DN, Campbell E. Arginine deprivation, growth inhibition and tumour cell death: 3. Deficient utilisation of citrulline by malignant cells. Br J Cancer. 2003;89(3):573-576.
13. Marzec M, Zhang Q, Goradia A, et al. Oncogenic kinase NPM/ALK induces through STAT3 expression of immunosuppressive protein CD274 (PD-L1, B7-H1). Proc Natl Acad Sci U S A. 2008;105(52):20852-20857.
14. Engl T, Relja B, Blumenberg C, et al. Prostate tumor CXC-chemokine profile correlates with cell adhesion to endothelium and extracellular matrix. Life Sci. 2006;78(16):1784-1793.
15. Acharyya S, Oskarsson T, Vanharanta S, et al. A CXCL1 paracrine network links cancer chemoresistance and metastasis. Cell. 2012;150(1):165-178.
16. Brat DJ, Bellail AC, Van Meir EG. The role of interleukin-8 and its receptors in gliomagenesis and tumoral angiogenesis. Neuro Oncol. 2005;7(2):122-133.
17. Roumeguère T, Legrand F, Rassy EE, et al. A prospective clinical study of the implications of IL-8 in the diagnosis, aggressiveness and prognosis of prostate cancer. Future Sci OA. 2017;4(2):FSO266.
18. Araki S, Omori Y, Lyn D, et al. Interleukin-8 is a molecular determinant of androgen independence and progression in prostate cancer. Cancer Res. 2007;67(14):6854-6862.

DOI 10.1007/s10330-021-0523-3
Cite this article as: Wang M, Wang L (Co-first author), Zhang Y (Co-first author), et al. Differential gene screening and functional analysis in docetaxel-resistant prostate cancer cell lines. Oncol Transl Med. 2022;8(2):94–99.

Oncology and Translational Medicine
DOI 10.1007/s10330-022-0568-8
April 2022, Vol. 8, No. 2, P100–P103

CASE REPORT

Immunotherapy induced hypothyroidism with hyperlipidemia: a case report and literature review

Yang Yang, Lilin He (✉)

First People's Hospital of Tianmen, Tianmen 431700, China

Abstract

In recent years, immune checkpoint inhibitors have been increasingly used in clinical practice. While considering the efficacy of immunotherapy, it is also necessary to be alert to immune-related adverse effects (irAEs). These include skin, gastrointestinal, liver, endocrine, and pulmonary toxicities. Here, we report a case of irAEs of hypothyroidism with marked hyperlipidemia during sintilimab administration.

Received: 26 March 2022
Revised: 11 April 2022
Accepted: 21 April 2022

Key words: immune-related adverse effects (irAEs); hyperlipidemia; hypothyroidism; immune checkpoint inhibitors (ICIs); sintilimab; immunotherapy

Sintilimab injection is an immune checkpoint inhibitor (ICI) and a recombinant, fully human immunoglobulin G-type programmed cell death protein 1 (PD-1) inhibitor. It has been approved since December 2018 for the treatment of relapsed or refractory classical Hodgkin lymphoma. Extensive clinical trials have been carried out in solid tumors such as lung, liver, gastric, and esophageal cancers, but few reports of related adverse reactions are available. Hyperlipidemia caused by immunotherapy is even rarer. Here, we report a case of immune-related adverse effects (irAEs) of hypothyroidism with marked hyperlipidemia during sintilimab administration and discuss its occurrence, characteristics, and treatment options to provide a reference for the follow-up of clinical safe application of ICIs (immune checkpoint inhibitors).

Case presentation

A 48-year-old female patient was treated in the outpatient department of Tianmen Traditional Chinese Medicine Hospital on March 18, 2020. Her chief complaints were intermittent dizziness and fatigue for more than 2 months, with no significant past medical history. Tumor markers investigation showed 60 4 ng/mL carcinoembryonic antigen (CEA) and 171 U/mL cancer antigen 199 (CA199). Abdominal ultrasound showed a space-occupying lesion (6.1 × 5.1 cm) in the right lobe of the liver.

She was treated at the Hubei Cancer Hospital on March 20, 2021. Abdominal computed tomography (CT) showed enlarged peripheral mesenteric lymph nodes and an invasion of the superior mesenteric artery by colon (hepatic flexure) cancer; the adjacent abdominal wall and pancreatic head may be involved. On April 1, 2020, the patient underwent radical resection for right colon cancer. Postoperative pathology revealed (right colon) mucinous adenocarcinoma (approximately 60%), moderately differentiated common type adenocarcinoma (approximately 40%), with large areas of necrosis that involved all muscularis to extramuscularis fibroadipose tissue (pT3). No vascular tumor thrombus or nerve invasion was noted. The superior and inferior resection margins, the mesorectum's root resection margins, the mesangial resection margins, and the omentum were nets. No cancer metastasis was observed in any of the 14 mesenteric lymph nodes. Immunohistochemistry: MSH2 (–), MSH6 (–), MLH1 (3 +, 90%), PMS2 (3 +, 70%), BRAF (V600E) (–), CD56 (–), CGA (+/–), syn (–), Ki67 (Li: 95%). Immunohistochemistry showed loss of mismatch repair proteins MSH2 and MSH6, suggesting possible microsatellite instability-high. Further confirmation by polymerase chain reaction was recommended, but the patient refused. After surgery, the patient was treated with one cycle of the XELOX regimen. On May 24, 2020, she was re-admitted to the Hubei Cancer Hospital with increased levels of tumor markers. Abdominal magnetic resonance imaging showed that there were still neoplastic lesions in the hepatic flexure of the colon, which may involve the adjacent abdominal wall and pancreatic head; the lymph nodes around the lesion may

✉ Correspondence to: Lilin He. Email: 372135535@qq.com

contain metastatic cells. Multiple metastases to the liver: Multiple lymph nodes were found in the hepatic hilar and retroperitoneal areas. The curative effect was evaluated by PD. Subsequently, two cycles of the XELIRI regimen plus bevacizumab targeted therapy were administered.

On July 13, 2020, the patient was admitted to our hospital's oncology department. Tumor marker CA125 was normal, CA724 > 300.00U/mL, CA199 17598.00U/mL, CEA 265.84 ng/mL; Fig. 1). Abdominal CT showed that after resection of colon cancer, metastatic tumors of the head of the pancreas and invasion of the superior mesenteric artery, superior mesenteric vein and multiple liver metastases were found. Since the patient's postoperative immunohistochemical findings suggested deficient mismatch repair, immunotherapy was possible. Fourteen cycles of immunotherapy with sintilimab were performed from July 17, 2020 to May 30, 2021. During the review, CA199 and CA724 showed a progressive decline to the normal range (Fig. 1), and the imaging review efficacy evaluation was a partial response (PR) (Fig. 2). On May 28, 2021, the tumor marker CA724 81.96 U/L significantly increased (Fig. 1). Therefore, fruquintinib-targeted therapy was added based on immunotherapy with sintilimab. On January 25, 2021, the imaging review efficacy evaluation was PR (Fig. 2).

Secondary hypothyroidism and hyperlipidemia developed during immunotherapy. The patient began to have hypothyroidism after 2 cycles of immunotherapy; thyroid-stimulating hormone (TSH) increased to 39.64 mIU/L, thyroxine (FT4) decreased to 2.85 pmol/L, and (tri-iodothyronine) FT3 decreased to 1.92 pmol/L, at which time levothyroxine was administered orally at a dose of 50 μg daily. A review after 21 days showed TSH 42 mIU/L, FT4 7.63 pmol/L, and FT3 2.81 pmol/L, and the dose of levothyroxine was increased to 75ug daily. Since then, FT3 and FT4 levels have risen to normal, but TSH is still elevated; hence, the patient continued to have subclinical hypothyroidism. By May 26, 2021, hypothyroidism recurred, evident by TSH 8.1 mIU/L, FT4 11.63 pmol/L, and FT3 3.2 pmol/L, while the patient developed very marked hyperlipidemia with triglycerides (TG) 30.89 mmol/L and total cholesterol (TC) 8.84 mmol/L. Fenofibrate Capsules (II) (Guangdong Xian Qiang), 0.1 g was given orally daily for lipid-lowering therapy. A review on August 10, 2021, revealed TSH 34 mIU/L, FT4 10.87 pmol/L, FT3 2.2 pmol/L. Consequently, the daily oral dose of levothyroxine was raised to 100ug, while the lipid-lowering therapy proved effective with TG 2.94 mmol/L, TC 5.81 mmol/L; fenofibrate treatment was continued. On November 16, 2021, a recheck revealed TSH, FT4, FT3, TC, and TG levels were within normal ranges. The daily oral dose of levothyroxine was 100ug, and fenofibrate was changed to atorvastatin. The last review date was March 13, 2022, and all of the above indicators were in the range, and the oral administration of levothyroxine and atorvastatin was continued.

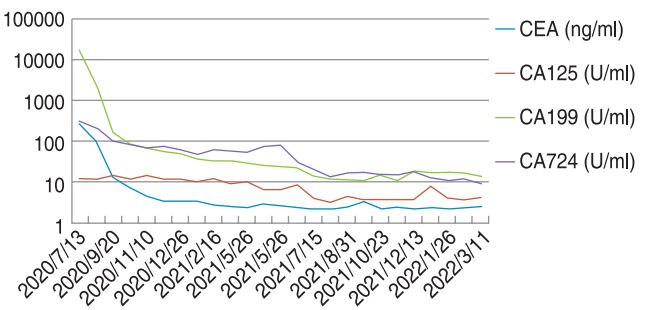

Fig. 1 The chart shows the trends of tumor markers during the course of immunotherapy in our hospital

Discussion

Colorectal cancer (CRC) is one of the most common cancers of the digestive tract in China. Its incidence and mortality rates have increased significantly over the past 30 years. A retrospective study showed that CRC has risen from sixth in common tumors to fourth [1]. Although its treatment is still based on fluorouracil and its derivatives, such as oxaliplatin and irinotecan, the long-term survival of patients remains to be improved. With the development of immunology and precision medicine, new immunotherapy drugs targeting programmed death-1 (PD-1) and its ligands (PD-L1 and PD-L2) have

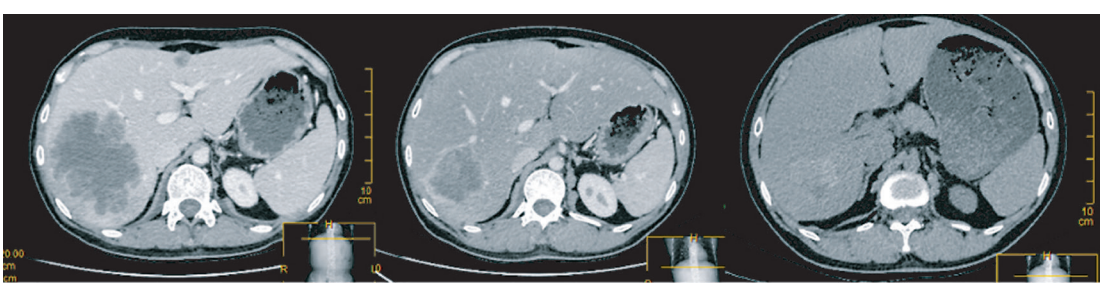

Fig. 2 CT revealed tumor masses at different times of the disease

been put into a new stage of tumor therapy. In recent years, PD-1 has achieved good results in treating solid and non-solid tumors, such as lung, breast, and liver cancers, and lymphoma [2-6].

Nivolumab and pembrolizumab, which were first marketed abroad in 2015, are the first PD-1 inhibitors to be marketed with remarkable clinical efficacy, but they also have adverse drug reactions (ADRs) such as immune-related pneumonitis, enteritis and rash. Sintilimab, a new class of drug developed independently in China, potently blocks the PD-1 / PD-L1 pathway and binds with a 50 fold higher affinity to the receptor than nivolumab, is durable and stable, can increase effector T cell infiltration in tumor tissues, and induces stronger antitumor immune responses [7]. Sintilimab, in combination with chemotherapy, can improve the short-term outcomes of patients with advanced CRC and has become an important option for prolonging patient survival.

However, while PD-1 inhibitors have significant therapeutic effects, there are also ADRs, such as fatigue, itching, diarrhea, erythema, nausea, myocarditis, and neurotoxicity [7-10]. Endocrine toxicity includes thyroid dysfunction and an acute hypophysis. The incidence of thyroid dysfunction is 5–10% (unrelated to tumor type) [11, 12]. PD-1 inhibitor single-agent-related endocrine toxicity often occurs within 10–24 weeks [13-15]. After 2 months of treatment, FT3 and FT4 levels decreased, and TSH levels increased. The treatment duration was consistent with the time of ADR.

Hyperlipidemia is a common clinical disease that can cause atherosclerosis. It is a high-risk factor for critical diseases such as coronary heart disease and pancreatitis. Hyperlipidemia is divided into two types: primary and secondary. Primary hyperlipidemia is a disorder caused by genetic or environmental factors, while secondary hyperlipidemia is caused by other factors, such as hypothyroidism. Clinical studies have shown that thyroid hormones can enhance the sensitivity of tissue to direct lipolytic hormones, reduce TG synthesis, and improve its clearance rate. Meanwhile, hypothyroidism and hyperlipidemia comorbidities are very easy. Hypothyroidism is generally associated with decreased myocardial contractility, decreased heart rate, reduced blood volume, and cardiac output and is also associated with elevated serum lipid levels.

Hypothyroidism-induced hyperlipidemia and decreased expression of low-density lipoprotein (LDL) receptors on the liver surface are associated with LDL particle oxidation. The role of FT4 in the human body is to enhance LDL activity by promoting mRNA secretion by LDL receptors in hepatocytes. In patients with hypothyroidism, the in vivo activity of LDL decreases, and damage to liver cells leads to a prolonged clearance time of LDL particles in serum, resulting in an increase in TC and TG levels [16]. Moreover, the binding of FT4 to the ApoB100 locus on LDL particles inhibits their oxidation of LDL particles. However, FT4 levels are too low for patients with hypothyroidism to provide sufficient antioxidant capacity, oxidizing LDL particles to form modified LDL, which cannot be recognized by LDL receptors, resulting in a large amount of low-density lipoprotein cholesterol accumulation [17].

Levothyroxine is a FT4 replacement therapy commonly used in clinics. This drug regulates thyroid function by improving thyroid hormone levels in patients. By exerting the effect of elevated serum TSH levels, it promotes an increase in blood lipid metabolism, thereby affecting blood lipid levels. Therefore, hyperlipidemia occurrence in this patient was related to long-term hypothyroidism.

Immune-related ADRs caused by PD-1 inhibitors sometimes appear later, even after the end of immunotherapy; therefore, regular monitoring and follow-up of thyroid function, lipid profile, renal function, and pituitary function are necessary after treatment. Most patients with hypothyroidism require long-term hormone replacement therapy and long-term monitoring and follow-up. Hypothyroidism and hyperthyroidism may occur during the treatment of hypothyroidism. Patients are currently recommended to be monitored for symptoms for at least 1 year after the end of PD-1 inhibitor therapy.

Conclusion

More immune-related toxicity may occur with the popularization of PD-1/PD-L1 inhibitors in clinical practice. The incidence of hyperlipidemia in this patient was related to long-term hypothyroidism. Monitoring toxicity is as important as evaluating efficacy during the course of PD-1/PD-L1 inhibitor monotherapy or combination therapy. The monitoring contents include biochemical tests and imaging studies, especially the indicators of renal function, thyroid function, lipid profile, and pituitary function, which are generally monitored once every 4 to 6 weeks. Due to partial toxicity's late-onset, monitoring symptoms for at least 1 year is recommended after treatment.

Acknowledgments

Not applicable.

Funding

Not applicable.

Conflicts of interest

The authors indicated no potential conflicts of interest.

Author contributions

All authors contributed to data acquisition, data interpretation, and reviewed and approved the final version of this manuscript.

Data availability statement

The data that support the findings of this study are available from the corresponding author upon reasonable request.

References

1. Zheng Y, Wang ZZ. Interpretation of global colorectal cancer statistics. Zhonghua Liu Xing Bing Xue Za Zhi. 2021;42(1):149-152.
2. Sun J, Zheng Y, Mamun M, et al. Research progress of PD-1/PD-L1 immunotherapy in gastrointestinal tumors. Biomed Pharmacother. 2020;129:110504.
3. Sun L, Zhang L, Yu J, et al. Clinical efficacy and safety of anti-PD-1/PD-L1 inhibitors for the treatment of advanced or metastatic cancer: a systematic review and meta-analysis. Sci Rep. 2020;10(1):2083.
4. Ni X, Xing Y, Sun X, et al. The safety and efficacy of anti-PD-1/anti-PD-L1 antibody therapy in the treatment of previously treated, advanced gastric or gastro-oesophageal junction cancer: A meta-analysis of prospective clinical trials. Clin Res Hepatol Gastroenterol. 2020;44(2):211-222.
5. Suzuki S, Haratani K, Hayashi H, et al. Association of tumour burden with the efficacy of programmed cell death-1/programmed cell death ligand-1 inhibitors for treatment-naïve advanced non-small-cell lung cancer. Eur J Cancer. 2022;161:44-54.
6. Fedorova LV, Lepik KV, Mikhailova NB, et al. Nivolumab discontinuation and retreatment in patients with relapsed or refractory Hodgkin lymphoma. Ann Hematol. 2021;100(3):691-698.
7. Wang J, Fei K, Jing H, et al. Durable blockade of PD-1 signaling links preclinical efficacy of sintilimab to its clinical benefit. MAbs. 2019;11(8):1443-1451.
8. Wang Y, Zhou S, Yang F, et al. Treatment-related adverse events of PD-1 and PD-L1 inhibitors in clinical trials: a systematic review and meta-analysis. JAMA Oncol. 2019;5(7):1008-1019.
9. Man J, Ritchie G, Links M, et al. Treatment-related toxicities of immune checkpoint inhibitors in advanced cancers: A meta-analysis. Asia Pac J Clin Oncol. 2018;14(3):141-152.
10. Ruggiero R, Fraenza F, Scavone C, et al. Immune Checkpoint Inhibitors and Immune-Related Adverse Drug Reactions: Data From Italian Pharmacovigilance Database. Front Pharmacol. 20209;11:830.
11. Barroso-Sousa R, Barry WT, Garrido-Castro AC, et al. Incidence of endocrine dysfunction following the use of different immune checkpoint inhibitor regimens: a systematic review and meta-analysis. JAMA Oncol. 2018;4(2):173-182.
12. Chang LS, Barroso-Sousa R, Tolaney SM, et al. Endocrine toxicity of cancer immunotherapy targeting immune checkpoints. Endocr Rev. 2019;40(1):17-65.
13. Puzanov I, Diab A, Abdallah K, et al; Society for Immunotherapy of Cancer Toxicity Management Working Group. Managing toxicities associated with immune checkpoint inhibitors: consensus recommendations from the Society for Immunotherapy of Cancer (SITC) Toxicity Management Working Group. J Immunother Cancer. 2017;5(1):95.
14. Postow MA, Sidlow R, Hellmann MD. Immune-related adverse events associated with immune checkpoint blockade. N Engl J Med. 2018;378(2):158-168.
15. Khan Z, Hammer C, Guardino E, et al. Mechanisms of immune-related adverse events associated with immune checkpoint blockade: using germline genetics to develop a personalized approach. Genome Med. 2019;11(1):39.
16. Tassi R, Baldazzi V, Lapini A, et al. Hyperlipidemia and hypothyroidism among metastatic renal cell carcinoma patients taking sunitinib malate. Related or unrelated adverse events? Clin Genitourin Cancer. 2015;13(2):e101-e105.
17. Su X, Peng H, Chen X, et al. Hyperlipidemia and hypothyroidism. Clin Chim Acta. 2022;527:61-70.

DOI 10.1007/s10330-022-0568-8
Cite this article as: Yang Y, He LL. Immunotherapy induced hypothyroidism with hyperlipidemia: a case report and literature review. Oncol Transl Med. 2022;8(2):100–103.

Oncology and Translational Medicine
DOI 10.1007/s10330-021-0540-0

April 2022, Vol. 8, No. 2, P104–P108

CASE REPORT

Nasal-type extranodal NK/T cell lymphoma in association with hemophagocytic syndrome: a case report and literature review*

Shuang Chen, Yongchu Huang, Yuchun Cao, Yong Zhang (✉)

Department of Dermatology and Venereology, Tongji Hospital, Tongji Medical College, Huazhong University of Science and Technology, Wuhan 430030, China

Abstract

We present a rare case of nasal-type CD56-negative NK/T-cell lymphoma. The patient developed hemophagocytic syndrome during diagnosis and treatment. The patient presented to our hospital (Tongji Hospital, Tongji Medical College, Huazhong University of Science and Technology, Wuhan, China) with "nasal congestion for 3 months and scattered erythema, nodules, and ulcers all over the body for 1 month." We analyzed clinical manifestations, skin histopathology, immunohistochemistry, and *in situ* hybridization results. Histopathology of the skin revealed a moderate amount of atypical lymphocyte infiltration between the entire dermis and collagen bundles. Immunohistochemistry showed the following: CD30 (+), TIA-1 (+), CD3(2GV6) (+), CD5 part (+), CD8 part (+), CD43 (+), CD56 (–), CD4 (–), CD20 (–), PAX5 (–), PCK (–), P63 (–), P40 (–), EGFR (–), Ki-67 (the hot spot LI is approximately 80%), and *in situ* hybridization EBER-ROCH (+). The diagnosis made was "NK/T cell lymphoma nasal type". This type of lymphoma is aggressive, progresses quickly, and has a poor prognosis. Early clinical manifestations are extremely atypical, especially in the absence of rash. Analysis of the skin manifestations of the disease has a positive effect on its early diagnosis, early treatment, and prognosis.

Received: 29 November 2021
Revised: 21 December 2021
Accepted: 20 January 2022

Key words: lymphoma; non-Hodgkin; lymphohistiocytosis; hemophilic

Extranodal NK/T cell lymphoma (ENKTCL) is overwhelmingly an Epstein-Barr virus (EBV) associated lymphoma, showing CD56 positive, low survival and aggressive clinical behavior [1]. Nasal-type extranodal NK/T cell lymphoma (ENKTCL-NT) has atypical early clinical symptoms and is often delayed due to lack of early diagnosis and treatment. Most ENKTCL-NT cases were derived from NK cells expressing CD3ε and CD56, with positive expression of CD56. CD56-negative ENKTCL-NT has been suggested as a distinct lymphoma subtype with fewer clinical cases [2]. Hemophagocytic lymphohistiocytosis (HLH) is considered as a rare heterogeneous disease caused by excessive secretion of inflammatory cytokines, which seriously endangers the lives of patients. HLH is divided into primary HLH and secondary HLH, and the latter is associated with many diseases, such as infectious diseases, hematological malignancies and connective tissue disease, mainly non-Hodgkin's lymphoma. ENKTCL has been shown to be a major trigger of lymphoma-associated hematophagocytic syndrome (LAHS) [3], the 2-year survival rate of ENKTCL patients with HLH was 14.7%, and that of patients without HLH was 77.5% [4]. ENKTCL combined with HLH is rare, with rapid and explosive course and variable presentation, seriously threatening the lives of patients. We report a case of CD56-negative ENKTCL-NT complicated with HLH. Through the analysis of the diagnosis and treatment process of this case, it is expected to provide evidence for improving the diagnosis and treatment effect.

Clinical data

Medical history

A 56-year-old man visited our hospital's Otolaryngology Department (Tongji Hospital, Tongji Medical College, Huazhong University of Science and Technology, Wuhan,

✉ Correspondence to: Yong Zhang. Email: 61112426@qq.com
* Supported by a grant from the National Natural Sciences Foundation of China (No. 81974308).

China) on September 14, 2020, due to nasal congestion for 3 months and scattered erythema, nodules, and ulcers all over the body for 1 month. Nasal congestion without an obvious cause occurred 3 months before the visit to our hospital, intermittent at first and then becoming continuous. Sinusitis was diagnosed and treated several times at another hospital; however, there was no obvious relief. Two months later, dark red infiltrating erythema, nodules, and ulcers repeatedly appeared on the patient's nose, trunk, and buttocks, with mild pain. During the illness, there were occasional headaches but no fever, cough, or other symptoms. The patient was transferred from the outpatient department to the Otolaryngology Department for inpatient treatment of a nasal mass. Nothing special was noted in the medical history of the patient. The patient reported no family history of similar diseases.

Skin histopathology, immunohistochemistry, bone marrow aspiration, and other related examinations were performed on the second day after admission. Anti-infectives were administered to treat symptoms. On September 18, 2020, the patient underwent sinuplasty under general anesthesia and sinus and nasal cavity lesion biopsy under nasal endoscopy. On September 21, 2020, he presented with acute fever. The highest body temperature reached 39.5 °C, and routine blood tests showed a white blood cell (WBC) count of 3.72×10^9/L, red blood cell (RBC) count 3.96×10^{12}/L, hemoglobin (Hb) level 128.0 g/L, platelet (PLT) count 111.0×10^9/L, and lymphocyte percentage 16.4%. After antipyretic treatment, the patient's body temperature did not decrease and the fever persisted. The pathological diagnosis of the bone marrow showed that the hyperplasia of the bone marrow was decreased, and hemophagocytosis was visible; combined with the results of skin histopathology, immunohistochemistry, and bone marrow aspiration, the patient was diagnosed with NK/T cell lymphoma on September 22, 2020 and transferred to the Oncology Department for treatment.

Routine blood tests on September 23, 2020 showed a WBC count of 3.18×10^9/L and PLT count 61.0×10^9/L. In view of the patient's continued decline in WBC and PLT counts, the treatments to increase WBC level (recombinant human granulocyte-macrophage stimulating factor), and PLT level (recombinant human interleukin-11), and an anti-infective treatment (moxifloxacin hydrochloride and cefoperazone natazobactam) were administered. However, the patient's condition was not relieved. On September 29, 2020, the patient developed persistent lower gastrointestinal bleeding. Routine blood tests on October 1, 2020, showed a WBC count of 3.17×10^9/L, lymphocyte count 0.52×10^9/L, lymphocyte percentage 16.4%, RBC count 2.26×10^{12}/L, Hb level 72.0 g/L, PLT count 53.0×10^9/L, fibrinogen level 1.32 g/L, triglyceride level 3.08 mmol/L, and ferritin level 3157.4 μg/L. The patient's RBC count, PLT count, Hb level, and fibrinogen level decreased rapidly, while triglyceride and ferritin levels increased significantly. The diagnosis was nasal-type NK/T-cell lymphoma (stage VI) with hemophagocytic syndrome. On October 1, 2020, the patient was treated with hormone plus VP-16. The patient still had a recurrent fever, and his condition rapidly deteriorated. The patient's family gave up treatment and patient was discharged on October 2, 2020. The patient died 2 days after discharge.

Physical examination

The following were noted upon examination: temperature of 37.2 °C, pulse rate 80 times/min, respiratory rate 20 times/min, and blood pressure 117/76 mmHg. The superficial lymph nodes throughout the body were not palpable or swollen. There were no obvious abnormalities on cardiopulmonary or abdominal examinations. Dermatological examination: infiltrating erythema with a diameter of approximately 1.5 cm × 3.0 cm was seen on the left side of the nose, with clear borders, ulceration in the center, thick brown scab overlying, and a small amount of purulent discharge (Fig. 1a). Infiltrating erythema and nodules with a diameter varying from 3.0 cm to 12.0 cm were scattered on the back, waist, and buttocks. Some skin lesions ruptured with scabs in the center (Fig. 1b). There were no obvious abnormalities in the oral mucosa or nails.

Auxiliary examination

9/15/2020 blood routine: WBC count 2.77×10^9/L, RBC count 3.88×10^{12}/L, Hb level 125.0 g/L, and PLT count 84.0×10^9/L. Activated partial thromboplastin time (APTT): 42.9 seconds (29.0–42.0 seconds).

9/17/2020 blood routine: Lymphocyte count 0.69×10^9/L, RBC count 3.65×10^{12}/L, Hb level 119.0 g/L, and PLT count 114.0×10^9/L.

9/29/2020: EBV nucleic acid in plasma and peripheral blood mononuclear cells were 1.14×10^4 and 1.54×10^4 copies/mL, respectively.

9/15/2020: Chest radiography showed no obvious abnormalities in the lungs, heart, and diaphragm.

9/16/2020: A facial computed tomography (CT) scan showed the density of the soft tissues of the left middle and lower nasal passages, which were not clearly demarcated from the turbinate. There was a possibility of tumor lesions being present in the newly identified parts.

9/20/2020: Pathological examination of the back skin tissue showed epidermal necrosis and scabs, and medium-density atypical lymphoid cell infiltration was observed around the whole layer of the dermis and between the collagen bundles (Fig. 2).

9/21/2020: A biopsy of the left nasal cavity and

Fig. 1 (a) Erythema and ulcer on the left-wing of the nose; (b) Scattered erythema, nodules, and ulcers on the back, waist, and buttocks

middle nasal passage showed nasal extranodal NK/T-cell lymphoma. Immunohistochemistry revealed the following: CD30 (+), TIA-1 (+), CD3(2GV6) (+), CD5 part (+), CD8 part (+), CD43 (+), CD56 (–), CD4 (–), CD20 (–), PAX5 (–), PCK (–), P63 (–), P40 (–), EGFR (–), Ki-67 (the hot spot LI was approximately 80%), and *in situ* hybridization EBER-ROCH (+) (Fig. 3).

9/30/2020: CT of the small intestine and colon dual-phase enhancement + tomography showed thickening and edema of the ileocecal valve and the intestinal wall

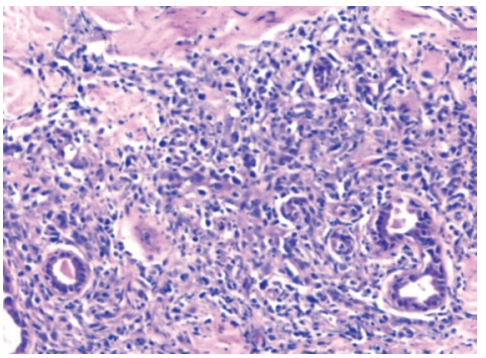

Fig. 2 Histopathology of the back skin (hematoxylin and eosin staining, × 100)

of the terminal ileum, increased and enlarged mesangial lymph nodes, thickening of the gastric wall of the gastric antrum, swelling of the Glisson sheath, and thickening and edema of the gallbladder wall. The spleen was slightly larger, bilateral inguinal lymph nodes were increased in number, peritoneum and mesangium were thickened and exuded, and abdominal and pelviceffusions were observed.

Discussion

ENKTCL is a rare type of non-Hodgkin lymphoma, which is considered to be closely related to EBV and usually affects the upper respiratory tract. Because it typically appears in the nasopharynx, the World Health Organization (WHO) classification includes both nasal and

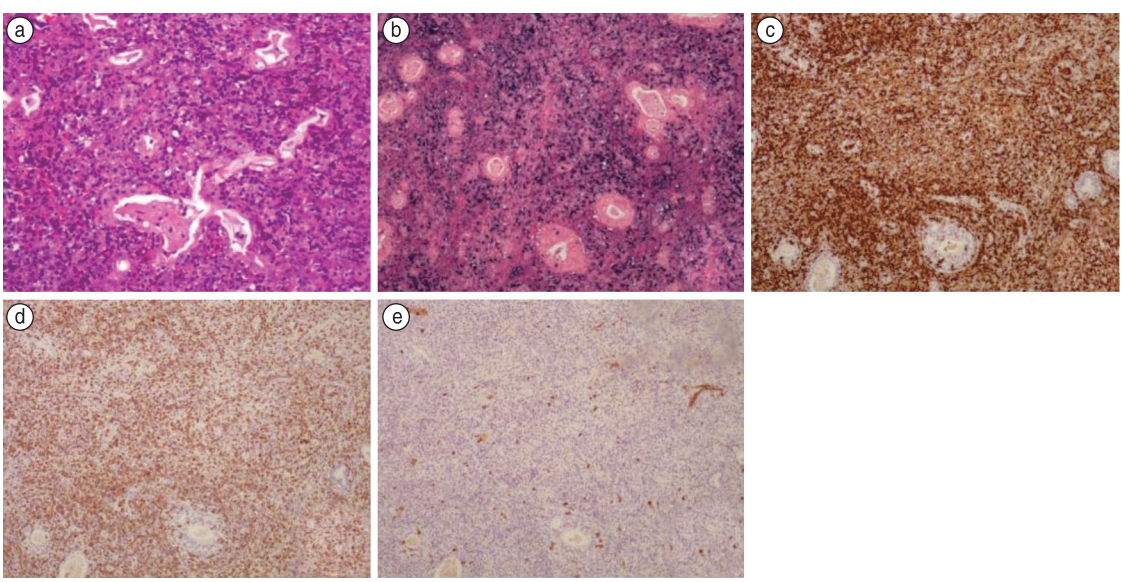

Fig. 3 Histopathology and immunohistochemistry of the left nasal cavity and middle nasal passage. (a) hematoxylin and eosin staining (x 200); (b) EBE-ROCH positive (× 200); (c) CD30 positive (× 200); (d) TIA-1 positive (× 200); (e) CD56 negative (× 200)

extranasal ENKTCLs in the same disease category. In light of its typical presentation in the nasopharynx, ENKTCL has also been classified as "nasal type" (ENKTCL-NT), and it has obvious regional and ethnic tendency. China is an area with a high incidence of ENKTCL-NT. The median age of onset for ENKTCL-NT is 45 years, with a reported incidence ratio of 4:1 (men : women) [5–6]. ENKTCL is characterized by prominent vascular destruction, tissue necrosis, and inflammatory cell infiltration [7]. Histologically, tumor cell infiltration usually manifests as vascular centrality and destruction, leading to band necrosis. Cytologically, the tumor cells were large, granular lymphocytes. Typical NK/T lymphomas mostly express T cell differentiation antigens (CD3 and CD45RO) or NK cell (CD56, CD2, and CD36) differentiation antigens, but not B cell differentiation antigens (CD20). In generalized cases, active hemophagocytic cells can be found in the liver, spleen, and bone marrow, leading to impaired liver function, hyperferritinemia, and pancytopenia [8–9].

HLH is a disease caused by the engulfing of blood cells by benign and reactive proliferating tissue cells in hematopoietic tissues, such as the bone marrow, spleen, and lymph nodes. It can be divided into primary and secondary cytophilia [secondary HLH (sHLH)] [10]. However, the pathogenesis of sHLH remains unclear. In sHLH, NK cells and cytotoxic T lymphocytes (CTL) are continuously abnormally activated, whereas cytotoxic effect defects or low function could result in antigens (pathogens, tumor cells, etc.) that cannot be effectively eliminated. These effects continue to stimulate and activate macrophages, leading to abnormal tissue cell proliferation and cytokine storms, which eventually cause high inflammation in multiple organs and immune damage to tissues and organs. Patients with NK/T-cell lymphoma are more prone to develop NK/T-cell lymphoma-associated hemophagocytic syndrome (LAHPS). Approximately 7.1% to 11.4% of ENKTCL cases were related to HLH. The prognosis of these patients is very poor, with a median survival of 30 days [11]. During the progression or treatment of lymphoma, 26.7%–47.8% of patients develop HLH. Disease progression or chemotherapeutic drugs may affect the clinical manifestations of LAHPS, leading to delays in diagnosis and treatment [12]. In addition, the following reasons may explain the occurrence of HLH. (1) NK/T-LAHPS is mostly associated with EBV infection. LAHPS related to EBV infection can express latent membrane protein (LMP-1), which activates the NF-κB pathway and upregulates cytokines (such as the expression of TNF-α and IFN-γ), consequently initiating a series of signal transduction pathways in cells and triggering a cytokine storm that finally leads to the occurrence of HLH. (2) NK/T cell lymphoma has obvious necrotizing lesions. Concurrent infections with focal necrosis can easily develop which may lead to increased cytokine levels and development of HLH [10–13].

In this case, the skin lesions showed erythema, nodules, and ulcers. The skin biopsy revealed epidermal necrosis, sparse medium-density atypical lymphocytes, and a small amount of tissue cell infiltration in the superficial and deep layers of the dermis. In addition, a biopsy of the sinus lesions revealed nasal-type extranodal NK/T-cell lymphoma. Based on the clinical manifestations, histopathology, immunohistochemistry, and *in situ* hybridization results, the patient was diagnosed with skin ENKTCL-NT. This was a rare case of CD56-negative ENKTCL. NK/T cell lymphomas are typically positive for CD3 (cytoplasm), CD56, cytotoxic markers (granzyme B, TIA1), and EBV. To the best of our knowledge, there are currently few reports of CD56-negative ENKTCL [14]. In a group of early ENKTCL patients, the survival rate of CD56-negative ENKTCL patients was significantly lower, indicating that CD56-negative ENKTCL can be regarded as a unique phenotype, and it is necessary to further optimize treatment strategies for this disease [15]. During the treatment of ENKTCL, the patient developed fever, progressive decline in blood cell counts, splenomegaly, hyperferritinemia, hypofibrinogenemia, and the presence of hematopoietic cells in the bone marrow, which met the five criteria in the HLH 2004 diagnostic guideline; thus, the patient was diagnosed with HLH. The prognosis of this disease in this patient was extremely poor, which is in line with previous reports in the literature [11]. The patient died within a short period. ENKTCL is a highly malignant, aggressive, and rapidly progressing tumor. Therefore, an early diagnosis is important. However, the early clinical manifestations of ENKTCL-NT are atypical, and they are easily misdiagnosed, especially when there is no rash. The patient's upper respiratory tract symptoms manifested as the first symptom, while skin erythema, nodules, and ulcers gradually appeared later. Unfortunately, he was misdiagnosed with sinusitis several times before being transferred to our hospital. Skin biopsy and other related examinations were performed promptly after admission, and the diagnosis was quickly confirmed. This case suggests that we should be vigilant about the possibility of ENKTCL-NT for persistent sinusitis, especially when it is accompanied by skin damage. Early nasal cavity, skin histopathology, immunohistochemistry or flow cytometry, and other related examinations are recommended for this type of disease to achieve early diagnosis and treatment.

Acknowledgments

Not applicable.

Funding

Supported by a grant from the National Natural

Sciences Foundation of China (No. 81974308).

Conflicts of interest

The authors indicated no potential conflicts of interest.

Author contributions

All authors contributed to data acquisition, data interpretation, and reviewed and approved the final version of this manuscript.

Data availability statement

Not applicable.

Ethical approval

Not applicable.

References

1. Shikama N. Local radiation for cutaneous T-cell lymphoma other than mycosis fungoides and Sézary syndrome. Chin Clin Oncol. 2019;8(1):8.
2. Yang J, Li P, Piao Y, et al. CD56-negative extranodal natural killer/T-cell lymphoma: A retrospective study in 443 patients treated by chemotherapy with or without asparaginase. Front Immunol. 2022;13:829366.
3. Liu YZ, Bi LQ, Chang GL, et al. Clinical characteristics of extranodal NK/T-cell lymphoma-associated hemophagocytic lymphohistiocytosis. Cancer Manag Res. 2019;11:997-1002.
4. Li N, Jiang M, Wu WC, et al. How to identify patients at high risk of developing nasal-type, extranodal nature killer/T-cell lymphoma-associated hemophagocytic syndrome. Front Oncol. 2021;11:704962.
5. Suzuki R. Pathogenesis and treatment of extranodal natural killer/T-cell lymphoma. Semin Hematol. 2014;51(1):42-51.
6. Haverkos BM, Pan Z, Gru AA, et al. Extranodal NK/T cell lymphoma, nasal type (ENKTL-NT): An update on epidemiology, clinical presentation, and natural history in north American and European cases. Curr Hematol Malig Rep. 2016;11(6):514-527.
7. Quan XY, Wu CZ, Lei L, et al. The prognostic potential of pretreatment C-reactive protein to albumin ratio in stage IE/IIE extranodal natural killer/T-cell lymphoma. Oncol Transl Med. 2019;5(4):162-169.
8. Yang D, Liu DH. Cutaneous extranodal NK/T-cell lymphoma: a clinicopathologic study of 10 cases. J Clin Dermatol (Chinese). 2020;49(6):342-346.
9. Tse E, Kwong YL. The diagnosis and management of NK/T-cell lymphomas. J Hematol Oncol. 2017;10(1):85.
10. Lehmberg K, Nichols KE, Henter JI, et al. Consensus recommendations for the diagnosis and management of hemophagocytic lymphohistiocytosis associated with malignancies. Haematologica. 2015;100(8):997-1004.
11. Wei L, Yang L, Cong J, et al. Using etoposide + dexamethasone-based regimens to treat nasal type extranodal natural killer/T-cell lymphoma-associated hemophagocytic lymphohistiocytosis. J Cancer Res Clin Oncol. 2021;147(3):863-869.
12. Yang XY, Li R, Shen LD. Research progress of extranodal natural killer/T-cell lymphoma-associated hemophagocytic syndrome. Med Recapitul (Chinese). 2015;21(7):1200-1203.
13. Geller S, Myskowski PL, Pulitzer M. NK/T-cell lymphoma, nasal type, γδ T-cell lymphoma, and CD8-positive epidermotropic T-cell lymphoma-clinical and histopathologic features, differential diagnosis, and treatment. Semin Cutan Med Surg. 2018;37(1):30-38.
14. Tse E, Kwong YL. Diagnosis and management of extranodal NK/T cell lymphoma nasal type. Expert Rev Hematol. 2016;9(9):861-871.
15. Wang L, Wang Z, Xia ZJ, et al. CD56-negative extranodal NK/T cell lymphoma should be regarded as a distinct subtype with poor prognosis. Tumour Biol. 2015;36(10):7717-7723.

DOI 10.1007/s10330-021-0540-0
Cite this article as: Chen S, Huang YC, Cao YC, et al. Nasal-type extranodal NK/T cell lymphoma in association with hemophagocytic syndrome: a case report and literature review. Oncol Transl Med. 2022;8(2):104–108.

中国外科大师的三会三知

做人要知足，
做学问要不知足

裘法祖

1914年12月—2008年6月

他是“人民医学家”

抗战回国效力，
用一生时间
成就少年理想

做人我只求四点：一身正气、两袖清风、三餐温饱、四大皆空。

做人要知足，做学问要不知足 他是“人民医学家”
抗战回国效力，用一生时间成就少年理想

裘法祖（1914 年 12 月—2008 年 6 月），医学家，中国科学院院士。我国普通外科学的奠基人和开拓者，器官移植外科创始人之一，在普通外科的成就推动了我国外科学的发展。他创造的外科手术方式被誉为“裘氏术式”。曾获何梁何利基金科学与技术进步奖，荣获全国先进科技工作者、“最美奋斗者”等称号。

摘自《科学家精神丛书》